eman ta zabal zazu

Universidad del País Vasco
Euskal Herriko Unibertsitatea

Faculty of Medicine. Department of Neurosciences

Signaling pathways in oligodendrocytes to promote myelin remodeling

DOCTORAL THESIS

Ana Palma Leiva

2022

Part of the results presented in this doctoral thesis have been publised in the following articles:

Palma, Ana, Juan Carlos Chara, Amaia Otxoa-Amezaga, Anna Planas, Carlos Matute, Alberto Pérez-Samartín, and María Domercq. “Clemastine Induces an Impairment in Developmental Myelination.” BioRxiv. 2021.12.14.472570. (2021). *Frontiers in developmental and cellular biology* (under review).

Matute, Carlos, Ana Palma, María Paz Serrano-Regal, Estibaliz Maudes, Sumanta Barman, María Victoria Sánchez-Gómez, María Domercq, Norbert Goebels, and Josep Dalmau. “N-Methyl-D-Aspartate Receptor Antibodies in Autoimmune Encephalopathy Alter Oligodendrocyte Function.” *Annals of Neurology* 87, no. 5 (2020).

This work was supported by:

- University of the Basque Country (UPV/EHU) - Ayuda de contratacion para formacion de personal investigador en la Universidad del Pais Vasco 2018
- Merck Serono (a business of Merck KGaA, Germany) - Grant for Multiple Sclerosis Innovation
- Spanish Ministry of Education and Science (SAF2013-45084-R and SAF2016-75292-R)
- Centro de Investigacion Biomedica en Red, Enfermedades Neurodegenerativas (CIBERNED)
- Basque Goverment (IT702-13)

A Ulpi y Angi

ABBREVIATIONS

aCSF	Artificial CSF
ANOVA	Analysis of variance
APC	Antigen presenting cell
APC (CC1)	Adenomatous polyposis coli clone CC1
Arg1	Arginase gen
ATP	Adenosine triphosphate
A.U.	Arbitrary units
BBB	Blood brain barrier
BDNF	Brain-derived neurotrophic factor
BSA	Bovine serum albumin
Calcein-AM	Calcein- acetoxymethyl
cAMP	Cyclic adenosine monophosphate
CAP	Compund action pontential
CIS	Clinically isolated syndrome
CNPase	2 ', 3'-Cyclic-nucleotide 3'-phosphodiesterase
CNS	Central nervous sistem
CNTF	Ciliary neurotrophic factor
CSF	Cerebrospinal fluid
DIV	Days in vitro
DMEM	Dulbecco's Modified Eagle's Medium
DPI	Day postimmunization
EAE	Experimental autoimmune encephalomyelitis
EDTA	Ethylenediaminetetraacetic acid
ERK	Extracellular signal regulated kinase
FACS	Fluorescence-activated cell sorting
FBS	Fetal bovine serum
Fc	Antibody receptor
FGF	Fibroblast growth factor

GABAergic	Gamma-aminobutyric acid-ergic
GLUT1	Glucose transporter 1
GPCR	G protein-coupled receptor
HLA	Human leukocyte antigen
Iba1	Ionized calcium binding adaptor molecule 1
IFN-ɣ	Interferon-γ
IGF-1	Insulin-like growth factor 1
IgG	Immunoglobulin G
IMDM	Iscove´s Modified Dubelcco´s Medium
iNOS	Inducible oxide nitrite synthase
MAG	Myelin-associated glycoprotein
MAPK	Mitogen-activated protein kinase
MBP	Myelin basic protein
MCT	Monocarboxylate transporter
MOG	Myelin oligodendrocyte glycoprotein
MRI	Magnetic resonance imaging
mRNA	Messenger RNA
MS	Multiple sclerosis
m-TOR	Mammalian target of rapamycin
Myrf	Myelin regulatory factor
NF-kB	Nuclear factor kappa-light-chain-enhancer of activated B cells
NF-L	Neurofilament L
NG2	Neuron-glial antigen 2
NGF	Nerve growth factor
NMDAR	N-methyl-D-aspartate receptor
NRG	Neuregulin
NT3	Neurotrophin-3
Olig2	Oligodendrocyte transcription factor 2
OPC	Oligodendrocyte progenitor cell

PB	Phosphate buffer
PBS	Phosphate buffer saline
PDGF	Platelet-derived growth factor
PDL	Poly-D-Lysine
PFA	Paraformaldehyde
PLP	Proteolipid protein
PPMS	Primary-progressive multiple sclerosis
pPCR	Quantitative polymerase chain reaction
ROI	Region of interest
RRMS	Relapsing-remitting multiple sclerosis
RT	Room temperature
SEM	Standard error of the mean
SMI-32	Neurofilament H Non-Phosphorylated protein
SPMS	Secondary progressive multiple sclerosis
T3	Tri-iodothyronine
T4	L -Thyroxine
TBS-T	Tris buffer saline tween-20
TEM	Transmission electron microscopy
Th	T helper cell
Treg	Regulatory T cell
WM	White matter
WT	Wild type
YFP	Yellow fluorescent protein

INTRODUCTION

1. OLIGODENDROCYTE AND MYELIN PHYSIOLOGY

More than half of the human brain is white matter, which supports rapid and synchronized transfer of information across the many gray-matter areas of the central nervous system (CNS). The function of white matter relies on oligodendrocytes, specialized glial cells for myelin formation. The myelin sheath is an extension of the oligodendrocyte plasma membrane that wrap axons in the CNS. After contacting the unmyelinated axons, oligodendrocytes start wrapping by spreading their membrane both radially and longitudinally, generating compacted areas, while also preserving uncompacted cytoplasmic channels for myelin component transport (Stadelmann *et al*., 2019) .

This compacted myelin is a multilamellar lipid structure that provides high electrical resistance and low transverse capacitance, both crucial for fast conduction velocity (Hartline & Colman, 2007; McDougall *et al*., 2018). Myelin sheaths distribution along the axons generate discrete areas named Nodes of Ranvier where the sodium channels are clustered, allowing the saltatory impulse propagation. Furthermore, oligodendrocytes provide axons with energy, essential for its survival and for the impulse propagation required for maintaining high impulse frequency (Moore *et al*., 2020; Nave, 2010). Fundamentally, fast and saltatory conduction leads to an advanced functional efficiency and complexity of the CNS in vertebrates (Hartline, 2008; Zalc *et al*., 2008).

1.2 Oligodendrocyte differentiation

Oligodendrocyte progenitor cells, OPCs, or NG2-glia, comprise a cell population of 5–10% of the total cells in the brain that can proliferate and generate mature, myelinating oligodendrocytes throughout life, but are also able to receive synaptic input from neurons. The extent and timing of differentiation could be influenced by the developmental origin, the environmental cues and/or their intrinsic properties. Interestingly, for OPCs in the adult brain it has been shown that their ability to proliferate and differentiate is region-dependant. Cells in grey matter regions have a longer cell cycle length and lower differentiation properties as compared to cells in the white matter (Dimou *et al*., 2008; Simon *et al*., 2011).

However, a recent single cell RNA-sequencing analysis of different populations of cells in the oligodendrocytic lineage could not identify region or age specific subpopulations of OPCs (Marques *et al*., 2016). In contrast, the authors identified a continuum of 12 different subpopulations ranging from OPCs to mature oligodendrocytes. Some of these cell populations were enriched in the developing brain pointing to intermediates in the oligodendrocyte lineage and suggesting that oligodendrocyte differentiation represents a series of linked cellular transformations.

1.3 Myelin biogenesis

Myelin is a poorly hydrated structure with a very particular molecular composition. The main constituents of myelin are lipids (70% of its dry weight) and proteins (30% of the dry weight), many of which are specific to myelin and are used to identify oligodendrocytes by immunohistochemistry (Salzer *et al*., 2008). The major CNS myelin proteins are Proteolipid Protein (PLP, 50% of myelin protein) and Myelin Basic Protein (MBP, 30% of myelin protein) among others, such as CNP (2',3'-cyclic nucleotide 3'-phosphodiesterase; 4% of myelin proteins), myelin-associated glycoprotein (MAG) and myelin oligodendrocyte glycoprotein (MOG) (Gould *et al*., 2008; Jahn *et al*., 2009, 2020). The specific lipid composition with high levels of saturated long-chain fatty acids, including cholesterol (46% of total lipids), phospholipids (26%) and glycolipids (20%), confers this membrane a solid molecular and metabolic stability (Poitelon *et al*., 2020). The biosynthesis of all these myelin components requires simple precursor molecules and consumes energy (Chrast *et al*., 2011). Cholesterol cannot cross the blood–brain barrier and it has to be synthesized through a highly energetic process of fatty acid synthesis, highlighting the importance of oligodendrocytes metabolic activity (Mathews & Appel, 2016; Maxfield & van Meer, 2010; Rinholm *et al*., 2011).

Last ultrastructural analysis revealed that myelin sheath formation starts as an extension of oligodendrocyte membrane with a triangular shape where the outer layer is in direct contact with the oligodendrocyte cell body, and the innermost layer with the axon (K. J. Chang *et al*., 2016). The myelination process involves two coordinated movements of the oligodendrocyte

membrane towards the axon (Snaidero & Simons, 2014) **(Figure 1)**. For the radial growth, the oligodendrocyte sends out the process which makes contact with the axon and the inner tongue wraps around it following a convex curve (Sobottka *et al*., 2011). Since the inner tongue is the primary growth zone in growing myelin sheaths, it leads the expanding membrane underneath the previously generated layers (Snaidero *et al*., 2014a, 2014b). The longitudinal growth implies membrane sheet widening along the axon. As the myelin length increases by lateral extension and start compacting, the lateral cytoplasmic loops move toward the edges of the myelin sheath forming the paranode (Müller *et al*., 2013). These paranodes are flanking the node, where the axonal sodium channels accumulate and increase in density (>1200/μm^2) **(Figure 2)** (Snaidero & Simons, 2014).

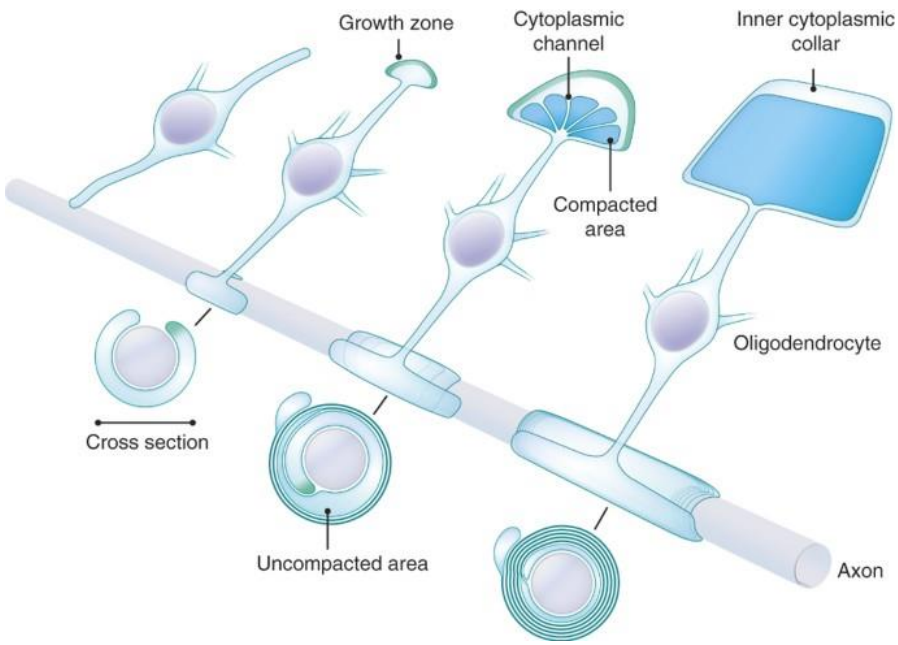

Figure 1. The current model of myelination in the CNS. From left to right: a newly differentiated oligodendrocyte extends a process to an unmyelinated axon. After contacting the axon, it starts wrapping by spreading its membrane. The growth zone for active membrane incorporation is shown in green. The myelin membrane grows both radially (more wraps) and longitudinally (longer sheath). When there are about three layers of myelin membrane, intracellular compaction initiates from the outermost layer toward the inner layers, preserving uncompacted cytoplasmic channels for material transport between the oligodendrocyte process and the growth zone (K. J. Chang *et al*., 2016).

Oligodendrocytes display two contact areas facing the periaxonal space, at the innermost layer of the internode and at the lateral edges of each myelin layer that form the paranode. Both regions are non-compacted structures that form a cytoplasmic compartment to communicate to the neuron. In the paranode, myelin is firmly attached to the axon by tight junctions. These junctions held together by the adhesion proteins Contactin and Caspr on the axonal surface, and Neurofascin-155 on the glial side (Salzer *et al*., 2008) **(Figure 2).** Besides, there are also autotypic tight junctions between compacted myelin layers of the internode, consisting of Claudin-11. These condensed cytoplasmic membranes attached in the internode by Claudin-11 are visualized by Transmission Electron Microscopy (TEM) as a major dense or electron-dense line (M). While the intraperiod line, or electron-light layer, correspond to closely oppose myelin membranes which are not fused (I) **(Figure 2)**.

Before MBP is expressed on the membrane surface, MBP mRNA is transported within cytoplasmic granules from the *nucleus* to the innermost layers where is translated to protein (Müller *et al*., 2013; Torvund-Jensen *et al*., 2018). The different myelin components are synthesized in oligodendrocytes at several subcellular localizations and are transported to the growing myeling sheath (Wake *et al*., 2011). This suggests the presence of a system of cytoplasmic-rich channels to allow myelin components trafficking and delivering of membrane vesicles to the inner tongue (White & Krämer-Albers, 2014). It is a complex system containing microtubules and vesicular carriers, for what oligodendrocytes modulate actin cytoskeleton dynamics in a site-specific manner. Actin filaments push the inner tongue forward and serve as tracks for the delivery of newly synthesized membrane, while they are depolymerized in the mature compact myelin. The myelin compaction proccess is governed by intracellular MBP-CNP dynamic; MBP promotes actin depolymerisation to facilitate myelin sheath compaction, while the presence of CNPase within the mature sheath ensures the formation of small uncompacted myelinic channels (Snaidero N *et al*., 2017).

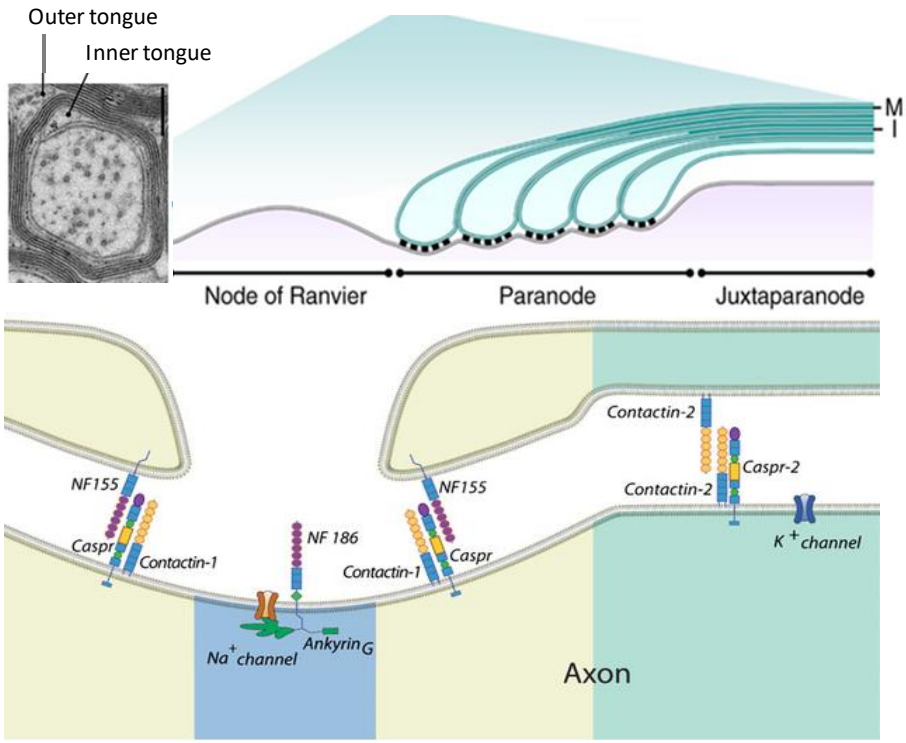

Figure 2. Structure of myelin and molecular domains along myelinated axons. Glial membranes at the ends of the sheaths are attached to the axonal membrane flanking the node, forming paranodes. Paranodal loops contain cytoplasm and are not compacted. Neuron-glia interactions at paranodes form paranodal axoglial junctions with the characteristic electron-dense transverse bands under EM. M indicates the major dense line, I the intraperiod line. Down, the magnification showing the major components of the node, paranode and juxtaparanode. At the juxtaparanode, contactin-2, expressed by both axons and glial cells, is involved in positioning the voltage-gated potassium channels. Adapted from K. J. Chang *et al*., 2016; Derfuss *et al*., 2010.

The cytoplasmic channels are gradually closed as myelin compaction spreads during development. However, many of them remain active in the adult nervous system, in which provide a functional connection of glial metabolites between the oligodrodroglial soma and the periaxonal space. Moreover, they can be re-formed to add more myelin wraps when myelination is promoted, suggesting that myelin is a highly dynamic and plastic structure regulated by both intrinsic and extrinsic cues (Lourenço *et al*., 2016).

1.3 Factors controlling innate myelination

The differentiation of OPCs towards mature oligodendrocytes follows several stages of cell maturation defined by morphological aspects and by the expression of specific-marker proteins (Emery, 2010). First, OPCs migrate away from the *neuroepithelium* of the ventricular/subventricular zone of the brain into the developing white matter where they differentiate into myelinating oligodendrocytes (Waly *et al*., 2014). During development, a greater number of OPCs proliferate in order to porperly match the axons to be myelinated, while a proportion of them are subsequently eliminated by apoptosis (Czopka *et al*., 2013; E. G. Hughes *et al*., 2013; R. H. Miller, 2002). The final number of oligodendrocytes is determined by the amount of target-derived growth and survival factors, such as platelet-derived growth factor (PDGF)-A, fibroblast growth factor (FGF)-2, insulin-like growth factor (IGF)-1, neurotrophin (NT)-3, and ciliary neurotrophic factor (CNTF) (Baumann & Pham-Dinh, 2001).

The speed at which signals propagate in a neural circuit is limited by the thickness of the myelin wrapping, the distance between nodes and the length of the exposed axon in the node; all parameters determined by axon diameter. Oligodendrocytes myelinate CNS axons through an orchestrated and precisely regulated process. Classical view supports that oligodendrocytes perform myelination following an innate program in the absence of exogenous signaling. Indeed, oligodendrocytes are able to wrap, in a coordinated way according to the diameter, electrically silent polystyrene fibres, supporting the hypothesis that myelination is a passive proccess controlled by the physical properties of axons (S. Lee *et al*., 2012; Mei *et al*., 2014). On the oher hand, there are new evidences suggesting that experience could induce dynamic changes in myelination during development and in adult life (Liu *et al*., 2016; Makinodan *et al*., 2012; Mangin *et al*., 2012). It has been hypothesyzed that the extent of myelin sheath formation may serve as a form of plasticity to adapt brain function to environmental *stimuli*.

1.3.1 Intracellular signals

Oligodendrocyte differentiation and myelin membrane synthesis is determined by an intrinsic transcriptional network (Bercury & Macklin, 2015). Oligodendroglial lineage cells express SOX10 and Olig2 over development but, as OPCs undergo terminal differentiation, they lose the expression of specific progenitor markers such as PDGFRα and NG2 and begin to express immature markers such as O4 and galactocerebroside (GalC) (Hornig *et al*., 2013). As OPCs mature, they begin to express the earliest myelin-related proteins as CNP (2', 3'-cyclic nucleotide 3'-phosphodiesterase) and adenomatous poliposis coli (ACP) marker, also known as CC1. Finally, myelinating oligodendrocytes express membrane markers related to feature myelin proteins, such as MBP, PLP, MAG and MOG **(Figure 3)**.

The complex mechanisms that control oligodendrocyte maturation induce changes at genome and molecular scale. The epigenetic regulation includes histone methylation, acetylation, chromatin remodeling, micro-RNAs, and noncoding RNAs. Modifications in the chormatine actively regulate the expression of cell cycle genes. Histone deacetylases (HDACs) form complexes that inhibit the expression of transcriptional repressors of differentiation, while miRNA-219 and miRNA-338 repress the activity of critical transcription factors and signaling pathways of the proliferative state, such as Sox5/6, Hes5, and PDGFRα (Dugas *et al*., 2010).

Once OPCs are polarized to finally differentiate into mature oligodendrocytes, active chromatine enables the transcription of pro-myelinating genes, such as *Myrf, Sox 10* and the transcription factor cyclic-AMP response element-binding protein (CREB), while repressing the expression of myelin inhibitor genes, including *E2f4* and *Yy1* (Bujalka *et al*., 2013; Tawk *et al*., 2011). Myrf is specifically induced during oligodendrocyte differentiation, and its ablation in knockout mice prevents the expression of most myelin genes, driving severe demyelination. CREB mediates the c-AMP-dependent stimulation of MBP synthesis and can be phosphorylated to promote cellular gene expression involving multiple protein kinases. For instance, the PtdIns (3,4,5) P3/Akt/mTor and ERK1/2-dependent signaling pathways are

activated to properly drive forward myelin sheaths synthesis (Ishii *et al*., 2014; Snaidero *et al*., 2014b, 2014a).

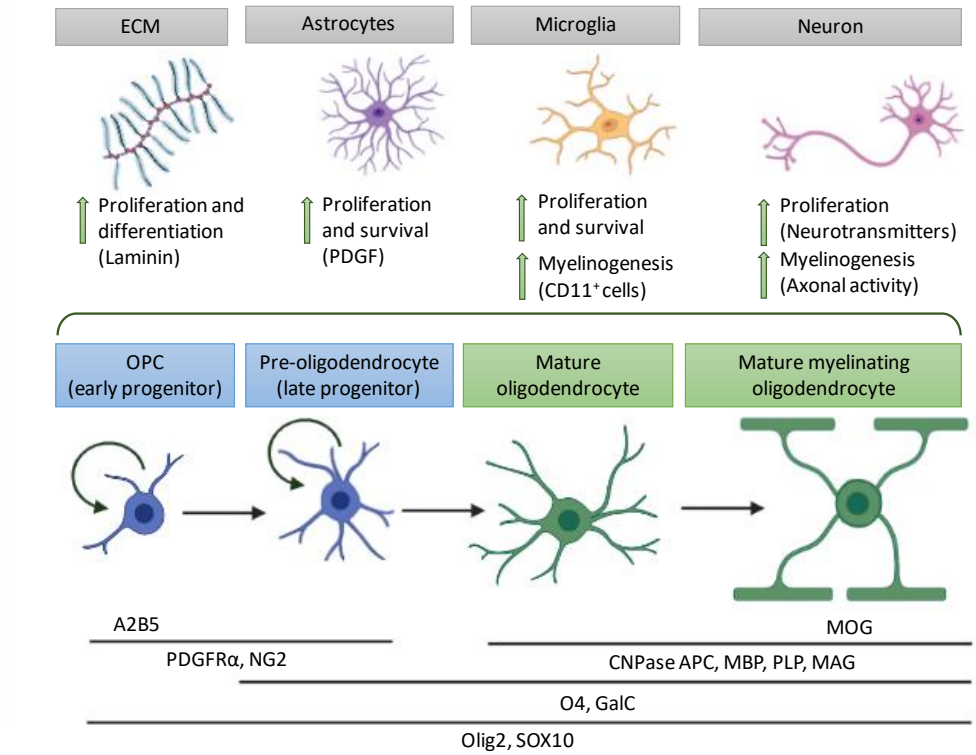

Figure 3. Schematic representation of the developmental stages of the oligodendrocyte lineage with exogenous regulators and intracellular transcriptional factors. Stage-specific markers and extracellular regulators of oligodendrocyte lineage cell progression from immature, migrating precursors to fully differentiated, myelinating oligodendrocytes. (Traiffort *et al*., 2016)

1.3.2 Exogenous factors

The main factor controlling myelinaton during development is the electrical activity of axons. The pioneer work of B. Barres and M. Raff already stablished that OPC proliferation and survival depens on the electrical activity of the axons (Barres & Raff, 1993). Premyelinating oligodendrocytes are transient cells that either differentiate into myelinating oligodendrocytes or undergo cell death processes. The survival of premyelinating oligodendrocytes can be influenced by factors released by active axons such as fibroblast growth factor (FGF), β1-integrin or glutamate (Fletcher *et al*., 2021). More recently, experiments in zebrafish revealed that neuronal activity directs myelination towards the

active axon (Almeida & Lyons, 2017; Hines *et al*., 2015; Mensch *et al*., 2015) and that myelin thickness and internode length is adapted to the requirement of the neuronal network (Ford *et al*., 2015; Seidl *et al*., 2010).

Oligodendrocytes express several neurotransmitter receptors that respond to synaptic inputs from electrically active axons, including GABA receptors, AMPA/kainate and NMDA receptors, adenosine receptors and muscarinic receptors (Fields & Stevens-graham, 2002; Mangin *et al*., 2012; Zonouzi *et al*., 2015). This way, myelination is deeply modulated by neuronal activity. Indeed, Wake *et al*. described that glutamate release from synaptic vesicles promoted myelination by increasing the local synthesis of MBP (Wake *et al*., 2011). Interestingly, the neuronal neuroregulin-1 (NRG1) interacts with the oligodendroglial ErbB2 and ErbB4 (family members of the epidermal growth factor receptors, EGFR) (Piaton *et al*., 2010), and increases oligodendrocytes sensitivity to glutamate by promoting the expression of NMDA receptors (Lundgaard *et al*., 2013). However, OPCs have no association with axonal membranes before starting myelination, suggesting that the NRG1/ErB signaling is not mandatory for innate myelination (A. N. Hughes & Appel, 2019).

Oligodendrocytes interact not only with axons, but also with the extracellular matrix (ECM) and other glial cells **(Figure 3)**. The ECM mediates the integration of growth factors and regulates the cytoskeletal dynamics. The activation of integrin and dystroglycan receptors of oligodendrocytes by ECM laminin contributes to the terminal steps of oligodendrocyte differentiation and myelination by modulating Fyn kinase, and to early stages of myelin formation by regulating small Rho GTPases (Lau *et al*., 2013). Microglia and astrocytes also promote oligodendrocyte survival and proliferation by secretion of growth factors such as PDGF and BDNF and by inducing the expression of transcription factor NF-kB p65 (Hagemeyer *et al*., 2017). A recent study decribes a transient subset of CD11c+ microglia that regulate CNS myelinogenesis via the release of IGF-1, a factor essential for myelination (Wlodarczyk *et al*., 2017).

In contrast to positive, negative signals in the CNS are crucial to control the spatiotemporal development of oligodendrocytes and prevent inappropriate ensheathment of axons. The

inhibitory regulators include the neuronal surface molecules PSA-NCAM (Charles *et al*., 2000) and LINGO1 (leucine-rich repeat and Ig-domain-containing 1) (X. Lee *et al*., 2007), the neurotrophin NGF (Chan *et al*., 2004), the oligodendroglial GPR17 (Y. Chen *et al*., 2009), Notch-1, and the astroglia-derived extracellular matrix molecule hyaluronan (Back *et al*., 2005).

1.4 Myelin plasticity and remodeling in the adult: adaptive myelination

Lately, accumulating evidences suggest that myelination is not restricted to the developmental period; rather, it now appears that myelin turns over and its patterns change throughout the lifespan, which may relate to experience-dependent changes in the function of neural circuits. In the adult brain, different regions display differing degrees of myelination. Indeed, TEM studies demonstrated the presence of unmyelinated and partially myelinated axons even at peak myelination in late adulthood (Tomassy *et al*., 2014). These partial myelination patterns in the adult brain give rise to a novel idea about activity-dependent myelin remodelling and neural network plasticity (E. G. Hughes *et al*., 2018).

In that way, myelin plasticity starts from the oligodendrogenesis process, which implies the generation of new mature and myelinating oligodendrocytes **(Figure 4)**. In the human and mouse cortex, myelinating oligodendrocytes are long-lived. In mice, the density of mature oligodendrocytes ($CC1^+$) in the somatosensory cortex increases throughout adulthood, and new myelin internodes accumulate in the superficial layers until ~2 years of age (Hill *et al*., 2018). In humans, ^{14}C dating studies reveals a high exchange rate of myelin (Yeung *et al*., 2014) and continuous generation of new oligodendrocytes in cerebral cortex (Scholz *et al*., 2010a). However, intracortical myelin content starts to decline after 50 years of age (Fletcher *et al*., 2021), an effect that is also observed after 2 years of age in the mouse somatosensory cortex (Hill *et al*., 2018).

The heterogeneous distribution of myelination in the adult brain allows additional forms of myelin plasticity including addition of new myelin sheaths or *de novo* myelination as well as changes in myelin sheath length and thickness (Wu *et al*., 2012) **(Figure 4)**. Once formed,

individual oligodendrocytes display heterogeneous myelin remodeling, with some internodes retracting, extending or remaining stable. However, the frequency of internode remodelling drastically decreases with age.

The formation of new internodes and remodeling of myelin sheaths also implies changes in the number and length of nodes of Ranvier (Cullen *et al*., 2021). A main feature of myelinated axons is the localization of voltage-gated sodium channels to nodes of Ranvier. It has been proposed that structural changes at nodes of Ranvier have an impact on action potential velocity because of the number and density of Na^+ channels. Therefore, node elongation increases the node capacitance, diminishing the conduction velocity (Arancibia-Cárcamo *et al*., 2017; Battefeld *et al*., 2019; C. Chen *et al*., 2004).

Finally, myelin thickness is also dynamic and is not only regulated by axon diameter. Most myelinated axons tend to have g-ratios (the diameter of the axon divided by the diameter of the axon and its myelin) close to the optimal value for conduction and nervous system efficiency; that means a *g*-ratio index around 0.6 (Chomiak & Hu, 2009). Recent studies demonstrate that optogenetic and pharmacogenetic stimulation of neurons increases myelin thickness. Moreover, specific up-regulation of ERK1/2 signaling in mature oligodendrocytes significantly increased myelin thickness in *corpus callosum* and spinal cord (Furusho *et al*., 2017; Jeffries *et al*., 2016). Nevertheless, whether the increase in myelin thickness is produced by recently differentiated OPCs or by pre-existing myelinating oligodendrocytes remains unclear.

Taken together, these data demonstrate that myelin plasticity is modulated locally and has multiple checkpoints, from the axon selection to internode extension and maturation. The local regulation cues include the axon diameter, cell-surface and/or secreted axonal molecules. Larger diameter axons tend to present higher myelination rates. However, the correlation between axonal diameter and propensity for myelination do not explain how a same caliber axon display unmyelinated regions, target for new internode formation. Additionally, several studies propose that oligodendrocytes subpopulations show different

myelination profiles over excitatory and inhibitory neurons due to the activity-dependent vesicular release (de Faria *et al*., 2021).

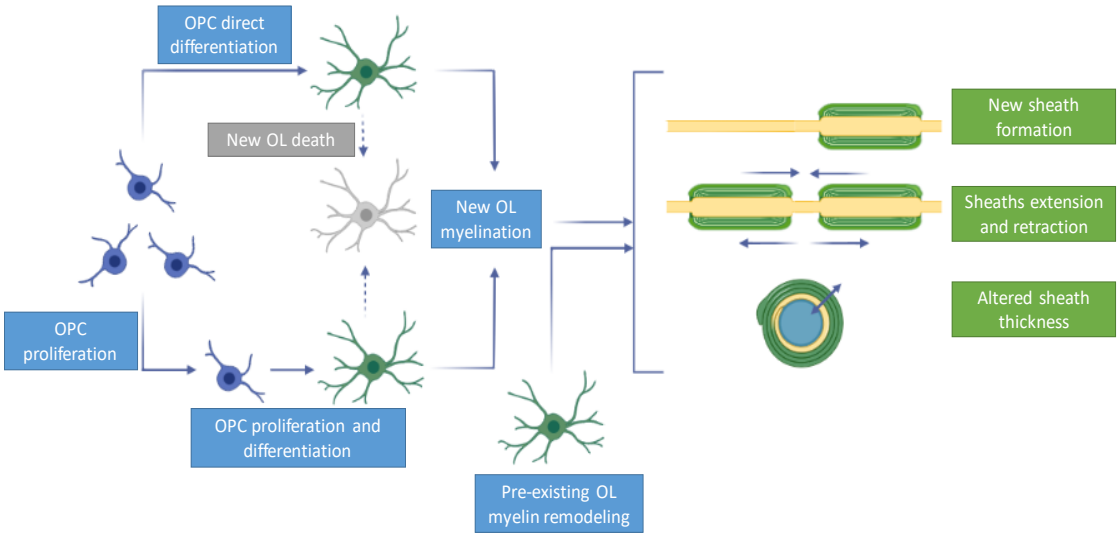

Figure 4. Forms of plasticity within the oligodendrocyte lineage. Oligodendrocyte precursor cells (OPCs) proliferate and a subset of these newly formed OPCs differentiate into new oligodendrocytes. Other existing OPCs directly differentiate into new oligodendrocytes. A subset of these new oligodendrocytes undergo cell death, whereas others stably integrate into the circuit and form new sheaths on previously unmyelinated axon segments. Existing oligodendrocytes can also undergoes plasticity in the form of altered sheath length and thickness, positioning of the myelin sheath, and changes in the length of individual nodes of Ranvier. Adapted from (Xin & Chan, 2020).

1.5 Functions of oligodendrocytes and myelin

Neurons rely on their myelinating partners not only for setting conduction velocity, but also for regulating the ionic environment and supporting their metabolic demands with energy-rich substrates. Oligodendrocytes also maintain long-term axonal integrity and neuronal survival, and the loss of this well-coordinated axon–glial interplay contributes to neurodegenerative and neuropsychiatric disorders (Stadelmann *et al*., 2019).

1.5.1 Conduction velocity and sculp neuronal circuits

The main role of mature oligodendrocytes is the formation of a myelin sheath around CNS axons which provides electrical insulation, decreasing the capacitance and increasing the resistance of the axonal membrane. A hallmark of myelinated fibers is saltatory nerve conduction, which enables faster and more efficient propagation of signals as compared with unmyelinated axons of the same diameter. Indeed, myelin sheaths increase nerve conduction velocity 20-to 100 time fold in comparison with non-myelinated axons (Hartline & Colman, 2007). To allow saltatory conduction, the paranodal junction separates voltage-gated sodium and potassium channels. This spatial segregation confined potassium channels to the juxtaparanodal and intermodal membrane to avoid the exposure to high potassium levels in the nodes, which can lead to inactivation of sodium channels and subsequent blocking conduction (Rash, 2010).

Myelination is a highly dynamic process, crucial for synchronizing complex neuronal networks. Circuit flexibility by myelin plasticity enhances motor skills and cognitive functions. Late studies demonstrate that social isolation leads to thinner and fewer myelin sheaths, an outcome that can be restored with social re-integration (Steadman *et al*., 2020). Besides, learning a new motor skill on a 'complex' running wheel promotes oligodendrogenesis and myelination (McKenzie *et al*., 2014). In healthy adults, at a functional and macroscopic level, piano playing, juggling, visuomotor training and learning language and mathematics have all been associated with increased white-matter volume in specific regions of the brain as measured by MRI (Bengtsson *et al*., 2005; Jolles *et al*., 2016; Lao *et al*., 2015; Scholz *et al*., 2010b). These recent fidings suggest that neuronal activity regulates *de novo* and adaptive myelination driven by experience and sensory imputs during learning and memory consolidation (Bechler *et al*., 2018).

1.5.2 Metabolic coupling

Apart from this well established function of myelination, oligodendrocytes are crucial for providing trophic and metabolic support to axons. During development, oligodendrocytes uptake glucose from bloodstream and N-acetyl-aspartate (NAA) from axons to provide

acetyl-CoA for myelin lipids synthesis. However, once the myelin sheath is formed, oligodendrocytes undergo a "metabolic switch" that reverses this metabolic cooperation between oligodendrocytes and axons (Krasnow & Attwell, 2016). Myelinated axons are isolated by the myelin from glucose in the extracellular space, and energy-rich substrates enter the axon exclusively at the nodes of Ranvier. Nodally sourced energy may support basal activity of axons with short internodes, but diffusion of energy substrates from the node to the internode could take minutes for larger-calibre axons (Harris & Attwell, 2012). Besides, glial cells can rapidly deliver metabolites directly to the internode in response to transient increases in demand of active myelinated fiber tracts (Kasischke *et al*., 2004; Pellerin & Magistretti, 1994). Similar to astrocytes, oligodendrocytes metabolize glucose to lactate or pyruvate through glycolysis, and transfer energy metabolites to neurons through cytoplasmic myelinic channels and monocarboxylate transporters (MCT1, MCT2) (Fünfschilling *et al*., 2012; Y. Lee *et al*., 2012b; Saab *et al*., 2013) **(Figure 5)**. This model of "oligodendrocyte-axon lactate shuttle" allows fast delivery of metabolites that contributes to ATP synthesis in neurons, fueling their energetic demands (Trevisiol *et al*., 2017).

1.5.3 Axonal survival

Notheworthy, oligodendrocytes also contribute by preserving long-term neuron connectivity and integrity (Saab *et al*., 2013). The axon degeneration phenotype of mice with myelin deficient in PLP or CNP, but not MBP, led to the discovery that oligodendrocytes support axonal integrity and survival independent of the physiological function of myelin (Griffiths *et al*., 2016; Lappe-Siefke *et al*., 2003). In white matter, the transfer of lactate or pyruvate from glycolytic oligodendrocytes via monocarboxylate transporter MCT1 and MCT2 to the neuronal compartment appears to be critical for axonal integrity (Y. Lee *et al*., 2012a; Rinholm *et al*., 2011). Measuring the activity-dependent synthesis of axonal ATP revealed that the pharmacological inhibition of lactate transporters provokes lower ATP level, with subsequent increase in axonal death (Trevisiol *et al*., 2017). Therefore, release of lactate to neuronal compartment by both astrocytes and oligodendrocytes, connected through gap junctions, is crucial for axons homeostasis and long-term survival.

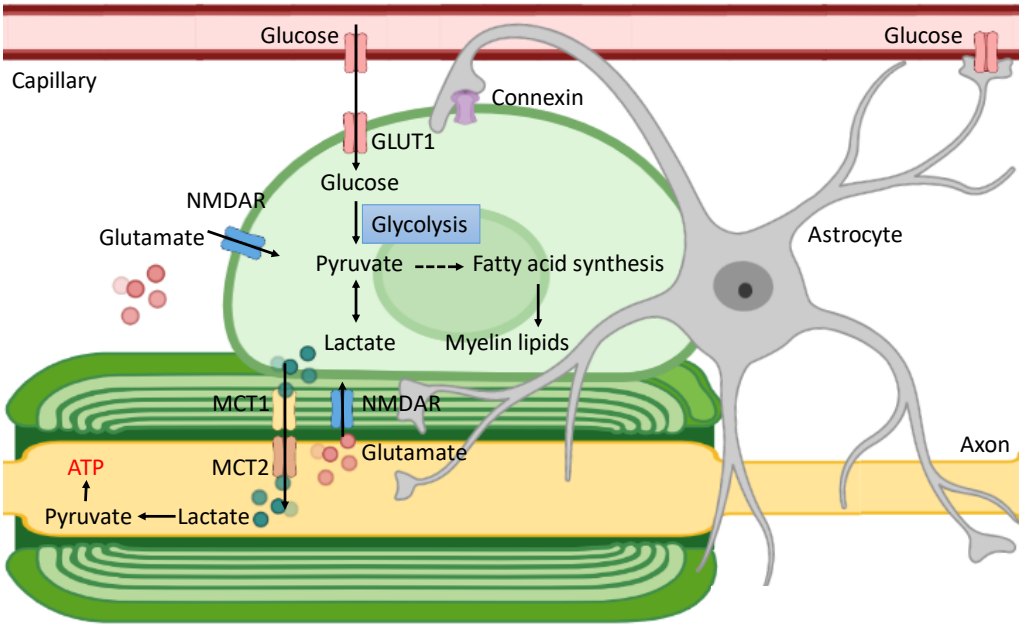

Figure 5. Hypothetical model of metabolic coupling between oligodendrocytes and myelinated axons. Oligodendrocytes import glucose through GLUT1 (and possibly via astrocytes and gap junctions; CX, connexin) for glycolysis. With the onset of myelination ('developmental switch'), glucose also serves the synthesis of fatty acid (FAS) and myelin lipids from acetyl-CoA. In postmyelination oligodendrocytes, glycolysis can produce sufficient ATP to support oligodendrocyte survival. Lactate can be directly transferred via monocarboxylic acid transporters (MCT1, MCT2), which reside in internodal myelin and the axonal compartment. Oligodendrocyte-axon lactate shuttle is driven by neuronal activity. Axonal released glutamate binds to oligodendrocyte-NMDARs leading to and increase in glucose uptake and its conversion into lactate. Note that myelinated axons, are separated by a thin periaxonal space from the oligodendroglial cytoplasm filling the inner loops of myelin ('cytosolic channel') and paranodal loops. Modified from Fünfschilling *et al*., 2012.

1.4 Neurotransmitter receptors in oligodendrocytes

The oligodendrocyte lineage expresses and responds to a broad range of receptor-ligand pairs (i.e., neurotransmitters and nuclear receptor) that can influence oligodendrocyte migration, proliferation, differentiation, and myelination, indicating their therapeutic potential. Many of these promising mediators, including acetylcholine (ACh) and glutamate (Glu), work through Ca^{2+} signaling, and the balance between Ca^{2+} influx and efflux can determine the temporal and spatial properties of oligodendrocytes (Marinelli *et al*., 2016).

1.6.1 Muscarinic receptors in oligodendrocytes

In the nervous system, muscarinic receptors (or mAChRs) are expressed by neurons and glial cells, and recognize acetilcholine (ACh). ACh was the first molecule identified as neurotransmitter and modulates basic cell functions including growth, survival, differentiation, and apoptosis. During neurogenesis, mAChRs activation promotes neuron proliferation, survival and differentiation. However, the specific mAChRs subtypes involved in OPCs proliferation and differentiation are not well characterized. Although OPCs exhibit all muscarinic receptors subtypes, M3, M1 and M4 are the most abundantly expressed (de Angelis *et al*., 2012). The expression of these receptors decreases with oligodendrocytes differentiation indicating that their activation is mainly required in early stages of oligodendrocyte development. Moreover, muscarinic receptors have different cellular locations, being the M3 and M1 in progenitor cell bodies and processes while the M4 is only localized in cell bodies (Fields *et al*., 2017).

Muscarinic receptors M3, M1 and M4 contribute to OPCs proliferation by modulating the expression of myelin proteins and oligodendrocytes receptors. According to this, mAChRs activation by muscarine agonist reduces MBP expression at both transcript and protein levels, while enhances the expression of PDGFRα receptor involved in OPC proliferation. M4 and M1/3 receptors are coupled to G_i and G_q proteins respectively; and their activation trigger different signaling pathways involving mitogen-activated protein kinase (MAPK), inositol triphosphate (IP3), and calcium mobilization (Ross Welliver *et al*., 2018). Despite that M2 receptors present low expression, M2 activation by its selective agonist reduces OPC survival, suggesting that they may impair terminal differentiation and myelination.

In the adult CNS, inhibition of muscarinic signaling promotes OPC and oligodendrocyte differentiation, leading to improved remyelination and myelin repair. Because of that, several muscarinic agonists and antagonists are currently under study (Eglen *et al*., 2001). Among these molecules, clemastine has arisen as the most promising pro-myelination drug. Clemastine is an antimuscarinic and anitihistaminic compound that efficiently crosses the blood-brain barrier with very few side effects and that promote OPC differentiation *in vitro*

and remyelination after demyelinating lesions (Liu *et al*., 2016; Mei *et al*., 2016; Wang *et al*., 2018). The efficacy of clemastine to promote remyelination has been proved after chemical demyelination, hypoxia, aging and Alzheimer's disease (Deshmukh *et al*., 2013; Z. Li *et al*., 2015; Mei *et al*., 2014). Recent studies described that the effect of clemastine on myelination is mediated through M1/M3 receptors. However, the mechanisms underlying its effect needs further characterization.

1.6.2 NMDA receptors in oligodendrocytes

The N-methyl-D-aspartate receptor (NMDAR) is one of the three glutamate ionotropic receptor, together with AMPA and kainate receptors. Originally, glutamate has been believed to mediate oligodendrocytes damage by acting only on calcium-permeable AMPA/ kainate receptors, but three separate studies (Káradóttir *et al*., 2005; Micu *et al*., 2006; Salter & Fern, 2005) demonstrated that NMDA receptors are present also in OPCs and myelinating processes of oligodendrocytes from cerebellum and *corpus callosum*.

NMDA receptors are ligand-gated cation channels, the interaction with its ligands (glutamate and glycine) allows positively charged ions to flow through the cell membrane, playing crucial roles in synaptic transmission and plasticity. Conventional structural conformation of NMDAR are heteromers of NR1 subunits, which bind to glycine, and NR2 (A, B, C, or D) subunits that bind glutamate (Burzomato *et al*., 2010). However, Juan C.Piña *et al* described the existence of native NR3-containing NMDARs (Piña-Crespo *et al*., 2010). NR1 and NR2/NR3 subunits combine to form receptor subtypes with distinct pharmacological properties, localisation, and ability to interact with intracellular messengers. Analysis of the pharmacological properties of NR1/NR3A/NR3B receptors demonstrated activation by glycine alone in the absence of glutamate (or NMDA) and insensitivity to the NR2 glutamate binding-site antagonist D-APV.

During development, OPCs form synapse-like structures with glutamatergic and GABAergic axons (Bergles & Jahr, 2000). According to this model, the 'postsynaptic' OPC compartment progressively transform into a growing oligodendroglial process as axonal glutamate release

promotes local MBP translation distally at ensheathment sites (Wake *et al*., 2011). In that way, the axon-OPC synapse turns into an axon-myelin synapse (AMS) for continued axon-mature oligodendrocyte communication in the myelinated nervous system (Micu *et al*., 2018) **(Figure 5)**. These axon-myelin synapses occur along the length of the internodes where axonal action potentials induce vesicular release of glutamate from the internodal axon into the periaxonal space. Activation of myelinic glutamate receptors (AMPA and NMDA) on the inner tongue of the myelin sheath, results in a Ca^{2+} increase within the thin cytosolic space of the myelin sheath, while does not elevate Ca^{2+} in the oligodendrocyte soma (Burzomato *et al*., 2010; Micu *et al*., 2018; Nave, 2010).

The molecular machinery responsible for vesicular fusion and neurotransmitter release requires Ca^{2+}, however internodal axons have restricted access to extracellular Ca^{2}+ leading to a necessity of intracellular source of Ca^{2+} ions. The expression of voltage-gated Ca^{2+} channels and AMPARs on the internodal axolemma permeate small amounts of Ca^{2+} ions in response to local depolarization. Other characteristic feature of AMS structure is that such NMDA receptors exhibit a weaker Mg^{2+} blockage. In contrast to synaptic endings where volumes are larger, only small amounts of ions change the local concentration within the periaxonal space. The relatively low Ca^{2+} permeability of NMDA receptors formed by NR1/NR3 subunits, coupled with their relative resistance to Mg^{2+} blockade at negative membrane potentials make NR1/NR3 receptors suited as mediators of physiological Ca^{2+} fluctuations in the axon-myelin synapses (Burzomato *et al*., 2010; Piña-Crespo *et al*., 2010).

The existence of different receptor subunits with distinct pharmacological properties suggests changing functionality of NMDAR. First characterization of NMDA receptors in oligodendrocytes by Káradóttir *et al* in 2005 describes that, in condition of oxygen and glucose deprivation, the activation of NMDA receptors (likely formed by NR1/NR2 heteromers) induce a Ca^{2+} influx to the myelin sheath with subsequent myelin damage and oligodendrocytes processes injury. During ischemia, the massive entry of extracellular calcium triggers a depolarization of the mitochondrial membrane and a production of

reactive oxygen species that culminate with the initiation of death cascades (Weilinger *et al*., 2016), which is reversed by blocking NMDAR.

However, once AMS structure is formed in mature oligodendrocytes, one important function is to couple electrical activity to the metabolic output from the oligodendrocyte. The release of glutamate in an activity-dependent manner activates glutamate receptors expressed on the AMS, allowing myelinating oligodendrocytes to detect and respond to axonal spiking activity. The increase of myelinic Ca^{2+} in response to active axons triggers lactate release from the oligodendrocyte, which is a metabolic fuel that support axonal energy. Moreover, activity-dependet activation of NMDA receptors increases the glucose transporter GLUT1 trafficking to the surface membrane, in order to adjust the glucose uptake capacity, and thus, to support the metabolic demand of ensheathing oligodendrocytes (Saab *et al*., 2016). Finally, Ca^{2+} fluctuations within the myelin sheath could affect to Ca^{2+}-sensitive targets, such as Ca^{2+}-sensing proteins (for example, calmodulin), phospholipases, proteases (for example, calpains) and protein arginine deiminases. These findings propose the NMDA receptors as novel therapeutic target for a wide range of diseases, including cerebral palsy, spinal cord injury, multiple sclerosis and stroke.

2. MYELIN PATHOLOGY

Given the major role of myelin in central and peripheral nervous system physiology, myelination defects outcome significant neurological manifestations. Myelin diseases comprise a heterogeneous group of hereditary and acquired pathologies present during adult life and early development. In genetic disorders, there is a primary failure in myelination that leads to hypomyelination and dysmyelination at a variable time after birth. In acquired disorders, myelin loss can occur as a result of direct or indirect damage to myelin sheaths during inflammation or immune attack, after acute insults or following neurodegeneration. Among the inflammatory demyelinating diseases, multiple sclerosis has high prevalence and not completely understood etiology. Myelin deficits have also been

associated to neurodevelopmental psyquiatric diseases and to autoimmune encephalitis, in which autoantibodies targeting myelin have been found (Duncan & Radcliff, 2020).

2.1 Neurodevelopmental diseases

Childhood neurodevelopmental diseases, including autism spectrum disorder (ASD), attention deficit hyper-activity disorder (ADHD), intellectual disability (ID) as well as some psychiatric disorders like schizophrenia, share cellular and histological alterations. Myelination abnormalities have been observed in schizophrenia, ASD, and ADHD (Galvez-Contreras *et al*., 2020; Graciarena *et al*., 2019; Onnink *et al*., 2015; Takahashi *et al*., 2011). The same is true for microglial dysfunction (Koyama & Ikegaya, 2015; Sellgren *et al*., 2019). Backed by genetic studies, these diseases share genetic risk alleles such as the contactin associated protein-like2 gene (*Cntnap2*) (Gdalyahu *et al*., 2015; Rodenas-Cuadrado *et al*., 2014). This leads to a new concept of a "neurodevelopmental continuum", in which complex neurodevelopmental diseases showing phenotypic overlap are included (Morris-Rosendahl & Crocq, 2020).

Disruption of neurogenesis and synaptic pruning, which occurs during the intrauterine period and later after birth, has been hypothesized to affect several childhood disorders (Givre, 2003). These reductive processes occur in concert with a precisely regulated growth process of myelination. Thus, regressive or pruning processes during childhood provide the volume (space) and possibly other resources necessary to support the crucial process of myelination (Bartzokis *et al*., 2001, 2004). The increase in conduction velocity and reduced energy consumption provided by myelination functionally compensates the regressive processes. The synaptic pruning, instead of reducing connectivity between different parts of the brain, allows myelination to increase functional connectivity of the remaining circuits (Bartzokis, 2004). Alterations in myelination, and thus, functional connectivity, affect processing speed, decision making, inhibitory controls and language, characteristics of psychiatric disorders.

Despite ASD has been considered as a brain connectivity disorder, emerging evidence suggests that oligodendroglial cells play a role in the etiology of ASD. Patients with ASD show

an aberrant growth pattern in several white-matter regions that varies throughout life. While some regions increase in their myelin volumen, other remain hypomyelinated. This myelin impairment is related to abnormal genetic expression of several transcriptional and growth factors including Olig1, Olig2, Sox10, PGFRA, Nkx2-2, Gpr17, IGF-1, and EGF. Given the heterogeneous etiology and pathophysiology of neurodevelopmental disorder that undergoes myelin impairment, understanding the molecular mediators involved in abnormal myelination patterns may represent an initial step to design therapeutic targets that help to improve social skills and disruptive behaviors observed in these patients.

2.2 Multiple sclerosis

Multiple sclerosis (MS) is a chronic inflammatory disease of the CNS characterized by widespread areas of focal demyelination. MS is the most prevalent neurological disease in young adults, afecting to 2.3 million people worldwide (Browne P *et al*., 2014). The estimated incidence of MS is about two-three times higher in females and increases with northern latitudes (Alonso & Hernán, 2008; Giovannoni *et al*., 2016), suggesting that MS is a heterogeneous disease asociated with multiple genetic and enrionmental risk factors (Huynh & Casaccia, 2013). Several genome-wide association studies demonstrate that the MS susceptibility is strongly related to the HLA *locus*, and to polymorphisms in genes regulating both innate and adaptive immunity. On the other hand, infection with Epstein Barr virus, low vitamin D levels or obesity have also been related to an increase in the susceptibility.

The principal feature of the disease are focal demyelinated lesions within the CNS, mainly due to an inflammatory reaction to myelin components. The migration of autoreactive lymphocytes across the blood-brain barrier leads to oligodendrocyte death and demyelination, glial activation and chronic neurodegeneration (Dendrou *et al*., 2015; Mahad *et al*., 2015; Polman *et al*., 2011). Nevertheless, the etiology of MS remains unclear and alternative etiopathogenic mechanisms have arisen during last decades. Latest studies suggest that primary death of oligodendrocytes and early axonal impairments contribute to MS initiation and progression. Demyelination results in slower conduction or complete failure of impulse transmission, leading to neuronal dysfunction and neurological symptoms.

The most common symptoms of MS include sensory and visual disturbances, spasticity, weakness, painful spasms, bladder dysfunction, tremor, ataxia, optic neuritis, fatigue, and dysphagia (Compston & Coles, 2008).

2.2.1 Multiple sclerosis phenotypic classification

The disease course and symptomatology of multiple sclerosis are heterogeneous, and need to be categorized by general patterns of disease manifestation. MS was firstly classified in four disease subtypes, based on the clinical course of the disease (Lublin & Reingold, 1996). However, new diagnosis criteria and new technologies, such as magnetic resonance imaging (MRI), re-defined the initial subtypes (Lublin *et al*., 2014; Thompson *et al*., 2018) **(Figure 6)**.

- Clinically isolated syndrome (CIS). This is the first clinical event of inflammatory demyelination and it is related with patients that present only a single relapsing episode. Even so, when CIS is accompanied by magnetic resonance imaging (MRI)-detected brain lesions, patients have 60-80% possibility to develop MS (D. Miller *et al*., 2005).
- Relapsing-remitting MS (RRMS). It is the most common form of MS, affecting aproximately 80% - 90% of patients. It is characterized by unpredictable acute exacerbations followed by complete or incomplete recovery. During relapses, MS pacients report symptoms of an acute inflammatory demyelinating event in the CNS, with duration of at least 24 hours and in absence of fever or infection (Polman *et al*., 2011). Relapses correspond with focal CNS inflammation and demyelination, as described by MRI.
- Secondary Progressive MS (SPMS). An initial relapsing course (RRMS) gradually progresses with irreversible neurological decline, while inflammatory lesions are no longer characteristic (Sand, 2015). Approximately, an 80% of RRMS patiens will evolve to SPMS, and a 40% of them within 20 years of the initial event. This phase is characterized by CNS atrophy and increased axonal loss.
- Primary Progressive MS (PPMS). Patients with primary-progressive MS (PPMS) experience a progressive decline in neurological functions from the onset and an absence of relapses (Figure 3). This form represents about 10% of MS cases (Koch *et al*., 2009), usually

patients tend to have a later age onset and the prognosis is worse compared to RRMS patients.

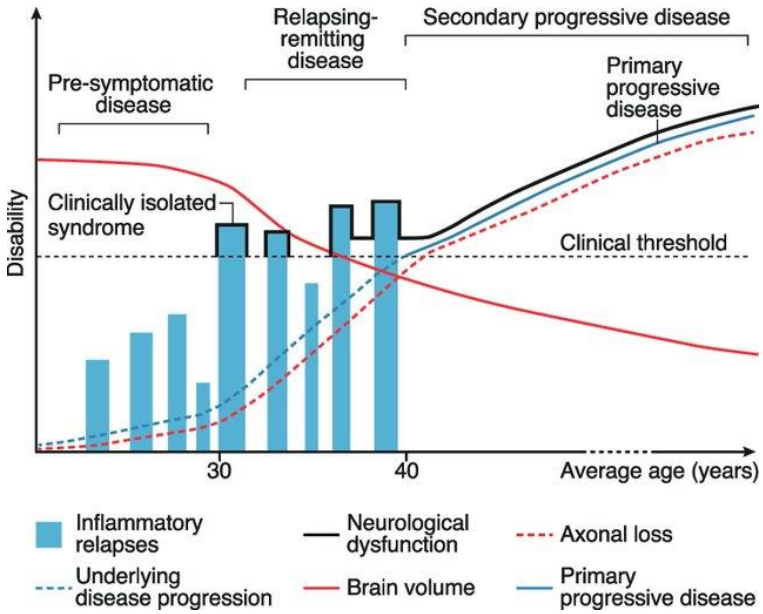

Figure 6. Diagram representing the clinical course of MS showing the progression of disability. The disease course and symptomatology of multiple sclerosis are heterogeneous, leading to categorize several disease subtypes according to general patterns of disease presentation. (Dendrou *et al*., 2015)

2.2.2 Etiology of multiple sclerosis

Multiple sclerosis initiation and progression are driven by complex pathogenic mechanisms that result in tissue injury within the CNS. Whether these pathogenic mechanisms trigger in the periphery ("outside-in" theory) or in the CNS ("inside-out" theory) is a remaining question (Matute & Pérez-Cerdá, 2005; Tsunoda & Fujinami, 2002) **(Figure 7)**.

The inflammatory process involves the activation and recruitment of T cells, macrophages and microglia to the lesions. In the "outside-in" model, autoreactive T cells cross the blood brain barrier (BBB) together with activated B cells and innate immune cells. Once in the CNS, activated T cells damage myelin directly by releasing toxins or indirectly by inducing release of toxins from activated macrophages and microglia. Autoreactive T cells recruit other cell

types from the periphery as macrophages, activated B cells, monocytes, dendritic cells and natural killes T cells, driving myelin loss, OL degeneration and axonal injury.

According to this theory, one of the most used animal model to study MS pathophysiology is the Experimental Autoimmune Encephalomyelitis (EAE). To induce the EAE, a variety of animal species (including mice, rats and non-human primates) are immunized with self-antigens derived from myelin proteins to generate autoreactive inflammatory CD4+ T helper 1 (Th1) cells and Th17 cells. These activated T cells infiltrate into the CNS where activate resident macroglia and astrocytes, and recruit macrophages and monocytes from circulating blood (Tompkins *et al*., 2002). Additionally, Freund's adjuvant and pertussis toxin are often administered to exacerbate the peripheral immune response. The peak of demyelination is reached between 10-15 days after injection and is primarily confined to the spinal cord, whereas in MS inflammatory lesions are mostly found in the brain (Dendrou *et al*., 2015). EAE animals develop a progressive paralysis that starts from the tail and continues to the himb limbs and ultimately the front limbs (Palumbo & Pellegrini, 2017). The clinical course varies with the immunopeptide and the animal strain used. While immunization with MOG peptied in C57BL/6 mice causes a chronic progressive disease, EAE induced with PLP peptide in SJL/J mice follows a relapsing-remitting course (Slavin *et al*., 1998).

The "inside-out" theory suggest that the axonal damage and oligodendrocyte death are the primary events that induce a secondary inflammation. Indeed, neurodegeneration might occur early in the disease course and not only secondary to myelin loss (Seehusen & Baumgartner, 2010). The most important evidence supporting this model is the histopathological finding of oligodendroglial apoptosis in the absence of immune cell infiltration at early stages of the disease described by Barnett and Prineas in patients who died during or shortly after the onset of a fatal relapse (Barnett & Prineas, 2004) .

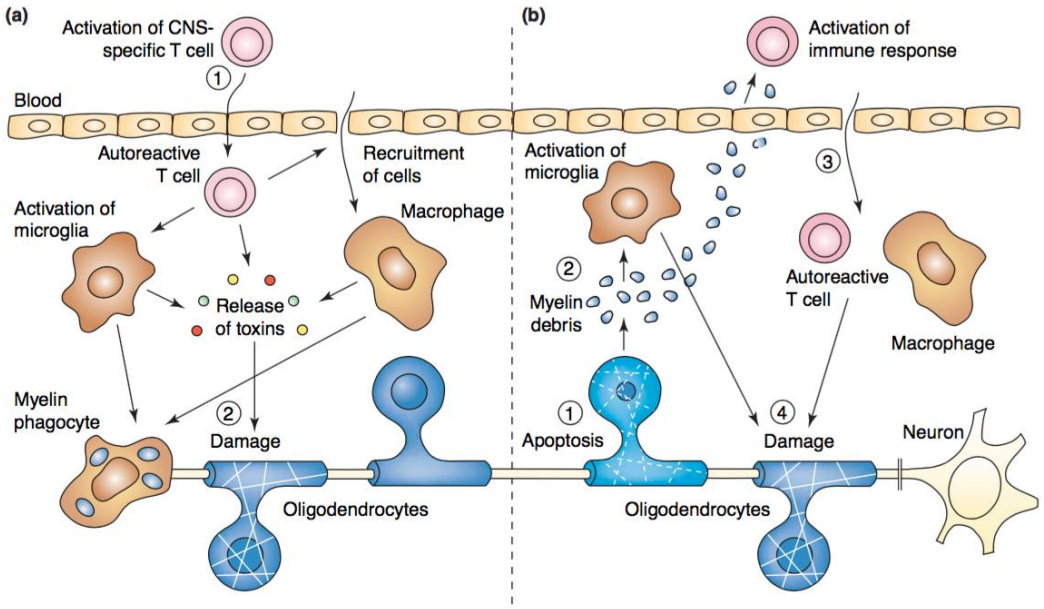

Figure 7. Alternative theories of lesion formation in MS. A) "Outside-in" theory: activated T cells enter the CNS (1) become utoreactive and destroy myelin directly by releasing toxins and cytokines or indirectly by inducing activation of microglia and recruiting macrophages from the periphery. This leads to myelin destruction, OL death and clearance of damage tissue by phagocytes (2). B) "Inside-out" theory: several factors can induce OL apoptosis (1) and large amounts of myelin debris are generated (2) exceeding the capacity of the phagocytic cells to clear them and triggering inflammation. Consequently, T cells and macrophages invade the CNS (3) and initiate the autoinmune attack of myelin (4). Adapted from (Matute & Pérez-Cerdá, 2005).

A viral infection, glutamate and other agents can cause extensive oligodendrocyte apoptosis or primary axonal degeneration in tissue foci and as a result, myelin debris and highly antigenic constituents are generated, promoting autoreactive lymphocytes infiltration in the CNS as a secondary event. Oligodendrocyte apoptosis can also be caused by increased extracellular levels of glutamate that cause oxidative stress and excitotoxicity in oligodendrocytes and this response has been associated with MS (Matute *et al*., 2001). For instance, glutamate concentration in cerebrospinal fluid is higher in acute compared with silent MS patients and controls subjects, demonstrating that glutamate-mediated excitotoxicity is a key etiopathogenic mechanisms of neurodegeneration and demyelination in MS (Stover *et al*., 1997). These observations contrast with the commonly held view that inflammation is a primary event in MS and suggest that, at least in a subset of MS,

autoimmunity might well be a secondary amplifying response to massive oligodendrocyte apoptosis. Alternatively, both models could act simultanously initiating a cascade of events and contributing to the pathogenesis of the disease.

2.2.3. Pathophysiology of multiple sclerosis

The pathological hallmark of MS is the accumulation of focal areas of demyelination and OL death in the white and grey matter of the brain, known as plaques or lesions. As the disease progresses, diffuse myelin decrease and axonal injury become evident, resulting in a more pronounced atrophy of the grey and white matter. These demyelinated areas can be partially repaired by remyelination, called "shadow plaques" (A. Chang *et al*., 2012) **(Figure 8)**. Inflammation and immune activation can be found at all stages of the diease, but it is more characteristic of the acute phase.

Immune dysregulation leads to altered 'crosstalk' between the innate and adaptive immune systems, mediating CNS damage in MS (Grigoriadis & van Pesch, 2015). Firstly, dendritic cells migrate across de blood brain barrier and secrete a variety of cytokines inducing T cell differentiation and activation. These activated Th1 and Th17 cells increase the BBB permeability by producing matrix metalloproteinases and radical oxygen species, promote the recruitment of monocytes from the bone marrow and produce cytokines that induce macrophage, microglial and astrocyte activation. Pro-inflammatory mediators, oxygen and nitric oxide radicals relased by activated cells drive myelin breakdown and axonal degeneration (Strachan-Whaley *et al*., 2014). Besides that, CD8+ T cells release pro-inflammatory mediators such as IL-17 and lymphotoxin, associated to axonal damage (Bitsch *et al*., 2000). Other cell types such as natural killer cells and B cells are also implicated in the immunopathogenesis of MS by producing cytokines and antibody/auto-antibody respectively. In contrast, there are evidence that microglia/macrophage activation counteracts pathological processes by providing neurotrophic and immunosuppressive factors and by promoting oligodendrocyte differentiation and recovery (Kotter *et al*., 2006; Lampron *et al*., 2015; Miron & Franklin, 2014).

Remyelination is an endogenous repair mechanism of the central nervous system (CNS) that restores lost myelin sheaths. This regenerative process can lead to complete remyelination of large and disseminated areas of demyelination in the CNS, with resultant functional recovery. However, at the chronic phase these repairing mechanisms are not as efficient as in the initial phases of the disease. A fail in the repairing mechanisms and an exhaustion of the neurological reserve determines the transition from RRMS to SPMS (Dendrou *et al*., 2015).

The origin of remyelinating oligodendrocytes in MS and in experimental models of demyelination has been the subject of considerable interest. Some evidence suggests that remyelinating oligodendrocytes arise from OPCs that reside either in or adjacent to demyelinated lesions (Münzel & Williams, 2013). OPCs migrate to the edge of the lession by secreted molecules from microglia, macrophages and astrocytes. Once OPCs are recruited into MS lesions and differentiate into myelinating oligodendrocytes (Franklin & Ffrench-Constant, 2017), mature oligodendrocytes give rise to shorter and thinner myelin sheaths than the original ones (g-ratio over 0.75) **(Figure 8)**.

Experimental proof that OPCs generate remyelinating oligodendrocytes comes from many transplant studies in de- and dysmyelinating models, as well as from toxin-induced demyelinating disorders. However, fate-mapping experiments published in *Nature* reveal an unexpected heterogeneity of oligodendrocytes throughout the MS-affected brain and raise questions about the role of adult oligodedrocytes in permanent lesion repair. *In vivo* studies shown that mature oligodendrocytes are able to reextend and recover their processes following damage. Sorted mature oligodendrocyte that were tansplantated into demyelinated areas were capable of myelinating axons *in vivo*. Similarly, mature oligodendrocytes at the edge of demyelinated lesions in the spinal cord, that overexpressed ERK1/2, extended processes into the lesions and remyelinated axons (Jeffries *et al*., 2016; Lin *et al*., 2013).

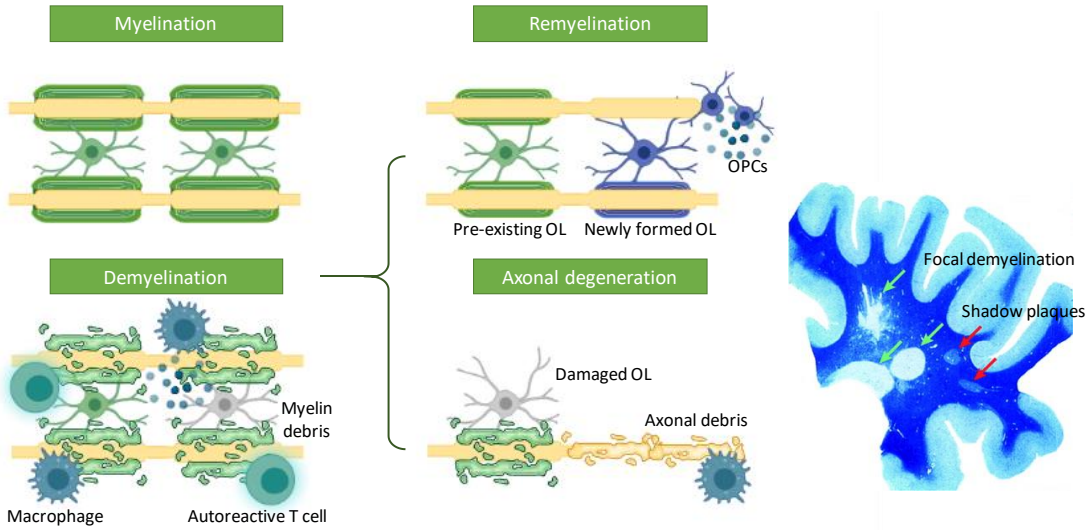

Figure 8. Mechanism of promoting remyelination. Following demyelination, which in the autoimmune disease multiple sclerosis is consequent to the pathological activation of T cells and macrophages, the myelin sheath is lost, but the underlying axon remains intact. This enables the naturally occurring regenerative response of remyelination to generate new sheaths from pre-existing mature oligodendrocytes, or newly formed oligodendrocytes by recruited OPCs. In the absence of remyelination, energy-efficient conduction cannot be restored, and the supportive role of the myelin is lost. This leads to energy deficiency, perturbed axonal transport and ultimately axonal degeneration. This degeneration can trigger a secondary inflammatory response, as illustrated by the presence of activated macrophages around the degenerating axon. (Right) Section from the brain of an MS patient stained with Luxol fast blue to identify subcortical white matter (WM). Green arrows indicate three areas of myelin loss which represent foci of chronic demyelination. Red arrows indicate areas of pale myelin staining which represent the shadow plaques where remyelination has occurred. Adapted from (Chari, 2007; Franklin & Ffrench-Constant, 2017).

Although remyelination is a consistent finding in MS, it is also well established that this process becomes inefficient, leading to mytocondrial disfunction and energy deficient, impaired axonal transport, and axonal degeneration. Consequently, neurological disability increases during disease progression (Sim *et al*., 2002). Several studies suggest that this failure in the repair process occurs due to an inhibition of oligodendrocyte myelination at the site of injury, rather than as a consequence of deficient OPC migration or proliferation (Falcão *et al*., 2018). For this reason, the major therapeutic challenge is to promote endogenous remyelination by stimulating adult OL myelination and OPC differentiation (Valny *et al*., 2017). In this sense, there are several remyelinating therapies under clinical

trials, such as histamine 1 receptor blocker Clemastine, the antibody anti-LINGO-1 Opicinumab, vitamin B family coenzyme Biotine, or the H3-receptor antagonist GSK239512 (Cunniffe & Coles, 2021; Eleuteri *et al*., 2017; Green *et al*., 2017; Sedel *et al*., 2016)

2.3 Autoimmune encephalitis: Anti-NMDA receptor encephalitis

Autoimmune encephalitis is a rare condition that entails behavioral change, cognitive deficits, seizures, as well as movement disorders. The reported incidence of autoinmune encephalitis is about 0.8 per 100,000 people, however the specific etiology is not well identified (Goodfellow & Mackay, 2019). There are different sub-types of autoimmune encephalitis characterized by antibodies to intracellular proteins, or extracellular synaptic proteins and cell surface antigens (Graus *et al*., 2010). Some forms of autoimmune encephalitis can start *de novo* whereas others are associated with lung, breast, ovarian or testicular malignancies and have poor prognosis (Broadley *et al*., 2019). These limbic encephalitis are named paraneoplastic autoimmune encephalitis and usually act against intracellular proteins located in the internal part of the synapse, cytoplasm or *nucleus* (Newman *et al*., 2016). The best characterized paraneoplastic auto-antibodies are anti-Hu/ANNA-1, anti-Ri/ANNA-2, anti-CV2/CRMP5 and anti-Ma2/Ta, that were first identified in the 1980s and 1990s.

Recent studies describe other auto-antibodies, among which the most common are the anti-N-methyl-D-aspartic acid receptor (anti-NMDAR), and anti- voltage-gated potassium channel (anti-VGKC) (Goodfellow & Mackay, 2019). Pathogenic antibodies binding the NR1 subunit of the N-methyl-D-aspartate receptor (NMDAR) are the most common cause of autoimmune encephalitis, and were firstly identified by Dalmau and colleagues in 2005 in both serum and cerebrospinal fluid (CSF) (Dalmau *et al*., 2017; Vitaliani *et al*., 2005). The clinical spectrum is wide, which represents a challenge for early diagnosis since the majority of cases are identified retrospectively. The principal form of NMDAR-e is related to young females (95% under 45 years, female-male ratio of 4:1) with a distinct neuropsychiatric syndrome (Dalmau *et al*., 2008; Titulaer *et al*., 2013). The typical presentation of NMDAR-e in adult usually comprises an initial prodrome of headache, fever, vomiting, diarrhoea and upper respiratory

tract symptoms **(figure 9)**. Then, a period of complex neuropsychiatric features, including memory deficits, psychosis, delusions or hallucinations, evolves to a severe and prolonged encephalitis with seizures, orofacial dyskinesia and autonomic dysfunction. Despite the frequency and intensity of the seizures tend to decrease as the disease evolves, formal electroencephalogram (EEG) evaluation is important to distinguish between seizure activity and movement disorders, to ensure appropriate treatment (Newman *et al*., 2016).

The progression of the disease within the months after the onset varies from patients. The vast majority of patients develop four or more core symptoms after a few months, while around 1% of patients have monosymptomatic manifestation of the disease, such as an isolated psychosis (Broadley *et al*., 2019). Generally, patients improve with early immunotherapy or treatment of the teratomas and recovery process is often in the reverse order of symptom presentation. However, aggressive immunotherapy carries significant risks of serious side-effects and, focal or generalized, seizures can be treatment resistant. Several studies documented associations between initial clinical findings including seizure control and cognitive deficits, and outcome measures of prognosis such as mortality, helpful for clinical guidelines (Goodfellow & Mackay, 2019; Newman *et al*., 2016).

Overactivity of NMDA receptors causing excitotoxicity is a proposed underlying mechanism for epilepsy, dementia, and stroke, whereas low activity produces symptoms of schizophrenia. In NMDAR-encephalitis, autoantibodies anti-NMDAR cause receptor internalization and reduced surface expression of NMDA receptors in neurons, leading to encephalitis symptoms that include psychosis, cognitive decline, seizures, and coma (Broadley *et al*., 2019). An intriguing feature of this disease is the dissociation between the severity of symptoms of most patients and the low frequency (~32%) of magnetic resonance imaging (MRI) abnormalities using standard clinical sequences (Dalmau *et al*., 2008). Yet studies with diffusion tensor imaging (DTI) and superficial white matter mean diffusivity show extensive changes in white matter integrity in most patients (Aurangzeb *et al*., 2017; Byun *et al*., 2015).

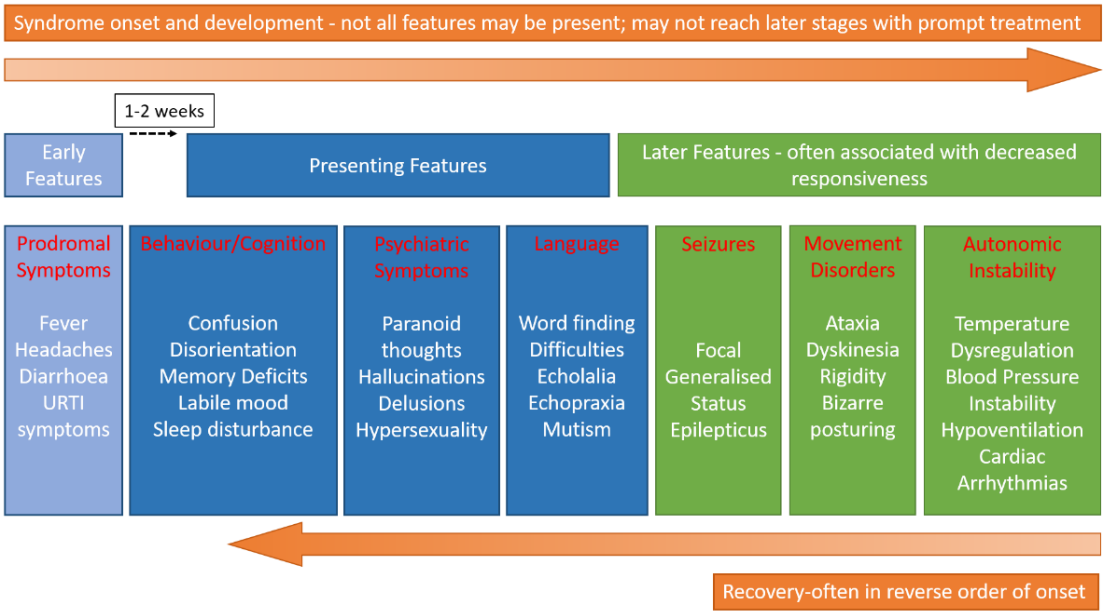

Figure 9. Usual acute clinical presentation of anti-N-methyl-D-aspartic acid receptor (NMDAR) encephalitis through various stages of development. (Newman *et al*., 2016)

HYPOTHESIS AND OBJECTIVES

Myelin directs node of Ranvier formation, enables rapid saltatory conduction and provides metabolic support to axons via the periaxonal space. As other brain structures, myelin is subject of plastic changes in response to electrical activity, that allow to fine tune circuits involved in motor learning and memory (McKenzie *et al*., 2014). Therefore, changes in the number or structure of myelin sheaths, node of Ranvier and periaxonal space may modulate axon conduction velocity. The importance of myelin for circuit function is made apparent by the severity of neurological diseases associated with its disruption. Abnormalities in myelination during development causes cognitive dysfunction and are associated to behavioral disturbances in neurodevelopmental psychiatric disorders such as Autism Spectrum Disorders. In multiple sclerosis, the complex etiopathology leads dysfunction and apoptosis of oligodendrocytes with subsequent demyelination and neurodegeneration. Finally, white matter damage is also present in autoimmune encephalopathy containing antibodies to N-methyl-D-aspartate receptors (NMDAR).

The main objective of this Thesis is ***to validate novel intervention strategies based on plastic myelination promotion*** in demyelinating neurological disorders. The specific objectives are as follows:

Objective 1. To explore the potential of clemastine to promote myelination during development

Neurodevelopmental disorders display a broad range of severity, ranging from cortical malformations incompatible with independent life to subtle impairments observed in affective pathologies. During embryonic development, oligodendrocytes shape the connectome. Previous data in the laboratory (Almudena Robledo's Master Thesis, unpublished) provide strong evidence that myelination is transiently impaired during development in cerebral cortex in mice deficient in contactin associated protein-like 2 (Caspr2) gene (Cntnap$^{-/-}$ mice), an animal model of autism (Peñagarikano *et al*., 2011). Myelin deficits have also been described in other models of autism (Gdalyahu *et al*., 2015). Thus, pharmacological intervention to promote or accelerate myelination could be a therapeutic option for, at least, a partial repair of erroneous perinatal brain development in

autism. Clemastine is to date the most promising pro-myelinating drug, likely due to its anti-muscarinic properties against the muscarinic receptor 1 (M1R) (de Angelis *et al*., 2012). However, little is known about the effect of clemastine in myelination during development or in the absence of previous myelin damage or demyelination. Therefore, we have explored here the therapeutic potential of clemastine to promote myelination during development. The specific aims of this objective are:

1.1 To characterize the effect of clemastine on oligodendroglial lineage *in vitro*

1.2 To assess the role of clemastine on myelination during development

1.3 To study the effect of clemastine on microglia-oligodendrocyte crosstalk during development

Objetive 2. To design a pharmacogenetic tool to selectively stimulate adult oligodendrocytes and to study their role in remyelination

According to the recently developed concept of "myelin plasticity," experience-dependent changes in myelin may modulate brain function through effects on signal synchronization (Hasan *et al*., 2019; Noori *et al*., 2020). Myelin plasticity occurs when newly-formed oligodendrocytes from OPCs remodel existing myelination. Similarly, remyelination is also dependent on OPCs, involving recruitment to the lesion, differentiation into myelin forming cells and remyelination of denuded axons, and the success of this depends on environmental context (Franklin & Ffrench-Constant, 2017). However, the specific role of mature oligodendrocytes on remyelination remain under debate. We hypothesize that mature oligodendrocytes could also be pivotal for remyelination. For that purpose we generated a pharmacogenetic tool using the cre-lox system, in which cre enzyme is expressed under the PLP promoter, a genetic marker of mature oligodendrocytes. In this study we tried to elucidate the role of mature oligodendrocytes signaling pathways after demyelination in the EAE model. The specific aims of this objective are:

2.1 To generate an animal model that allows to selectively stimulate mature oligodendrocytes

2.2 To study the effect of acute and chronic activation of oligodendrocytes in myelination and nerve impulse transmission

2.3 To analyze the consequences of oligodendrocyte activation in demyelinating diseases

Objective 3: To analyze the role of oligodendroglial NMDA receptors in autoimmune encephalitis

Like neurons, oligodendrocytes express NMDAR, which play a critical role in supplying lactate to axons in order to sustain proper propagation of action potentials (Saab et al., 2016). Thus, stimulation of NMDAR by glutamate released from axons, results in a translocation of the glucose transporter GLUT1 into the oligodendrocyte plasma membrane and myelin compartment, enhancing glucose uptake and glycolytic support of fast spiking axons. Recent studies have identified a group of human disorders in which synaptic receptors are directly targeted by autoantibodies (Dalmau et al., 2017). In particular, autoantibodies to the GluN1 subunit of the NMDAR cause receptor internalization and reduced surface expression in neurons, leading to encephalitis symptoms that include psychosis, cognitive decline, seizures and coma. However, post-mortem analysis of the brain from encephalitis autoimmune patients revealed white matter damage. Here, we tested the hypothesis that the function of NMDAR in oligodendrocytes may also be impaired in patients with anti-NMDAR encephalitis leading to white matter alterations. The specific aims of this objective are:

3.1. To characterize the activity of NMDAR in cultured oligodendrocytes

3.2. To determine the effect of CSF from patients with autoimmune encephalitis on NMDAR functionality

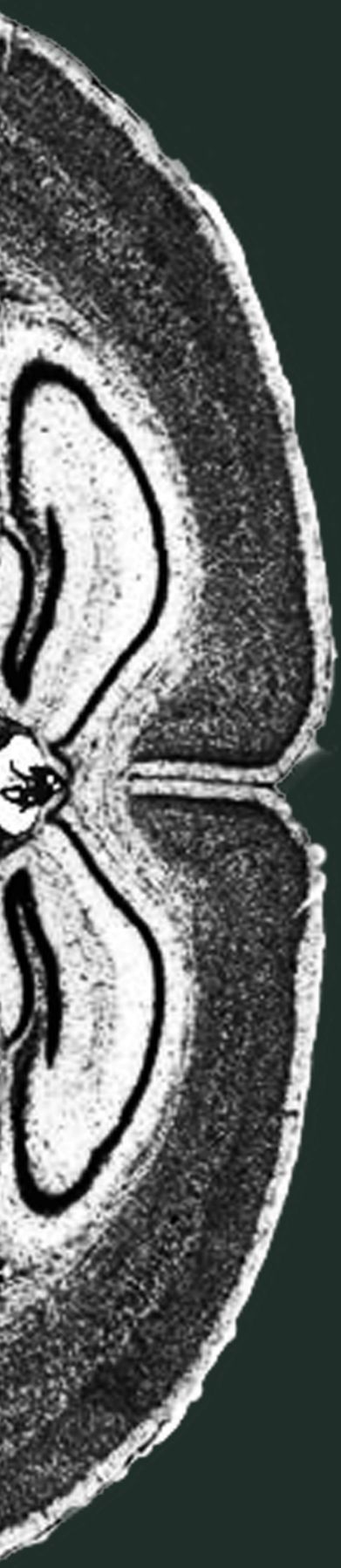

MATERIALS AND METHODS

1. ANIMALS

All experiments were performed according to the procedures approved by the Ethics Committee of the University of the Basque Country (UPV/EHU), following the European Directive 2010/63/EU. Animals were handled in accordance with the European Communities Council Directive. Animals were kept under conventional housing conditions (22 ± 2 temperature, 55 ± 10% humidity, 12-hour day/night cycle and with ad libitum access to food and water) at the University of the Basque Country animal unit. All possible efforts were made to minimize animal suffering and the number of animals used.

Experiments were performed in C57BL/6 wild-type, $CD11c^{+}$ eYFP (kindly provided by Dr. Ana Planas, Institute of Biomedical Research from Barcelona) and PLP-$CreERT2^{+}$/$hM3Dq^{+/+}$ mice.

1.1 PLP-$CreERT2^{+}$/ $hM3Dq^{+/+}$ mice generation

R26-LSL-Gq-DREADD mice (from Jackson laboratory) allow the inducible Cre expression of the hM3Dq gene. Designer receptor exclusively activated by designer drugs (DREADD), permits spatial and temporal control of G protein signaling *in vivo*. These systems utilize G protein-coupled receptors (GPCR) engineered to respond exclusively to synthetic small molecules ligands instead of their endogenous ligands. In that case, human muscarinic 3 receptor (hM3Dq) present two amino acid substitutions [Y149C3.33/A239G5.46] that abolish receptor affinity for the native ligand, acetylcholine [ACh], but allow receptor binding and subsequent activation by the small pharmacologically inert molecule clozapine-N-oxide [CNO] **(Figure 10)**. Thus, hM3Dq activation via CNO binding induces the canonical Gq pathway.

R26-LSL-Gq-DREADD allele randomly integrates into the mouse genome as a transgene without affecting its functionality. This construct presents a loxP-flanked STOP cassette; and a coding region for the mutant G protein-coupled receptor hM3Dq together with two reporting proteins, the yellow-green fluorescent protein mCitrine and the hemagglutinin epitope-tagged (HA-hM3Dq-pta-mCitrine).

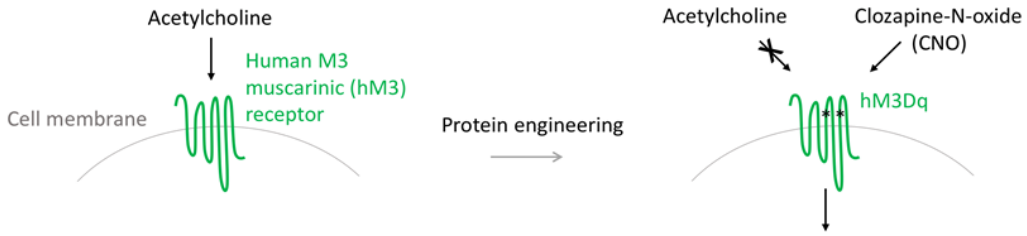

Figure 10. DREADD receptor. hM3 receptor molecularly modified to recognize Clozapine-N-oxide.

The R26-LSL-Gq-DREADD mice were crossed with PLP-CreERT2 mice (assigned by Dr. F. Kirchhoff), which express the Cre recombinase after administration of tamoxifen specifically to oligodendrocytes **(Figure 11)**. Cre enzyme recognizes 34 base pair DNA sequences called loxP ("*locus* of crossover in phage P1"). Placement of Cre under the control of the regulatory sequence of the myelin proteolipid protein (PLP) promoter allows tissue-specific expression of Cre in mature oligodendrocytes. In order to induce specific temporal Cre activity, the enzyme is fused to a mutated ligand-binding domain for the human estrogen receptor (ERt). Upon the introduction of tamoxifen (an estrogen receptor antagonist), the Cre-ERt construct is able to penetrate the *nucleus* and induce targeted mutation. Thus, following cre-mediated removal of an upstream floxed-STOP cassette, expression of HA-tagged hM3Dq and mCitrine yellow fluorescent protein are observed.

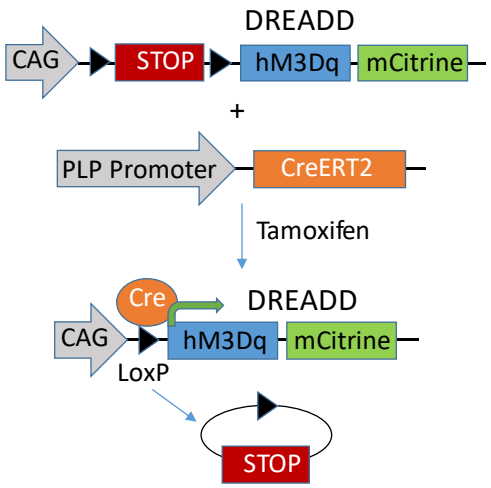

Figure 11. Pharmacogenetic tool. Genetic design of PLP-CreERT2^{+}/hM3Dq$^{+/+}$ mice

2. HUMAN SAMPLES.

The cerebrospinal fluid from 7 patients included in the study were selected from a previously reported cohort of cases with anti-NMDAR encephalitis (Titulaer *et al*., 2013). All 7 patients fulfilled criteria of anti- NMDAR encephalitis (Dalmau *et al*., 2017), and their random selection was based on the amount of cerebrospinal fluid (CSF) available for the current studies. The median age was 16 years (range = 10–25 years), and 4 were female. In all cases, the CSF was obtained during the acute stage of the disease, and all were negative for glial autoantibodies such as aquaporin-4, myelin oligodendrocyte glycoprotein, and glial fibrillary acidic protein. By the time of diagnosis (in all cases within 4 weeks of disease onset), 6 patients had normal clinical MRI studies, and 1 had a 0.2mm abnormality on fluid-attenuated inversion-recovery (FLAIR)/T2 sequences in the right temporal lobe. NMDAR antibody titers were determined by serial dilutions of CSF using a cell-based assay (median = 1/160, range = 1/20–1/640). For controls, we used the CSF of 3 patients with noninflammatory mild cognitive decline and 4 patients with normal pressure hydrocephalus who were negative for NMDAR antibodies. Pooled CSF from the 3 patients with the highest NMDAR antibody titers (all >1:80) was immunoabsorbed with HEK293T cells expressing the GluN1 subunit of the NMDAR or cells not expressing this subunit, as previously reported (Höftberger *et al*., 2015). A recombinant monoclonal human antibody (SSM5) derived from intrathecal plasma cells of a patient with anti-NMDAR encephalitis and a control isotype against an irrelevant antigen (12D7) were used in some assays.

3. IN VIVO MODELS

3.1 Animal treatments

3.1.1 Tamoxifen administration

Tamoxifen (Sigma #T5648) is dissolved in Mygliol812 (Caesar & Loretz) to a stock solution of 10 mg/ml. For PLP-CreERT2^{+}/hM3Dq$^{+/+}$ adult mice (P27), tamoxifen was administered by intraperitoneal injection (27G needle) at 80 mg/kg for three consecutive days, followed by a washing period of 15 days. PLP-CreERT2^{-}-hM3Dq mice were used as control to analyse

effective recombination. Pup PLP-CreERT2^{+}/hM3Dq$^{+/+}$ mice (P15) were treated with the same tamoxifen dosis (80 mg/kg) for two consecutive days, followed by a washing period of 5 days until P20. These pup animals will be used for oligodendrocytes culture derived from optic nerve.

3.1.2 Chronic CNO treatment

After tamoxifen administration, adult PLP-CreERT2^{+}/hM3Dq$^{+/+}$ recombined animals (P45) were treated with Clozapine N-oxide (Tocris #4936) by intraperitoneal injection at 1mg/kg solved in saline solution (Stock dilution at 100mM in DMSO. The treatment was administered for 15 days on daily basis (P60). Control PLP-CreERT2^{+}/hM3Dq$^{+/+}$ mice were treated with DMSO vehicule solution.

3.1.3 Chronic Clemastine treatment

C57BL/6 wild-type mice were daily treated with vehicle or clemastine (#1453 Tocris; 50mg/kg solved in 10% DMSO) by intraperitoneal injections from postnatal day 5 (P5) to P21. CD11c^{+} eYFP mice were treated from P5 to P10 following the same protocol.

3.2 Experimental autoimmune encephalomyelitis (EAE) induction

EAE was induced in 8-10 week old female PLP-CreERT2^{+}/hM3Dq$^{+/+}$ and C57BL/6 wild-type mice mice by subcutaneous immunization with 300 µl of myelin oligodendrocyte glycoprotein 35-55 (MOG 35-55; 200 µg; Sigma) emulsioned in incomplete Freund's adjuvant (Sigma) supplemented with 8 mg/ml *Mycobacterium tuberculosis* H37Ra. *Pertussis* toxin (500 ng/0.1 ml; Sigma) was injected intraperitoneally on the day of immunization and again 2 days later to facilitate and improve the development of the disease.

In this model, mice begin to show neurological signs around 10-12 days postimmunization (dpi). The motor deficits increase with the time reaching a maximum peak around day 20 postimmunization, followed by a partial and slow recovery. Motor symptoms were recorded daily and scored from 0 to 8 as follows:

0, no detectable signs

1, weakness in the tail

2, paralysed tail

3, paralysed tail and weakness in hindlegs

4, paralysed tail and hemiparalysis of hindlegs

5, complete hindlimb paralysis

6, paralysis of hindlegs and rigidity in forelegs

7, tetraplegia

8, moribund

PLP-CreERT2^{+}/hM3Dq$^{+/+}$ mice were daily treated with CNO 1mg/kg from 10 day post-immunization (PI). To analyze the specific effect of CNO administration in the course of the EAE, the following control groups were added to the experimental paradigm:

- PLP-CreERT2+/hM3Dq+/+ mice treated with vehicule solution from day 10 PI.
- C57BL/6 wild-type mice tamoxifen administered previously to the immunization.
- C57BL/6 wild-type mice treated with CNO from day 10 PI.

4. IN VITRO MODEL

4. 1 Optic nerve-derived oligodendrocyte culture.

Primary oligodendrocyte cultures were performed as previously described (Barres *et al*., 1992) with modifications (Matute, Sánchez-Gómez, Martínez-Millán, & Miledi, 1997). Optic nerves were extracted from P12 Sprague Dawley rats or P20 PLP-hM3Dq, and meninges were removed in supplemented (2 µl/ml gentamicin, 1 mg/ml BSA and 2 mM glutamine) HBSS (Sigma- Aldrich) under magnifying scope. Briefly, optic nerves were freed of their meninges and then digested with collagenase (1.25 mg/ml; Sigma-Aldrich), trypsin (0.125%; Sigma-Aldrich) and deoxyribonuclease (0.004%; Sigma-Aldrich) for 40 min at 37°C. Afterwards, the enzymatic reaction was stopped by 10% FBS in DMEM (Gibco) and centrifuged at 1000 rpm for 5 min. Then, the pellet was resuspended in 1 ml of the same

solution and the resulting cell suspension was gently passed through needles of different gauges (21G, 23G, and 25G) and filtered through a 40 µm nylon mesh (Millipore). Cell number was determined with 10 µl of sample with 1:1 tripan blue staining (Sigma-Aldrich) and the rest of the cell suspension was centrifuged at 1000 rpm for 10 min. Cells were seed into 24-well plates bearing 14-mm diameter coverslips coated with poly-D-lysine (10 mg/ml) at a density of 10.000 cells/well for immunocytochemistry 50.000 cells/well for lactate measurements, or 100.000 cells/well for western blot. For calcium imaging, oligodendrocytes were seeded in µ-Dish 35 mm Ibidi plates (#81158) at a density of 10.000 cells/plate. Cells were kept in DMEM supplemented with 2 mM glutamine, 1 mg/ml BSA (fraction V), 5 mg/ml bovine pancreatic insulin, 100 mg/ml human transferrin, 40 ng/ml sodium selenite, 60 ng/ml progesterone, 16 mg/ml putrescine, 30 ng/ml 3,39,5-triiodo-L-thyronine, 40 ng/ml L-thyroxine, 10 ng/ml ciliary neurotrophic factor (Boehringer Mannheim) and 1 ng/ml neurotrophin-3 (Promega), called $SATO^{+}$ medium **(Table 1)**. However, for differentiation studies, cells were kept without trophic factors CNTF and NT3 ($SATO^{-}$) Cultures were maintained at 37°C and 5% CO2, and fresh medium was added every day.

Reagent	Concentration	Company
Dulbecco's Modified Eagle Medium (DMEM)	Base medium	Gibco
Insulin	5 µg/ml	Sigma-Aldrich
Penicillin/Streptomycin	100 U/ml	Lonza
BSA	1 mg/ml	Sigma-Aldrich
L-Glutamine	2 mM	Sigma-Aldrich
N-Acetyl L-Cystein	6.3 mg/ml	Sigma-Aldrich
Transferrin	100 µg/ml	Sigma-Aldrich
Putrescine	16 ng/ml	Sigma-Aldrich
Progesterone	60 ng/ml	Sigma-Aldrich
Sodium selenite	40 ng/ml	Sigma-Aldrich
Triiodotironine (T3)	30 ng/ml	Sigma-Aldrich
L-Tyroxine (T4)	40 g/ml	Sigma-Aldrich
Ciliary neurotrophic factor (CNTF)	10 ng/ml	Peprotech
Neurotrophin 3 (NT-3)	1 ng/ml	Peprotech

Table 1. SATO medium composition

4.2 Primary mixed glial culture

Primary mixed glial cultures were prepared from the cerebral cortex of neonatal rats and mice (P0-P2) following the protocol described by McCarthy and De Vellis (1980) with modifications. Cell suspension was obtained by mechanical and enzymatic dissociation of the cerebral cortex and was seeded in 75 cm^2 surface culture flasks previously treated with poly-DLysine (PDL). Flasks were maintained in Iscove´s Modified Dubelcco´s Medium (IMDM; Gibco) supplemented with 10% fetal bovine serum (FBS) at 37°C, with 5% of CO2 in a humidified incubator

4.2.1 Microglia culture

Approximately 15 days after performing the culture, microglia were isolated by mechanical shaking. Free-floating microglia were collected from shaken astrocyte flasks and purified by pre-plating on bacterial plastic dishes (Sterilin). Microglia were maintained in Petri dish 24-48 hours minimum with Dulbecco's Modified Eagle's Medium (DMEM) supplemented with 10% FBS. Microglia were tripsinized and seeded in PDL-coated µ-Dish 35 mm (Ibidi #81158) coverslips at 10,000 cells/well for calcium imaging. Cells were cultivated in DMEM + 10% FBS at 37°C, with 5% of CO^2 in a humidified incubator and were used after 24 hours.

4.2.2 OPC culture

OPCs were obtained from the same primary mixed glial cultures used to isolate microglia. After microglia isolation from the flasks, the remaining OPCs present on the top of the confluent monolayer of astrocytes were dislodged by shaking flasks overnight. OPCs were purified from microglial cells by plating on bacterial Petri dishes. The non-adherent cells (OPCs) were further collected and seeded in PDL-coated µ-Dish 35 mm (Ibidi #81158) at a density of 10,000 cells/well in complete SATO medium (SATO+).

5. TECHNIQUES

5.1 PLP-CreERT2^{+}/ hM3Dq$^{+/+}$ mice genotyping

DNA from PLP-CreERT2^{+}/hM3Dq$^{+/+}$ mice tissue was isolated using KAPA HotStart® Mouse Genotyping Kit, following the manufacturers' instructions. Genotyping was performed by PCR of genomic DNA using GoTaq® Hot Start Polymerase kit and 5µM of each oligo-primer **(Table 2)**. Final PCR products were analyzed using gel electrophoresis (4.62 µM Tris-Base, 1.25 µM EDTA, 28.3 µM Boric.ac and 2% agarose).

Target gene	Forward (5'->3')	Reverse (5'->3')
PLP-CreERT2	CAGGGTGTTATAAGCAATCCC	CCTGGAAAATGCTTCTGTCCG
R26-22887 Mutant	CGCCACCATGTACCCATAC	GTGGTACCGTCTGGAGAGGA
R26-oIMR9021	AAGGGAGCTGCAGTGGAGTA	CCGAAAATCTGTGGGAAGTC

Table 2. Primers used for PLP-CreERT2^{+}/hM3Dq$^{+/+}$ mice genotyping

5.2 Immunofluorescence

5.2.1 Cultured oligodendrocytes

Cells were fixed in 4% paraformaldehyde (PFA) for 15 min, washed in 0.1 M PBS for three times and then stored at 4°C. Cells were permeabilized and blocked in 4% normal goat serum (NGS, Palex), 0.1% Triton X-100 (Sigma-Aldrich) in 0.1 M PBS (blocking buffer) for 1 h and incubated with primary antibodies overnight at 4°C (Table 2). Then, cells were washed in 0.1% Triton X-100 in 0.1 M PBS (washing buffer) and incubated with the fluorochrome conjugated antibodies in blocking solution for 1 h at RT. After that, cells were washed and incubated with DAPI (4 µg/ml, Sigma-Aldrich) for 10 min. Then, cells were washed again twice and coverslips were mounted on glass slides with Glycergel Mounting Medium (Dako #C0563)

5.2.2 Animal tissue

Mice were anesthetized with intraperitoneal injection of chloral hydrate (500 mg/kg) and transcardially perfused with 0.1 M sodium phosphate buffer (pH 7.4) followed by 4% PFA in the same buffer for 15-20 minutes. The brains were extracted and postfixed with the same fixative solution for 4 h at RT, placed in 30% sucrose in 0.1 M PBS at 4°C and then kept in cryoprotectant solution (30% ethylene glycol, 30% glycerol and 10% PB 0.4 M in dH2O) at -20°C. The tissue was cut using a Leica VT 1200S vibrating blade microtome (Leica microsystems) to obtain coronal 40 µm-thick sections.

Free-floating vibratome sections or cerebral slices were permeabilized and blocked with 0.1% Triton X-100, 4% NGS in 0.1 M PBS for 1 h at RT and were incubated with primary antibodies overnight at 4°C with gently shaken **(Table 3)**. Slices were then washed three times in 0.1% Triton X-100 in 0.1 M PBS and were incubated with containing fluorochrome-conjugated antibodies in blocking solution and DAPI (4 µg/ml) at RT for 1 h. After that, slices were washed for three times in 0.1% Triton X-100 in 0.1 M PBS and were mounted on glass slides with ProLong™ Gold (Invitrogen #P36930).

For labeling specific paranode and node markers, an antigen retrieval protocol was performed. Free-floating sections were incubated in R-Universal epitope recovery buffer for heat-induced antigen unmasking (Aptum) for 5 min at 95°C followed by 5 min at RT and then were washed in cold 0.1 M PBS twice. For MBP staining, slices were permeabilized in 100% ethanol at -20°C for 5 min and washed in 0.1 M PBS for three times. After permeabilization, sections were blocked in 10% NGS, 0.1% Triton X-100 in 0.1 M PBS for 1 hour at RT. For PDGFr-α labelling, Triton X-100 was only used during the blocking step.

Antibody	Host	Concentration	Company
APC (CC1)	Mouse	1:200	Calbiochem
Caspr	Mouse	1:500	Neuromab
CD68-Alexa 488	Rat	1:100	BioRad
GFP	Rat	1:1000	Nacalai
Iba1	Rabbit	1:1000	Wako
iNOS	Mouse	1:500	BD Bioscience
Ki67	Rabbit	1:200	Vector
MBP	Mouse	1:1000	Biolegend
NaV1.6	Rabbit	1:250	Alomone
NF-L	Rabbit	1:500	Cell Signaling
NG2	Rabbit	1:200	Millipore
Olig2	Mouse	1:1000	Millipore
PDGFRα	Rabbit	1:200	Santa Cruz
P2Y12	Rabbit	1:200	Anaspec
pERK	Rabbit	1:250	Cell Signaling
SMI-32	Mouse	1:1000	Covance
IgG Rabbit-Alexa 488	Goat	1:500	Invitrogen
IgG Rabbit-Alexa 594	Goat	1:500	Invitrogen
IgG Mouse-Alexa 488	Goat	1:500	Invitrogen
IgG Mouse-Alexa 594	Goat	1:500	Invitrogen

Table 3. Antibodies used for immunohistochemistry

5.2.3 Analysis of fluorescence immunostaining images.

Images were acquired with the same settings for all samples within one experimental group. Zeiss LSM800, Zeiss LSM880 Airyscan and Leica TCS SP8 confocal microscopes were used to adquire the images. For oligodendrocyte differentiation analysis in cultured oligodendrocytes, the number of MBP^+ cells, $NG2^+$ cells and $ki67^+$ cells was blindly counted (5 fields per coverslip from at least 3 different experiments performed in triplicate, 40X objetive). Data was shown in percentage from total cells in the field. To measure MBP^+cells area, 45-50 cells were analyzed per condition. Cells were outlined with the MBP labelling as the defining parameter for the region of interest (ROIs) using the Image J software (NIH). The morphology of MBP^+ cell was analysed by *sholl* analysis pluggin (Image J software) to determine cell complexity and the number of branches and junctions. To analyze pErk

activation, the results were expressed as changes in fluorescence intensity relative to those seen in control conditions.

Fluorescence immunostaining images from mouse tissues were taken with Leica TCS SP8 laser scanning microscope or Zeiss LSM880 Airyscan using 20X objective, 40X or 63X oil-immersion objectives to generate z-stack projections. Images analysis was carried out in 2-3 sections per animal from 3-6 mice per experimental group. For MBP intensity analysis, images were taken in *corpus callosum* and cortex with the same settings for all experiments and mean value along the stack profile was quantified with Image J software. To analyse the percentage of myelinated axons, stack z-images were taken with 63X oil-immersion objectives in layers II-III of cerebral cortex. We used a generated macro able to: I) distinguish transversal NF-L labelled axons on the basis of size and circularity parameters, and II) to determine whether the axons selected were surrounded by a myelin ring. The number of myelinated axons were normalized to the total number of axons per area.

To analyze oligodendrocyte stages, the percentage of APC^+ cells and $NG2^+$ cells vs total number of Olig2+ cells was quantified from random areas of *corpus callosum*, retrosplenial cortex and primary somatosensory cortex. For nodes of Ranvier number and length, images from *corpus callosum* and cortex were taken with Zeiss LSM800 microscope, using the 63X oil-immersion objective. To measure node of Ranvier length, 50 nodes per animal were randomly selected and analyzed. For the internode length, z-stack images from cerebral cortex were taken with Zeiss LSM800 microscope using the 40X objective. Maximal projections of z-stack images were used to determine MBP staining length between two nodes of Ranvier.

To analyze microglia activation, immunoreactivity of Iba1+, inducible oxide nitrite synthase (iNOS), P2Y12 and CD68 was calculated in 63X images from Leica TCS SP8 confocal microscopes. Z-stack images from cerebral cortex were taken with the same settings for all experiment and mean value along the stack profile was quantified with Image J software. From $Iba1^+$ images, individual cells were segmented and skeletonized in order to analyze microglia morphology. The number of branches and junctions, as well as the number of

intersections at determined distance from the soma was analysed using the *sholl* pluggin (Image J software).

To determine the percentage of oligodendrocytes expressing hM3Dq receptor after tamoxifen administration, m-citrine signal was amplified using anti-GFP primary antibody. The number of GFP^+ oligodendrocytes was normalized versus the total number of oligodendrocytes ($Olig2^+$ cells) or mature oligodendrocytes (APC^+ cells), and expressed in percentage. Images were taken at 40X with Zeiss LSM800 microscope from at least two slices from three mice.

Lession area in spinal cord sections from EAE mice were counted in 40X images acquired using a Leica TCS STED SP8 confocal microscope. White matter (WM) area and lesion area were defined as ROI on the basis of MBP immunostaining using the Image J software (NIH). To quantify axonal damage images were acquired using a Leica TCS STED SP8 confocal microscope and SMI-32 immunereactivity was calculated with the ImageJ software (NIH) and normalized to WM area defined as ROI.

5.3 Electron Microscopy

Mice were perfused with 4% formaldehyde, 2.5% glutaraldehyde (Electron Microscopy Sciences) and 0.5% NaCl in phosphate buffer, pH7.4, as described (Möbius *et al*., 2010). The brains were postfixed with the same fixative solution overnight at 4ºC. The tissue was sagitally cut using a Leica VT 1200S vibrating blade microtome (Leica) to obtain 200 µm-thick sections. Tissue sections were postfixed in 2% OsO_4, dehydratateed in ethanol and propylenoxide and embedded in EPON (Serva) for 24h at 60ºC. Ultrathin sections (50 nm thickness) were obtained by Leica Ultracut S ultramicrotome (Leica) and contrasted with 4% uranyl acetate (30 min) and lead citrate (6 min). EM pictures were taken with a Zeiss EM900 electron microscope (Zeiss). G-ratio (100-150 myelinated axons per animal) was calculated as the ratio of the diameter of axons (A) plus the inner tongue (I) divided by the diameter of the whole fiber (M), measured using Image J software and 8,000x magnitication images. The number of myelinated axons were quantified using 1,000x magnification images.

5.4 Cytosolic Ca^{2+} Imaging

Measurements of cytosolic [Ca^{2+}] were carried out as previously described (Ruiz *et al*., 2014). Prior to recording, cells were loaded with Fluo-4 AM (1 mM; Molecular Probes, Invitrogen) in the culture medium for 30 min at 37ºC. Afterward, the culture medium ($SATO^{+}$, $SATO^{-}$ or DMEM 10%FBS) was removed and the cells were maintained in extracellular solution (NaCl 140mM, KCl 5 mM, $MgCl_2$ 2mM; $CaCl_2$ 2mM, Glucose 10mM and HEPES 10mM, pH:7,4) at 37°C, with 5% of CO^2 in a humidified incubator. Fluo-4 AM- was excited at 488 nm, and the images were acquired through a 40X objective by an inverted LCS SP8 confocal microscope (Leica, Germany) at an acquisition rate of 1 frame/15 s during 5-10 min. For data analysis, a homogeneous population of 15–25 cells was selected in the field of view and cell somata selected as ROIs. Background values were always subtracted and the magnitude of the response was expressed as area under curve (AUC) in comparison to control conditions. Data expressed as F/F0_+ SEM (%) in which F represents the fluorescence value for a given time point and F0 represents the mean of the resting fluorescence level.

To study the effect of CSF from anti-NMDAR encephalitis on NMDA-mediated cytosolic [Ca^{2+}], oligodendrocytes were incubated with each individual patient or control CSF sample (diluted 1:50) at 37C for 4 hours before Fluo-4AM loading. Then, oligodendrocytes were exposed to NMDA applied together with glycine (both at 100µM). For each individual patients' CSF or control CSF, this experiment was repeated 3 times in oligodendrocyte cultures grown in identical conditions.

For calcium recording in acute cerebral slices the mice were anesthesized by isoflurane before depitation and their brain were removed from the skull immersed in an ice-cold oxygenated (5% CO_2 / 95% O_2 pH 7.4) slice preparation solution containing: NaCl 87mM, KCl 3mM, $NaHCO_3$ 25mM, NaH_2PO_4 1.25 mM, $MgCl_2$ 3mM, $CaCl_2$ 0.5mM, Sucrose 75mM and Glucose 25mM. Sagittal slices of 300µm were prepared with a vibratome (Leica VT 1200s) and transferred to a nylonbasket slice holder for incubation in artificial cerebrospinal fluid (ACSF) at 34ºC containing: NaCl 126mM, KCl 3mM, $NaHCO_3$ 25mM, NaH_2PO_4 1.2 mM, $MgCl_2$ 2mM, $CaCl_2$ 1mM, and Glucose 15mM. The slices were allowed to recover in ACSF with

continuous oxygenation for at least 30min. Before imaging, slices were incubated with 1 µm Fluo-4AM (Life technologies) in ACSF at room temperature for half an hour. Fluo-4 AM was dissolved in DMSO with 4.5% Pluronic F127 (Life technologies). Subsequently, the slices were washed twice and immersed in extracellular solution containing: NaCl 126mM, KCl 3mM, $NaHCO_3$ 25mM, NaH_2PO_4 1.2 mM, $MgCl_2$ 1mM, $CaCl_2$ 2.5mM, and Glucose 15mM.

5.5 Western blotting

After each treatment, cultured oligodendrocytes were washed in cold 0.1 M phosphate buffered saline (PBS) twice and cells were scraped in 40 µl of sample buffer (62.5 mM Tris pH 6.8, 10% glycerol, 2% SDS, 0.002% bromophenol blue and 5.7% β- mercaptoethanol in dH2O) per treatment (2 wells/treatment and 80,000 cells/well). All this process was performed on ice to enhance the lysis process and avoid protein degradation. After that, samples were boiled at 95°C for 10 min.

Protein samples were separated by SDS-PAGE in 3-8% Tris-Acetate and 4-20% Tris- Glycine polyacrylamide gels (Bio-Rad), according to the molecular weight of proteins. Electrophoresis was conducted in a Tris-Tricine buffer (100 mM Tris, 100 mM Tricine, 0.1 SDS% in dH2O, pH 8.3) by using the Criterion cell system (Bio-Rad). Gels were transferred to nitrocellulose membrane by using a Trans-Blot® Turbo™ Transfer System (Bio-Rad). Membranes were blocked for 1 h at room temperature (RT) in blocking solution, which consisted of TBST buffer (20 mM Tris, 1.4 M NaCl, 0.05% Tween-20 in dH2O, pH 7.6) supplemented with 5% bovine serum albumin (Sigma-Aldrich). Then, they were incubated with mouse anti-MBP (1:1000; Biolegend) in the same solution overnight at 4°C with gentle shaking. Afterwards, membranes were washed three times with TBST and incubated with secondary antibody (rabbit anti-β-actin, 1:5000 from Sigma-Aldrich) conjugated to horseradish peroxidase (HRP) in blocking solution for 1h at RT.

Immunoreactive proteins were detected by using enhanced electrochemical luminescence (Super Signal West Dura or Femto, Pierce) and ChemiDoc XRS Imaging System (Bio-Rad). Band signal was quantified by densitometry using Image Lab software (Bio-Rad) and were

normalized with actin and provided as the mean ± S.E.M of at least three independent experiments.

5.6 Fluorescence-activated cell sorting (FACS)

Animals were anesthetized by isoflurane and sacrificed by decapitation. The brains and spinal cords were extracted, homogenized and digested mechanically and enzymatically. Homogenates were centrifuged through a continuous 60% Percoll gradient to remove the myelin and other cell debris. To avoid non-specific binding of the antibodies, Fc receptors (antibody receptors) were blocked with TruStain FcX antibody (BioLegend) for 10 minutes at 4°C in FACS buffer (0.1% Bovine serum albumin, BSA and 1 mM EDTA in PBS). For cellular labelling, a mix of fluorochrome-conjugated antibodies (Table 4) was prepared and the incubation was simultaneous (30 minutes, 4°C). Stained cells were washed and resuspended in 300 µl FACS buffer for acquisition in the flow cytometer or for cell sorting.

For microglia sorting, samples were sorted using CD11b and CD45 to distinguish between resident microglia ($CD11b^{+}/CD45^{low}$) and macrophages ($CD11b^{+}/CD45^{high}$) (Szulzewsky *et al*., 2015) using a FACSAria IIIu (BD Bioscience).

5.7 qPCR and Gene expression profiling

Microglia RNA from mice samples (lumbar spinal cord, lymph nodes and spleen) was isolated using Trizol (Invitrogen) according to manufacturer's instructions. Subsequently, from 1 µg of total RNA cDNA synthesis was conducted using SuperScript III retrotranscriptase (200 U/µl; Invitrogen) and random hexamers as primers (Promega). RNA from sorted microglia was isolated using RNeasy Plus Micro Kit (Quiagen) and cDNA synthesis was conducted using AffinityScript Multiple Temperature cDNA Synthesis Kit (Agilent Technologies Inc) and random hexamers as primers (Promega).

Gene expression of microglia RNA were further analysed using a 96.96 Dynamic Array™ integrated fluidic circuit (Fluidigm) real-time PCR and GenEx software **(Table 4)**. Results were

depicted as relative gene expression according to the ΔΔCq method (2−ΔΔCt) and expressed in base 2 logarithmic scale.

Target gene	Forward (5'->3')	Reverse (5'->3')
Itgax	GAACATATCCCTGGGCCTGTC	CACAGTAGGACCACAAGCCAA
Spp1	GCTTTTGCCTGTTTGGCATT	AATCAGTCACTTTCACCGGGAG
ApoE	AGGTCCAGGAAGAGCTGCAG	GTGCCGTCAGTTCTTGTGTGA
IGF-1	AGAAGTCCCCGTCCCTATCG	CCTTCTCCTTTGCAGCTTCG
CD68	CAAGCCCAAATTCAAATCCG	CCAAGCCTTTCTTCCACCC
H2-Ab1	AGGGCGGAGACTCCGAAA	GAAGTAGCACTCGCCCATGAAC
Arg1	GGATTGGCAAGGTGATGGAA	CGACATCAAAGCTCAGGTGAA
Bdnf	TCCAAAGGCCAACTGAAGCA	CTGCAGCCTTCCTTGGTGTA
C3	AGGGAGTGTTTGTGCTGAAC	GCCAATGTCTGCCTTCTCTAC
Ccl2	AGCAGCAGGTGTCCCAAA	TTCTTGGGGTCAGCACAGAC
Cd36	GGTGTGCTAGACATTGGCAAA	GACTTGCATGTAGGAAATGTGGAA
Cd86	CATGGGCTTGGCAATCCTTA	ATTGAAATAAGCTTGCGTCTCC
Chi3l3	GCCCACCAGGAAAGTACACA	CCTCAGTGGCTCCTTCATTCA
Clec7a	ACCACAAGCCCACAGAATCA	AGGAAGGCAAGGCTGAGAAA
Mrc1	CACAAAGCCATGCTGTAGTACC	GTAAAACCCATGCCGTTTCCA
Nos2	GAGGAGCAGGTGGAAGACTA	GGAAAAGACTGCACCGAAGATA
P2ry12	GATGCCAGTCTGCAAGTTCC	TTGACACCAGGCACATCCA
Trem2	ACCTCTCCACCAGTTTCTCC	AGTACATGACACCCTCAAGGAC
Tyrobp	GCTGAGACTGAGTCGCCTTA	CTCTGTGTGTTGAGGTCACTGTA

Housekeeping gene	Forward (5'->3')	Reverse (5'->3')
B2m	ACTGACCGGCCTGTATGCTA	ATGTTCGGCTTCCCATTCTCC
Ppia	AGGGTTCCTCCTTTCACAGAA	TGCCGCCAGTGCCATTA

Table 4. Sequences for mouse primers used for qPCR

5.8 Oxigen-Glucose Deprivation (OGD) *in vitro*

OGD (1h) was achieved by incubating oligodendrocytes in an anaerobic chamber, in which O_2 was replaced with N_2, and glucose with sucrose in an extracellular solution containing 130 mM NaCl, 5.4 mM KCl, 1.8 mM $CaCl_2$, 26 mM $NaHCO_3$, 0.8 mM $MgCl_2$, and 1.18 mM NaH_2PO_4, (pH 7.4). Oligodendrocytes culture medium was then replaced by this solution

(supplemented with sucrose 10mM 95% N_2 /5% CO_2, or glucose 10mM oxygenated with 95% O_2 /5% CO_2) prior to OGD to deplete the remaining glucose from extracellular spaces. Iodoacetic acid (IAA) was added to sucrose OGD solution to further inhibit glycolisis. After 1 hour of OGD, extracellular solution was replaced with medium and O_2 supply restored. CNO was present during the OGD (1 hour), and reoxygenation (24 hours) periods. Cell survival was determined 24 hours after OGD by Calcein-AM method (Life Technologies), using a colorimetric assay (Cytotoxicity Detection Kit; Roche Diagnostics) according to the manufacturer's instructions.

5.9 Cell viability assay

Cultured oligodendrocyte cell viability was measured 24 h after treatment by Calcein-AM method (Life Technologies). Cells were incubated with Calcein-AM at 1 µM and 37°C for 30 min in fresh culture medium and then, were washed in pre-warmed 0.1 M PBS for three times. Emitted fluorescence was measured by a Synergy HT (Biotek) spectrophotometer using excitation wavelength at 485 nm and emission at 528 nm. Values were represented as means or a percentage of cell survival in comparison with control cells (control cells, 100% viability).

5.10 Lactate measurements

5.10.1 Lactate assay kit

L(+)-Lactate is a metabolic compound formed by the enzyme Lactate Dehydrogenase (LDH) in proliferating cells and during anaerobic conditions. L(+)-Lactate present in the oligodendrocyte culture medium was detected using Lactat assay kit (Sigma #MAK064) according to the manufacturer's instructions. In this assay, lactate concentration is determined by an enzymatic assay, which results in a colorimetric (570 nm) product, proportional to the lactate present. Samples were centrifuged at 13,000g for 10 minutes and deproteinized with a 10 kDa MWCO spin filter to remove insoluble material and lactate dehydrogenase. The soluble fraction was assayed directly or kept at -80ºC.

5.10.2 FRET sensor for lactate

Oligodendrocytes were transfected with Laconic plasmid (3µg/10^6cells) using Amaxa™ Basic Nucleofector™ Kit for Primary Mammalian Glial Cells (lonza) following the manufacturer's guidelines. Then, oligodendrocytes were seeded into µ-Dish 35 mm plates (Ibidi) at 5.000 cells/plate and incubate with SATO$^+$ 0,1% FBS at 37°C and 5% CO_2 for 48h before assay. Afterward, the culture medium was replaced by extracellular solution (NaCl 140mM, KCl 5 mM, $MgCl_2$ 2mM; $CaCl_2$ 2mM, Glucosa 10mM and HEPES 10mM, pH:7,4) at 37°C, with 5% of CO_2 in a humidified incubator.

Laconic is a genetically encoded FRET sensors for lactate (Mächler *et al*., 2016). Laconic consists of a N-terminal mTFP (462 nm excitation /492 nm emission), followed by the LldR flanked by linkers, and finally a C-terminal mVenus (515 nm excitation /527 nm emission). The images were acquired through a 40X objective with a Zeiss LSM880 Airyscan microscope at an acquisition rate of 1 frame/10 s during 5 min. For data analysis, cell somata of 10-15 cells was selected as ROIs from 3 independent experiments. Background values were subtracted and data expressed as mTFP/mVenus fluorescence ratio.

5.11 Metabolism Analysis

Real time measurements of OCR and ECAR were performed using a Seahorse XFe96 Extracellular Flux Analyzer (Agilent). Oligodendroglial cells were seeded as a monolayer in a 96-well microplate and the analysis was performed following the manufacturer instructions. Before the assay, cells were washed and equilibrated in the XF Assay modified DMEM medium for 30 min at 37ºC. The real levels of oxygen consumption rate were determined in response to the sequential addition of oligomycin (2 mM), FCCP (1 mM) and rotenone/antimycin A (0.5 mM). Basal mitochondrial respiration was calculated as the last measurement before addition of oligomycin – non-mitochondrial respiration (minimum rate measurement after Rot/AntA). Spare capacity was calculated by subtracting basal respiration from the maximum rate measurement after addition of FCCP. Basal extracellular acidification rate (ECAR) was estimated by the last measurement before addition of CNO – the minimum

rate before oligomycin. All these parameters were obtained using the Agilent Report Generator.

5.12 Electrophysiology

Mice were anesthetized and decapitated and the brain was rapidly removed and placed in ice-cold (4◦C) cutting artificial cerebrospinal fluid (ACSF) containing (in mM): 215 Sucrose, 2.5 KCl, 26 $NaHCO_3$, 1.6 NaH_2PO_4, 20 Glucose, 1 $CaCl_2$, 4 $MGCl_2$, and 4 $MgSO_4$ bubbled with a mixture of 95% O_2/5% CO_2. Coronal slices, 400-µm thick, were cut on a Leica VT1200S vibratome and transferred to a warmed (~36°C) solution of low Ca^{2+} ACSF (ACSF) containing (in mM): 124 NaCl, 2.5 KCl, 10 Glucose, 25 $NaHCO_3$, 1.25 NaH_2PO_4, 1.25 $CaCl_2$, and 2.6 $MgCl_2$ for recovery (30 min). Then, acute coroncal slices were mantained at 30ºC in normal ACSF (nACSF) containing (in mM): 124 NaCl, 2.5 KCl, 10 Glucose, 25 $NaHCO_3$, 1.25 NaH_2PO_4, 2.5 $CaCl_2$, and 1.3 $MgCl_2$ during the recording. Compound action potentials (CAPs) were evoked by electrical stimulation of the *corpus callosum* with a bipolar electrode (CE2C55, FHC, USA) and were recorded with a pulled borosilicate glass pipette (1.6 MΩ resistance) filled with NaCl 3 M within the contralateral *corpus callosum*. Stimulation intensities ranged from 30 to 3000 µA (100µs pulses, Master-8, AMPI, Israel), and the recording strength was adjusted to evoke supramaximal stimulation (Tekkök & Goldberg, 2001).

Conduction velocity values for myelinated (N1) and partially myelinated (N2) fibers were calculated as the slope of a straight line fitted through a plot of the distance between the recording and stimulating electrodes *versus* the response latency (time to N1 and N2 respectively) in 4 different distances from the recording electrode (500, 1000, 1500 and 2000 µm).

To study acute pharmacological effects on propagated compound action potentials (CAPs), acute slices were perfused (1 mL/min) with aCSF continuously bubbled with 95% O2/5% CO_2 for 30 minutes (stimulus pulse of 30 µs duration, delivered every 30 s).

To simulate ischemia, glucose was replaced with 10 mM sucrose, and 95% O_2 /5% CO_2 was replaced with 95% N_2 /5% CO_2 for 30 minutes, followed by a recovery period of 30 minutes

perfused with normal ACSF. All compounds and antagonists were applied concomitantly with ischemia stimulation and recovery phase. Peak amplitudes and latencies were calculated using custom written routines in pCLAMP 10.0 (Molecular Devices, USA) and the baseline of the stimulus artefact was substracted in all cases.

To analyze CAPs amplitude after high frequency stimulation (HFS) recordings, CAPs from interhemispheric fibres were recorded at 0.2 Hz to obtain baseline, and then were challenged with a gradual increase in stimulation frequency (from 1 to 100 Hz), with each stimulus trainlasting 30 s. For 1 and 5 Hz stimulations, CAPs were continuously recorded. For 10, 25, 50, and 100 Hz stimulations, CAPs were sampled after a burst of each 100 *stimuli* with an inter-burst interval of 300 ms. CAP area of the graded responses were analyzed for each treatment group (2.1 ms after stimulus onset) and normalized to baseline.

6. STATISTICAL ANALYSIS

Data are presented as mean ± s.e.m. with sample size and number of repeats indicated in the figure legends. Statistical analysis were performed using absolute values and GraphPad Prism software (GraphPad Software) applying the corresponding statistical treatment for each experiment, as mentioned in figure captions. Comparisons between two groups were analysed using paired Student's two-tailed t-test for data coming from *in vitro* experiments and unpaired Student's two-tailed test for data coming from *in vivo* experiments, except in MOG-EAE experiments where statistical significance in neurological score was determined by Mann-Whitney U test. Comparisons among multiple groups were analysed by one-way ANOVA analysis of variance followed by Tukey *post hoc* test. Statistical significance was considered at $p < 0.05$.

RESULTS

PART I. ROLE OF CLEMASTINE IN MYELINATION DURING DEVELOPMENT

1.1 Clemastine increases proliferation of the oligodendroglial lineage *in vitro*

Previous studies have shown that clemastine and other muscarinic antagonists promote oligodendrocytes differentiation *in vitro* (Liu *et al*., 2016; Mei *et al*., 2016; Wang *et al*., 2018). Therefore, we analyzed the acute (24h) and chronic (3 days *in vitro*, DIV) effect of clemastine in oligodendrocyte cultures from optic nerves of P12 rats.

Initially, we verified that these treatments did not significantly affect the viability of oligodendrocytes using increasing concentrations of clemastine up to 250nM. Cell viability was assessed using Calcein-AM method as previously described (Ruiz *et al*., 2014). Clemastine did not significantly modifiy basal oligodendroglial survival **(Figure 12.A)**. Then we analyzed whether clemastine (250nM) could affect to oligodendrocyte survival under pathological conditions, either protecting or increasing cell death (Figure 12.B). For that, we performed an *in vitro* chemical ischemia model in which glucose and oxygen are replaced by sucrose and nitrogen (Oxygen glucose deprivation, OGD). Ischemic condition was further enhanced by iodoacetic acid (IAA), an inhibitor of glycolysis (Domercq *et al*., 2010). However, we did not observe any significant difference in oligodendrocyte survival between control and clemastine treated cells, neither in mild (IAA 20µM) nor severe (IAA 50µM) ischemia.

Once we analyzed the viability of oligodendrocytes exposed to clemastine, we studied its effect on oligodendrocyte proliferation and differentiation by immunocytochemistry. We quantified the number of $NG2^+$ OPCs and $Ki67^+$ OPCs (a proliferation marker), after 24 hours and 3 days of treatment *in vitro*. Results showed a significant increase in the number of $NG2^+$ cells **(Figure 13.A)** and $Ki67^+$cells **(Figure 13.B)**, suggesting that clemastine modulates the proliferation of OPCs.

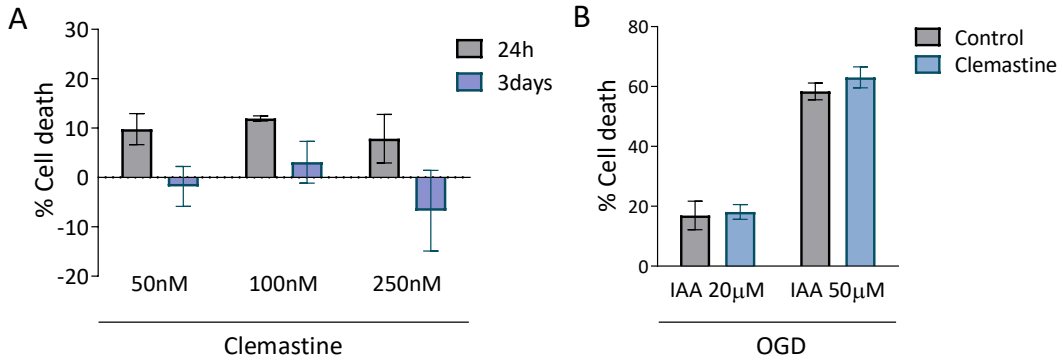

Figure 12. A. Cell viability assays in oligodendrocytes *in vitro* after exposure to increasing concentrations of clemastine (24h and 3DIV). **B.** Cell death after ischemia *in vitro* induced by oxygen and glucose deprivation (OGD) in the presence of iodoacetic acid (IAA) (20µm and 50µm) in control and clemastine (250nM) treated oligodendrocytes. Data represent mean ± s.e.m. from n = 3 independent experiments performed in triplicate.

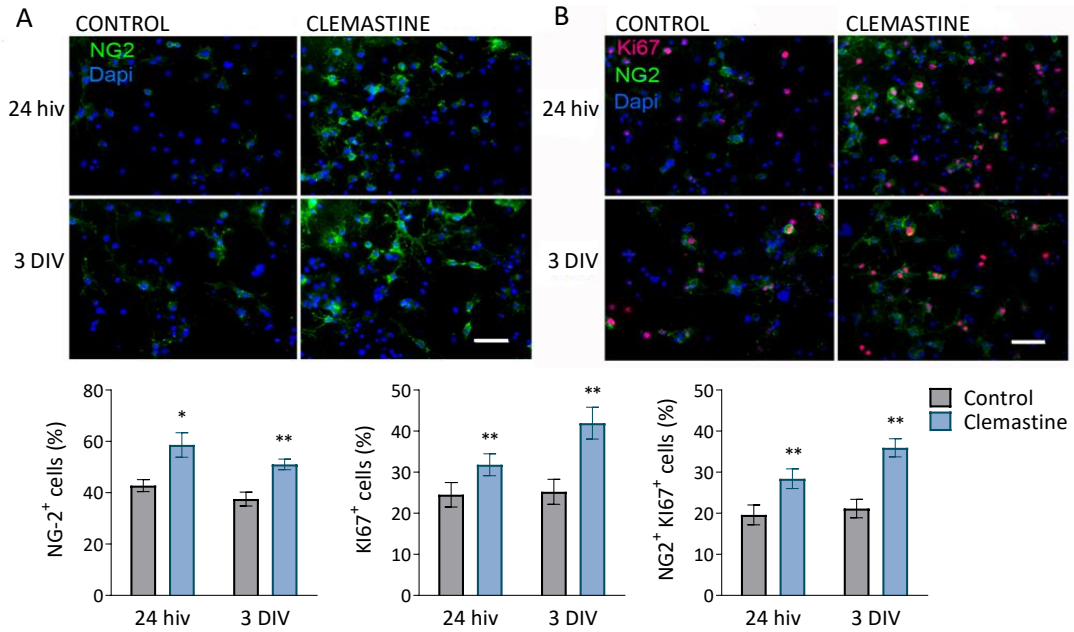

Figure 13. Effect of clemastine on the proliferation and differentiation of cells of the oligodendroglial lineage in cultures from the optic nerve of P12 animals. **A**. Quantification of $NG2^+$ cells in presence and absence of clemastine (250 nM, 24 h and 3 DIV). **B.** Effect of clemastine on proliferation, analyzed by the quantification of $Ki67^+$ cells and double labeled cells ($NG2^+$ $Ki67^+$). Data expressed in percentage vs total number of cells (n = 3 independent experiments). Scale bar = 50 µm. *p<0.05, **p<0.01

Next, we quantified the number of mature and myelination oligodendrocytes using the MBP (myelin basic protein) marker. However, contradicting previous results (Mei *et al*., 2014, Mei *et al*., 2016), the treatment with clemastine did not promote the differentiation in oligodendrocyte cultures, neither after 24 hours nor 3 days *in vitro* **(Figure 14.A)**. This result was further confirmed by western blot analysis. Indeed, the expression of MBP was significantly reduced in oligodendrocytes after 3 days of treatment with clemastine **(Figure 14.B)**.

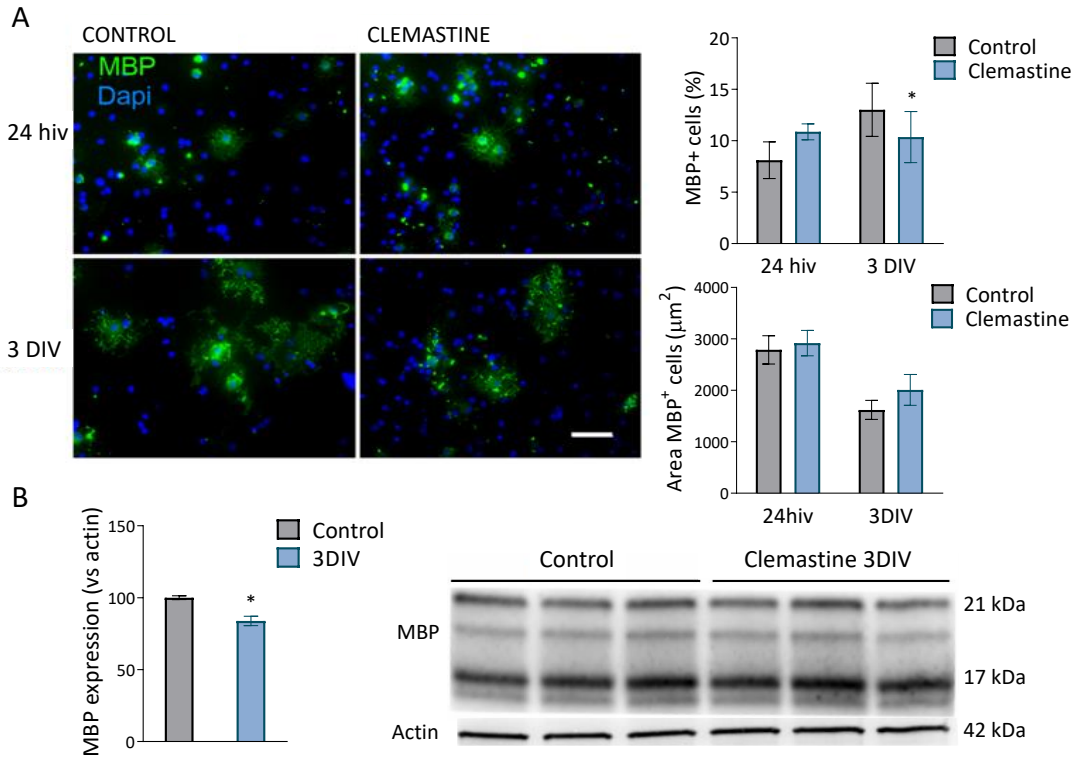

Figure 14. Effect of clemastine on the differentiation of oligodendroglial lineage cells *in vitro*. **A.** Quantification of the number of mature MBP⁺ oligodendrocytes cells in the presence and absence of clemastine (250 nM, 24 hiv and 3 DIV) and analysis of oligodendrocyte area, an indicative of its morphology. Data expressed in percentage vs total number of cells per area **B**. MBP expression in oligodendrocytes in control and clemastine treated cultures, as analyzed by western blot. MBP expression was normalized to actine. n = 3 independent experiments performed in triplicate. Scale bar = 50 µm. *p<0.05.

To exclude that the absence of effect in the differentiation is due to the concentration of clemastine, we incubated the cells with increasing concentrations (250nM, 500nM and 1 µM). Again, higher concentrations of clemastine induced an increase in proliferation but we did not observe any effect on differentiation **(Figure 15)**.

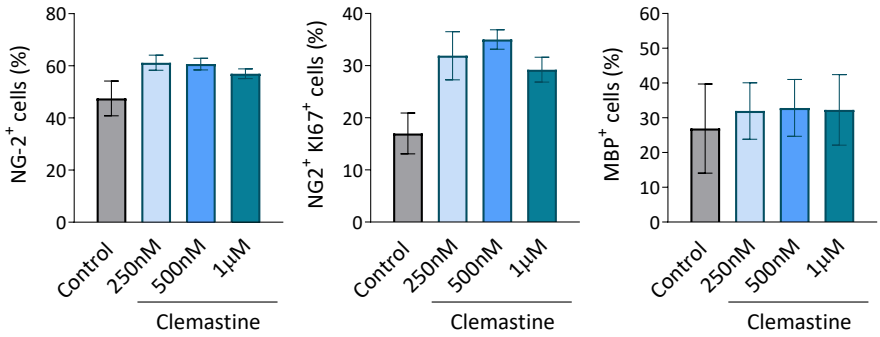

Figure 15. Effect of increasing concentrations of clemastine in OPCs proliferation, as analyzed using the OPC marker NG2 and the proliferation marker Ki67; and in oligodendrocyte differentiation, as analyzed using the myelin marker MBP. Analysis performed in cultured oligodendrocytes from rat-P12 optic nerve (n = 3 independent experiments).

1.2 Clemastine antagonizes the muscarinic acetylcholine receptor subtype 1 (Chmr1)

Previous reports described that the action of clemastine is due to the interaction with the muscarinic cholinergic receptor Chrm1 (Mei *et al*., 2016). Muscarinic M1 receptors, however, are genetically expressed more abundantly in OPCs than in mature oligodendrocytes **(Figure 16)**, and this may modulate both OPC proliferation and differentiation (de Angelis *et al*., 2012; Deshmukh *et al*., 2013; Mei *et al*., 2014).

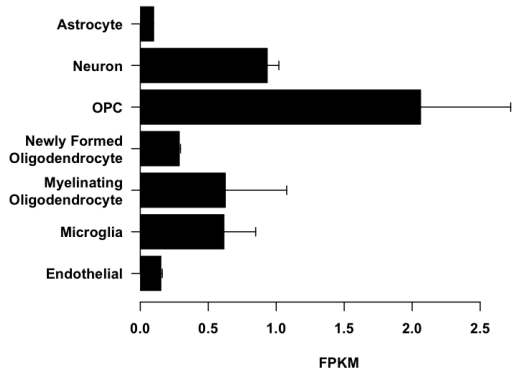

Figure 16. Gene expression of the muscarinic receptor Chrm1 in oligodendroglial lineage cells and other cell types of the brain, according to data obtained from Zhang *et al*. (2014).

In order to identify the cellular subtype and the mechanism of action of clemastine, we performed intracellular calcium imaging using the Fluo-4 indicator in cultured oligodendrocytes. To determine the magnitude of the response in OPCs and in mature oligodendrocytes, the recordings were performed at 24 hours and 3 days *in vitro* (24hiv, 3DIV) **(Figure 17.A)**. According to the genetic expression profile of Chrm1, the number of cells that respond to muscarine, as well as the magnitude of the response (area under the curve) were significantly higher in OPCs (24 hiv cultured oligodendrocytes) than in oligodendrocytes (3 DIV cultured oligodendrocytes) (**Figure 17.B)**. In addition, the cellular response was corroborated in acute cerebral slices from PLP-DsRed mice, that allow to identify mature oligodendrocytes **(Figure 17.C)**.

Altogether, these experiments confirm the abundant expression of functional M1 receptors in OPCs, and their role in OPC proliferation *in vitro*, but not in differentiation. However, given that these results are controversial based on previous literature (Liu *et al*., 2016; Mei *et al*., 2016; Wang *et al*., 2018), and the limitations of the *in vitro* models, we further characterized the effect of *in vivo* clemastine treatment in C57BL/6 wild-type mice.

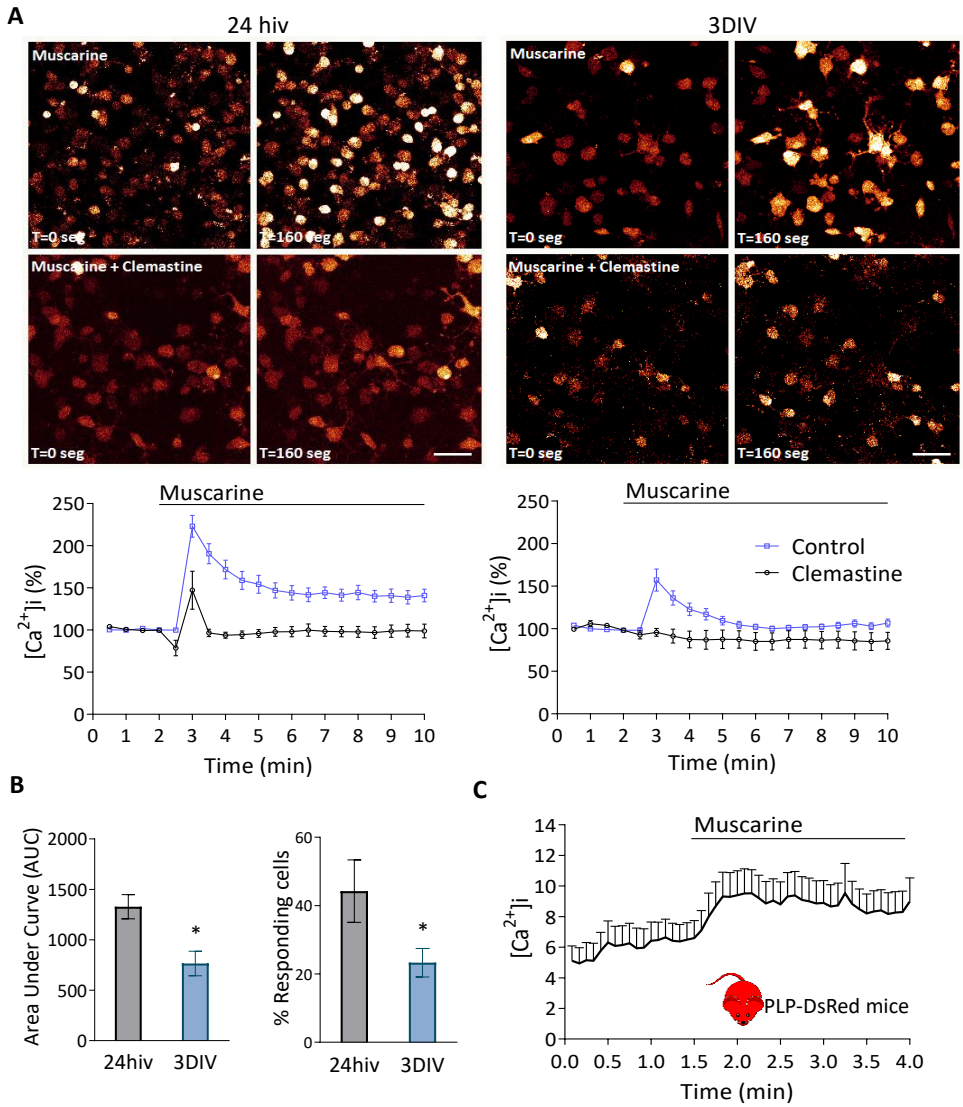

Figure 17 Oligodendrocytes express functional muscarinic receptors *in vitro*. **A**. Images and traces of Ca^{2+} responses in oligodendrocytes at 24 hiv and 3 DIV following application of muscarine (500 nM) using Fluo-4. Data represent average ± SEM of values obtained from more than 50 cells from 3 different cultures. **B**. Quantification of the number of cells that respond and the area under the curve. **C.** Calcium imaging recording in acute cerebral slices from PLP-DsRed mice. Muscarine induces an increase in intracellular calcium in $DsRed^{+}$ oligodendrocytes. Data come from n = 3 PLP-$DsRed^{+}$ mice. Scale bar = 50 µm. Recordings were performed with the calcium indicator Fluo4. * $p<0.05$.

1.3 Clemastine induces oligodendrocyte differentiation *in vivo*

Clemastine, as well as other M1R antagonists such as benzotropine, promote remyelination in animal models of multiple sclerosis (Deshmukh *et al*., 2013; Mei *et al*., 2014), after hypoxia (Cree *et al*., 2018; Wang *et al*., 2018) and prevent demyelination secondary to aging and in Alzheimer's disease (J. F. Chen *et al*., 2021; Wang *et al*., 2020). On the other hand, abnormalities in myelination during development cause cognitive dysfunction and are associated to behavioral disturbances in neurodevelopmental psychiatric disorders. However, little is known about the effect of clemastine in the absence of myelin abnormalities or demyelinaton.

To determine whether clemastine treatment *in vivo* promotes myelination during development, we treated mice with clemastine (50mg/kg/day, i.p.) or vehicle from postnatal day 5 to 20, a time window coincident with myelination and within the critical period of brain plasticity **(Figure 18.A)**. We first quantified the population of OPCs and mature oligodendrocytes using antibodies against PDGFRa and CC1 (anti-APC), respectively. We performed blinded cell counts in three different areas, *corpus callosum* (CC), retrosplenial cortex (Rsp Ctx) and primary somatosensorial cortex (SSp Ctx), on anatomically equivalent brain sections and normalized our counts using the pan-OL marker Olig2.

In contrast to our *in vitro* results but in concordance with previous *in vitro* and *in vivo* studies (Mei *et al*., 2014, 2016), clemastine induced a significant increase in the proportion of APC^+ oligodendrocytes in *corpus callosum* as well as in the cerebral cortex **(Figure 18.B)**. In parallel, we detected a decrease in the proportion of $PDGFR^+$ OPCs in *corpus callosum*. In contrast, no change in the number of $PDGFR^+$ OPCs was detected in cerebral cortex **(Figure 18.C)**. These results indicate that the treatment with clemastine during development promotes the maturation of the oligodendroglial lineage by increasing the percentage of APC^+ oligodendrocytes, particularly in the *corpus callosum*.

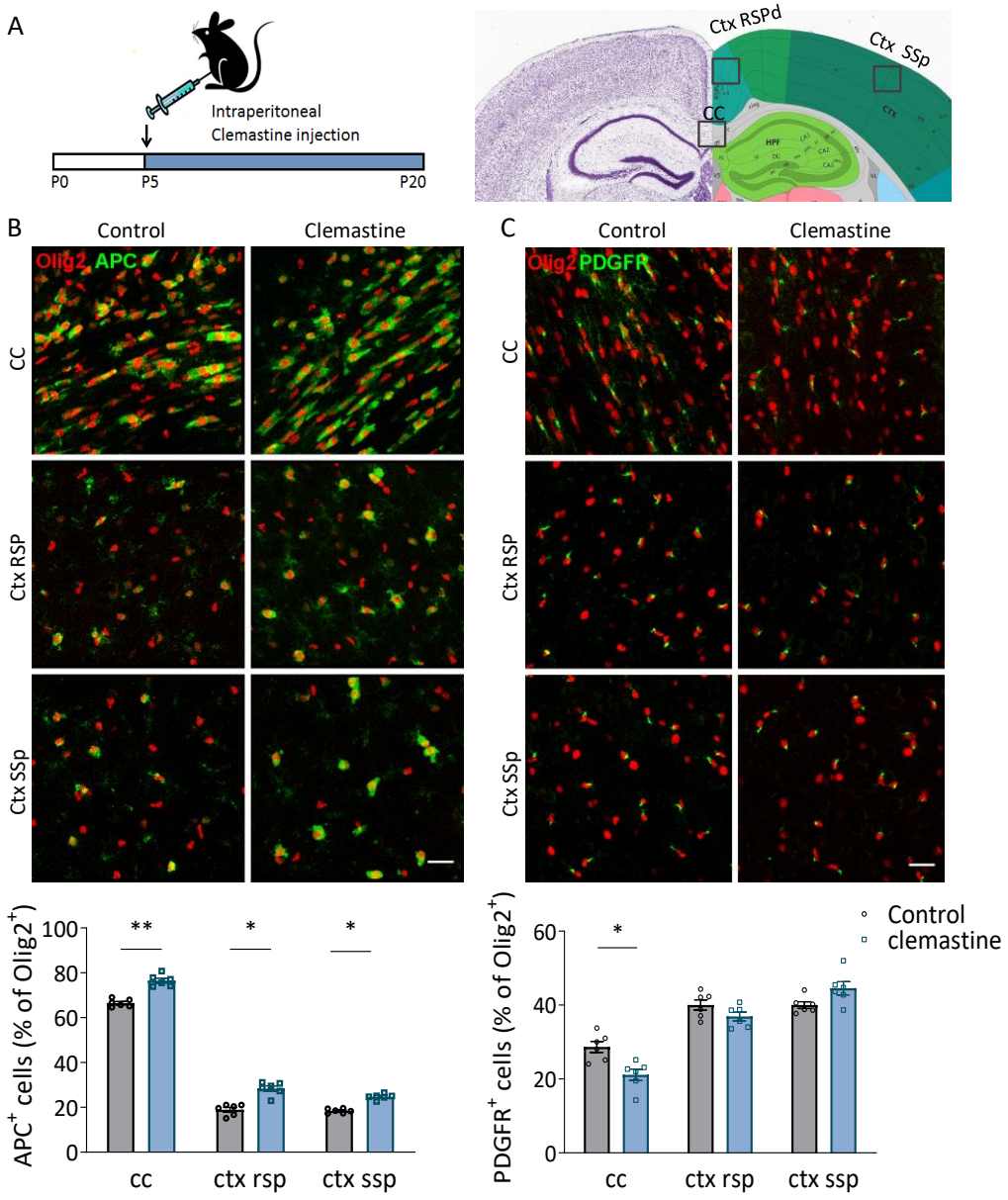

Figure 18. A. Schematic representation of clemastine treatment (50µg/kg; i.p.) during development. The analysis was performed in *corpus callosum* (cc), retrosplenial cortex (ctx rsp) and primary somatosensory cortex (ctx ssp). **B, C.** Compressed confocal z stack images of APC$^+$ mature oligodendrocytes (B) and PDGFR$^+$ oligodendrocyte precursor cells (C; OPCs) in cc, ctx rsp and ctx ssp of control and clemastine-treated mice. Below, average of the percentage of mature oligodendrocytes (B) or OPCs (C) vs total Olig2$^+$ oligodendroglial cells (Olig2$^+$) (n= 6 mice per experimental group). Scale bar = 50 µm. *p<0.05, **p<0.01.

1.4 Conduction velocity in *corpus callosum* decreases after clemastine treatment.

As clemastine induced a clear increase in oligodendrocyte differentiation in the *corpus callosum*, we hypothesized that this would translate into accelerated myelination and a subsequent increase in the conduction velocity in white matter. To test this idea, we measured the propagation of compound action potential (CAPs) in the *corpus callosum* by performing electrophysiological recordings in acute coronal brain slices. CAPs were evoked by a bipolar stimulating electrode and recorded by a field electrode placed at varying distances across the *corpus callosum* **(Figure 19.A).**

Surprisingly, our results revealed that action potentials transmission is significantly slower in myelinated axons (N1) of clemastine-treated mice compared to control mice **(Figure 19. B)**. In contrast, the conduction velocity in unmyelinated axons (N2) is similar between groups **(Figure 19. B)**. Examining the relationship between stimulus intensity and response magnitude (input-output curve) revealed that myelinated axons in clemastine-treated mice tend to be more excitable than those in control mice **(Figure 19.C).** Therefore, we concluded that clemastine induced a delay in action potential propagation despite the effect in oligodendrocytes differentiation.

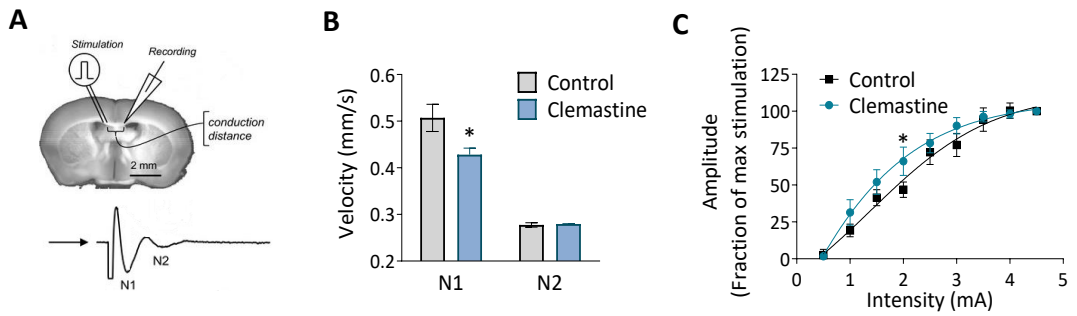

Figure 19. A. Schematic representation of compound action potentials (CAPs) recording in *corpus callosum* of 400µm coronal slices. **B.** Conduction velocity corresponding to N1 and N2 peaks in vehicle (n= 12) and clemastine-treated mice (n= 10). For each mouse, the average measure come from at least four different sections recorded three times. **C.** The input-output relationship for N1 myelinated fibers is left-shifted in clemastine-treated *corpus callosum* (n= 10-12). *p<0.05

1.5 Clemastine reduces the number of nodes of Ranvier and myelinated axons in *corpus callosum*.

Since the increase in the percentage of mature oligodendrocyte is not accompanied by an increase in the conduction velocity of N1 fibers in *corpus callosum*, myelination was further studied by performing histological analysis both by confocal and transmission electron microscopy (TEM). The speed of action potential conduction depends on the length and the number of the nodes of Ranvier, in addition to myelin sheaths number and structure. Therefore, node length is plastic and refined in response to electrical activity (Arancibia-Cárcamo *et al*., 2017). We immunolabeled coronal brain sections with antibodies against contactin-associated protein (Caspr) and sodium-gated channels 1.6 (Nav1.6) to visualize paranodes and nodes of Ranvier respectively. By identifying regions of dense Nav1.6 staining that were clearly flanked by abutting $Caspr^+$ paranodes, we quantified the length of individual nodes within *corpus callosum* in control and clemastine-treated mice. We did not find any change in nodal length **(Figure 20.A)**. However, we detected a significant reduction in the number of nodes of Ranvier in clemastine-treated mice **(Figure 20.A)**. We measured the length of internodes that were flanked on each end by $Caspr^+$ paranodes. We found that clemastine treatment tend to increase internode length, although the differences were not significant **(Figure 20.B)**. The high density of myelin sheaths in *corpus callosum* made it difficult to look for differences using confocal microscopy.

So, we next used TEM to visualize myelination. TEM images were taken of the *corpus callosum* directly above the dorsal hippocampus from anatomically equivalent tissue sections from control and clemastine-treated mice. We observed that the number of myelinated axons was reduced after clemastine treatment **(Figure 20.C)**. Myelin thickness was assessed by g-ratio calculation (axon diameter/total outer diameter of myelinated fiber). G-ratio analysis revealed thinner myelin sheaths in small caliber axons (0-0.5 µm) of treated animals, while no differences were found in axons from 0.5 to 1 µm diameter, indicating that the changes observed in myelin thickness depend on axons diameter **(Figure 20.C)**. Taken together, our findings suggest that, although clemastine treatment during development initially enhances oligodendrocyte differentiation, functional myelination is impaired.

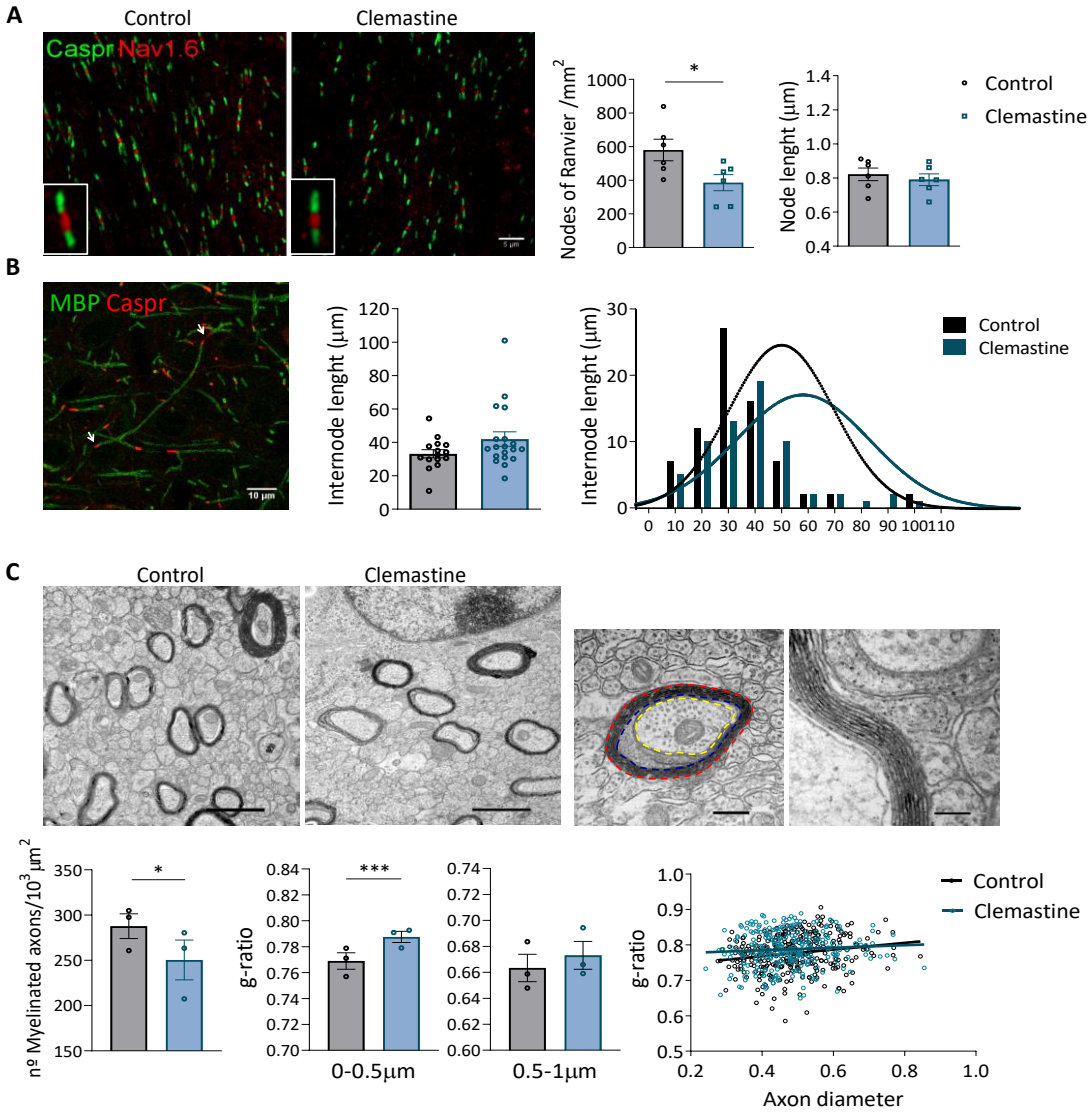

Figure 20. A. Representative confocal images of nodes of Ranvier ($Na_v1.6$; red) and paranodes (Caspr; green) in *corpus callosum* of control and clemastine treated mice. Scale bar = 5 µm. Rigth, histograms show average node of Ranvier number and length in control and clemastine-treated mice (n= 6 per experimental group). **B.** Representative confocal images of MBP^+ myelin internodes (green) flanked by two $Caspr^+$ paranodes (red; arrows). *Right*, average and cumulative internode length distribution in control and clemastine-treated mice (n= 6 per group). Scale bar = 10 µm **C.** Representative electron microscopy images of myelinated axons within *corpus callosum* in control and clemastine treated mice. Graphs represent the average of myelinated axons (at least 60 different images per animal from n= 3 mice per group), the mean g-ratios for small and bigger axons (100-150 axons in control and clemastine-treated mice) and the distribution of g-ratios for control and clemastine-treated mice (n=3 mice per group). *p<0.05; *** p<0.001

1.6 Clemastine treatment modifies the expression of activation markers and morphology of microglia in developing brain.

In addition to electrical activity, a new player in developmental and adaptive myelination is microglia cells (Geraghty *et al*., 2019; Wlodarczyk *et al*., 2017). Chmr1, the receptor mediating clemastine-effect in oligodendrocytes, is also expressed in microglia, as reported from previous RNAseq analysis (Zhang *et al*., 2014) **(Figure 16)**. Indeed, cultured microglia cells exposed to muscarine showed a significant increase in cytosolic calcium, as revealed with Fluo4- calcium imaging **(Figure 21)**. We hypothesized that the impairment in myelination during development could be related to the interaction of clemastine with microglia cells. Hence, we analyzed the impact of clemastine on microglial cells during development.

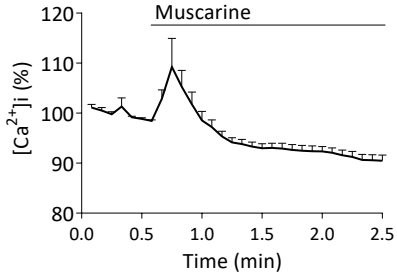

Figure 21. Recordings of Ca^{2+} responses in microglia *in vitro* following application of muscarine (100 µM) using Fluo-4 indicator. Data represent average ± SEM of values obtained from more than 50 cells from 3 different cultures.

Clemastine treatment did not alter the number of microglia cells nor the immunoreactivity of $Iba1^{+}$, ruling out a global impact on microglial population **(Figure 22.A)**. Additionally, we examined the morphology of $Iba1^{+}$ microglia from control and treated mice. For that, we quantified the number of branches and junctions per cell, as well as the cellular complexity as determined by *sholl* analysis. Both data demonstrated an increase in the morphology complexity and ramification in microglia from clemastine treated mice **(Figure 22.B)**. Since the activation state of microglia is determinant for the remyelination capacity of OPCs (Zabala *et al*., 2018), we wondered whether clemastine could alter microglia activation state. Clemastine induced a massive reduction in the expression of iNOS, a proinflammatory marker, as well as the expression of the phagocytic marker CD68 **(Figure 22.C, D)**. All these data suggest that clemastine impacts on microglia cells too during development.

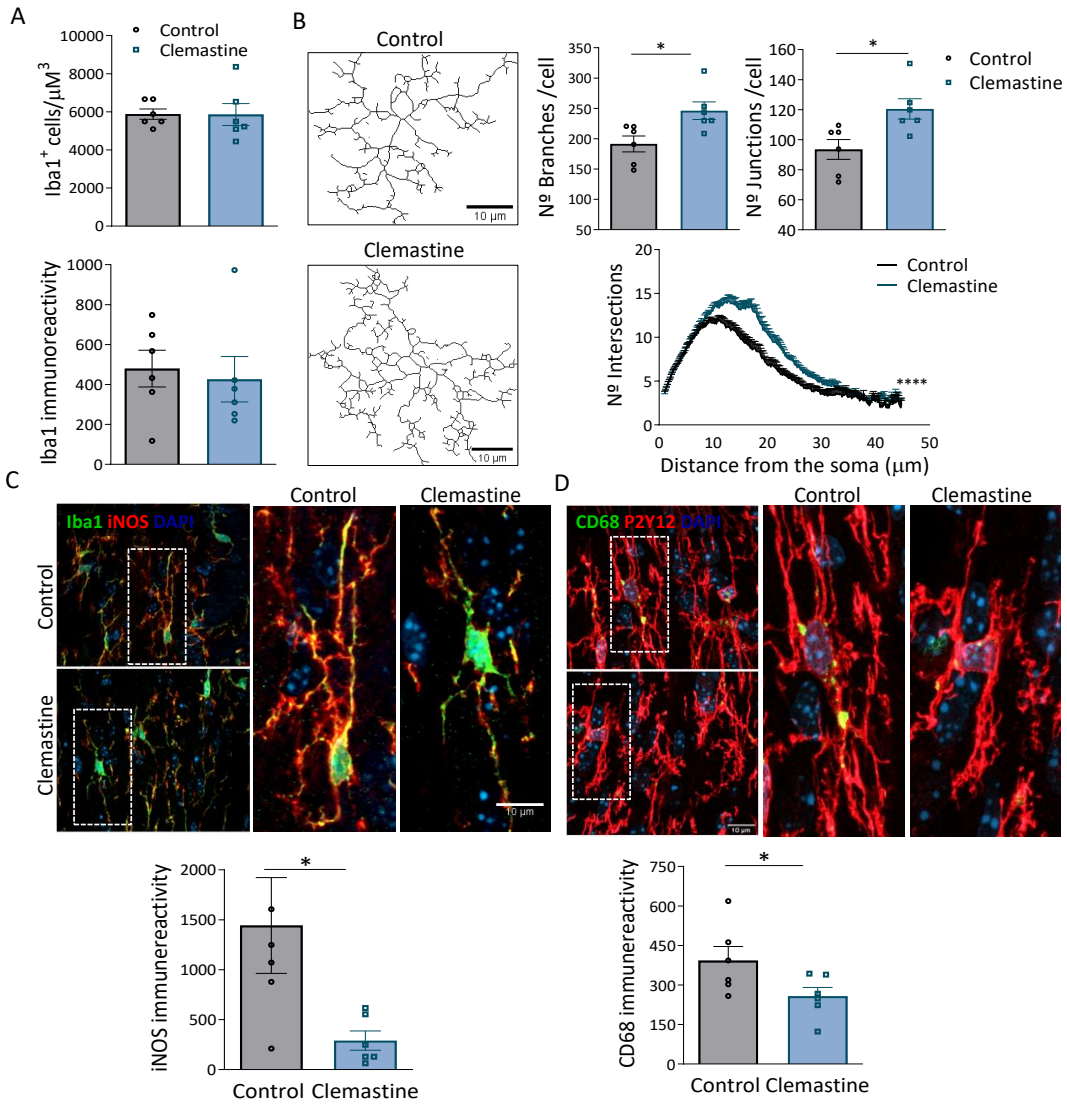

Figure 22. A. Quantification of the number of Iba1+ microglia cells as well as Iba1 staining intensity in *corpus callosum* of control and clemastine-treated mice. **B.** Representative skeletonized images of microglia used for morphological analysis. Scale bar = 10 µm. Graphs show average of the number of branches, junctions and *sholl* analysis of microglia in control and clemastine-treated mice. **C, D.** Representative compressed z confocal images showing the expression of iNOS, a pro-inflammatory marker, and CD68, a phagocytic marker, in Iba1^{+} microglia in *corpus callosum* of control and clemastine-treated mice. Scale bar = 10 µm. Graphs show the average P2y12 and CD68 staining intensity (n= 6 mice per group). *p<0.05.

We further explored the expression of pro-inflammatory/anti-inflammatory genes, lipid and phagocytosis markers as well as growth factors involved in developmental myelinogenesis and adaptive myelination (Geraghty *et al*., 2019; Wlodarczyk *et al*., 2017) in FACS isolated microglia. Although we did not find changes in pro-inflammatory markers, we observed a significant upregulation of anti-inflammatory markers **(Figure 23.A)**. In contrast, the expression of ApoE and CD36, genes involved in metabolism and phagocytosis respectively, was significantly downregulated. Notably, clemastine induced a significant reduction in *IGF* expression in microglia **(Figure 23.A)**. CD11c$^+$ microglia has been described as a microglial subset expressed transiently in *corpus callosum* during development that play a pivotal role in myelinogenesis since it is the main source of IGF, a growth factor essential for myelinogenesis.

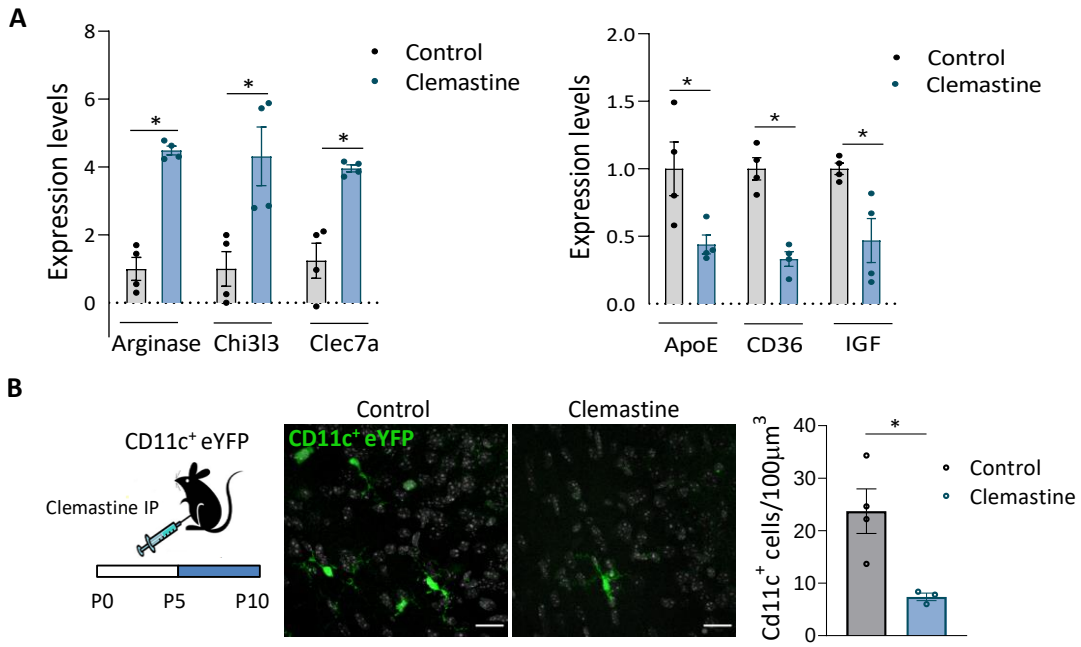

Figure 23. A. Gene expression of *Arginase*, *Chi3l3* and *clec7a*, anti-inflamatory markers, of *ApoE*, a disease associated marker, of *CD36*, a phagocytic marker and of *IGF*, a growth factor involved in myelinogenesis. The expression levels of genes are presented using fold-change values transformed to Log2 format compared to control (n= 4 mice per group). **B.** Analysis of the number of CD11c$^+$ cells in control and clemastine treated CD11-eYFP mice. Representative z confocal images and histogram showing that clemastine reduced the number of CD11c$^+$ cells (n= 3-4 mice per group). Scale bar = 20 µm.*p<0.05.

We next analysed, using $CD11c^+$ eYFP reporter mice, the impact of clemastine in this cell type population. Since $CD11c^+$ microglia is a transient population that disappears early during development, we treated mice with clemastine from P5 to P10. Blind analysis showed that clemastine treatment reduced the number of $CD11c^+$ microglia in *corpus callosum* **(Figure 23.B)**. Altogether, these results are consistent with the hypothesis that activation of muscarinic receptors expressed in microglia with clemastine can impair myelin development.

PART II. IMPACT OF PHARMACOGENETIC STIMULATION OF OLIGODENDROCYTES IN MYELINATION / REMYELINATION

2.1 PLP-CreERT2^{+}/hM3Dq$^{+/+}$ mice generation

To investigate the consequences of activating adult oligodendrocytes *in vivo*, we used Designer Receptors Exclusively Activated by Designer Drugs (DREADD) based technology (Armbruster *et al*., 2007). DREADDs are mutationally modified muscarinic acetylcholine (ACh) receptors, which can be specifically expressed in a targeted cell population and exclusively activated by the designer drug clozapine N-oxide (CNO), but not by their endogenous ligand ACh (Armbruster *et al*., 2007; Rogan & Roth, 2011). In this study, we used the excitatory Gq-DREADDs inserted into PLP+ oligodendrocytes to selectively activate mature oligodendroyctes, not OPCs. Cre-dependent excitatory Gq-DREADD mice (R26-LSL-Gq-DREADD or hM3Dq$^{+/+}$ mice (Jackson laboratory) were crossed with PLP-CreERT2 mice (assigned by Dr. F. Kirchhoff) to express hM3Dq in PLP+ oligodendrocytes. PLP-CreERT2 mice express the Cre recombinase enzyme in mature oligodendroctyes after tamoxifen administration, providing specific spatial and temporal control of hM3Dq expression. Using this pharmacogenetic tool we studied the effect of acute and chronic stimulation of mature oligodendrocytes on myelination, remyelination, metabolic coupling and axon-oligodendroglial survival.

The generation of these transgenic mice was crucial for the development of the entire project. To address this, R26-LSL-Gq-DREADD mice (hM3Dq$^{+/+}$) were crossed with PLP-CreERT2 mice to generate PLP-CreERT2/hM3Dq$^{+/+}$ mice, following the next breeding scheme **(Figure 24)**:

- Firstly, HM3Dq homozygous (hM3Dq$^{+/+}$) mice were bred with PLP-CreERT2 mice. From these offspring we selected animals PLP-CreERT2^{+} and heterozygotes hM3Dq-loxP (hM3Dq$^{+/-}$) **(Figure 24.A)**.
- Then, PLP-CreERT2^{+}/hM3Dq$^{+/-}$ mice were bred with homozygous mice hM3Dq (hM3Dq$^{+/+}$). Approximately 25% of the offspring of this cross was homozygous for the

hM3Dq gene and hemizygote for PLP-CreERT2. These mice were selected following Mendelian law in combination with qPCR, to establish the final colony **(Figure 24.B)**.

- Finally, we amplified the colony by breeding homozygous hM3Dq$^{+/+}$ and hemizygotes PLP-CreERT2 mice (hereinafter termed PLP-CreERT2^{+}/hM3Dq$^{+/+}$ mice or hM3Dq$^{+/+}$ mice) **(Figure 24.C)**. Control littermates PLP-CreERT2^{-}/hM3Dq$^{+/+}$, lacking PLP-Cre, as well as PLP-CreERT2^{+}/hM3Dq$^{+/+}$ mice without CNO treatment were used as controls.

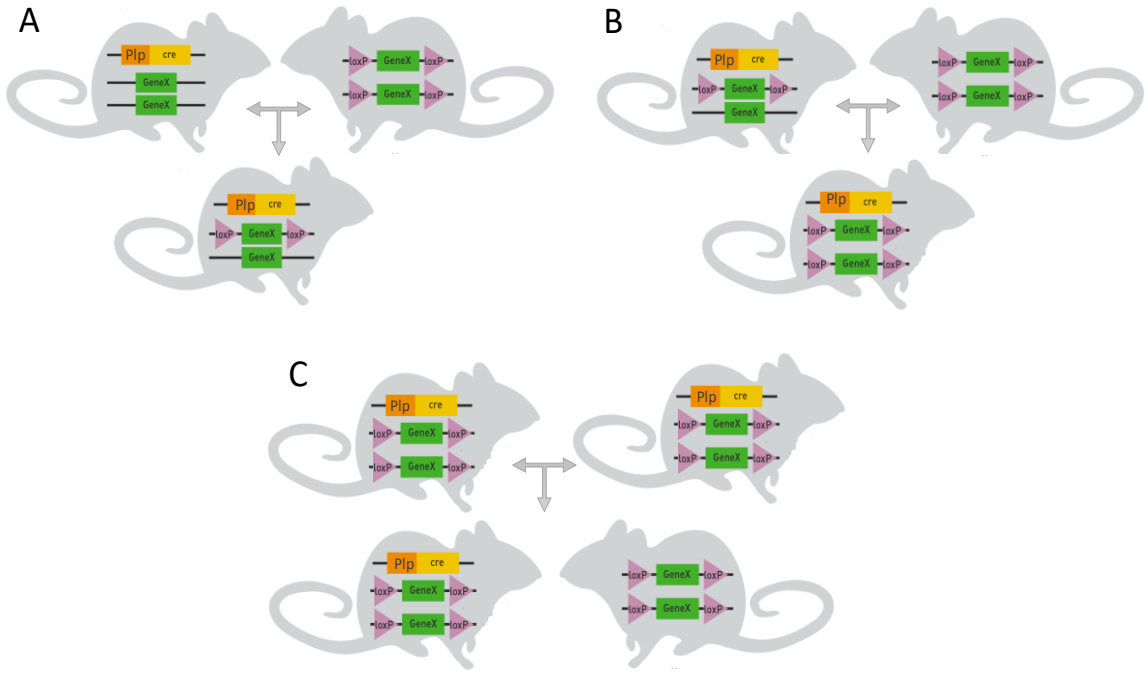

Figure 24. Schematic representation of the breeding steps to generate PLP-CreERT2/hM3Dq$^{+/+}$ transgenic mice **A.** Homozygous hM3Dq$^{+/+}$ mice were breed with PLP-CreERT2 mice. **B.** The PLP-CreERT2^{+}/hM3Dq$^{+/-}$ mice were backcrossed to homozygous mice hM3Dq (hM3Dq$^{+/+}$) to obtain the final colony PLP-CreERT2^{+}/hM3Dq$^{+/+}$. **C**. Breeding PLP-CreERT2^{+}/hM3Dq$^{+/+}$ mice give us PLP^{+} and PLP^{-} littermates, the latter ones used as controls.

2.2 Functional characterizaction of PLP-CreERT2^{+}/hM3Dq$^{+/+}$ mice

We characterized the degree of recombination in PLP-CreERT2^{+}/hM3Dq$^{+/+}$ mice after tamoxifen administration by means of Cre-mediated reporter expression. Tamoxifen was administered to P27 mice by intraperitoneal injection for three consecutive days, and after a washout period of 15 days, the animals were perfused to histologically quantify the

percentage of hM3Dq^{+}GFP^{+} oligodendrocytes **(Figure 24.A)**. First, we analyzed the recombination in *corpus callosum* and within the layers II-III of three different regions of the cerebral cortex (ventral and dorsal retrosplenial cortex and primary somatosensory cortex).

The number of GFP^{+} oligodendrocytes was normalized versus Olig2^{+} cells, a pan-oligodendrocyte marker **(Figure 24.B)**. We obtained a recombination level of 80-90 % in *corpus callosum* and in the retrosplenial area of the cerebral cortex. The percentage of recombination decreased progressively through dorsal areas of cerebral cortex. This result indicates that the percentage of OPCs differentiated into mature oligodendrocytes varies between different cerebral regions as expected according to temporal control of myelination. Thus, *corpus callosum* and retrosplenial cortex are myelinated before than somatosensory cortex. However, Cre-mediated reporter expression demonstrated that virtually all recombined cells were of mature APC^{+} oligodendrocytes **(Figure 24.C)**. Since the recombination was performed at P27, the lower percentage of APC^{+} GFP^{-} oligodendrocytes could represent oligodendrocytes that differentiated after tamoxifen administration.

Then, in order to functionally evaluate the expression of the hM3Dq receptor, we performed calcium imaging recordings in oligodendrocytes *in vitro* and in slices. For cultures, PLP-CreERT2^{+}/hM3Dq$^{+/+}$ pups were treated with tamoxifen for two days (P14-15), and after five days of washing **(Figure 24.A)**, we performed cultures of oligodendrocytes derived from the optic nerve according to previously described methodology (Barres *et al*., 1992). Acute stimulation with clozapine-N-oxide (CNO; 100 µM) produced a significant increase in intracellular calcium concentration, as revealed by Fluo-4 confocal imaging **(Figure 24.D)**. Some cells, as can be seen in the graph, presented an oscillating or rhythmic stimulation pattern, characteristic of metabotropic receptors. In addition, CNO also induced calcium signaling in subcortical white matter oligodendrocytes in acute slices **(Figure 24.E)**. Collectively, these data demonstrate that CNO evokes a specific and robust activation response in mature oligodendrocytes expressing the hM3Dq receptor and therefore the transgenic mice are a valuable genetic tool to analyze the impact of this activation in oligodendrocyte function.

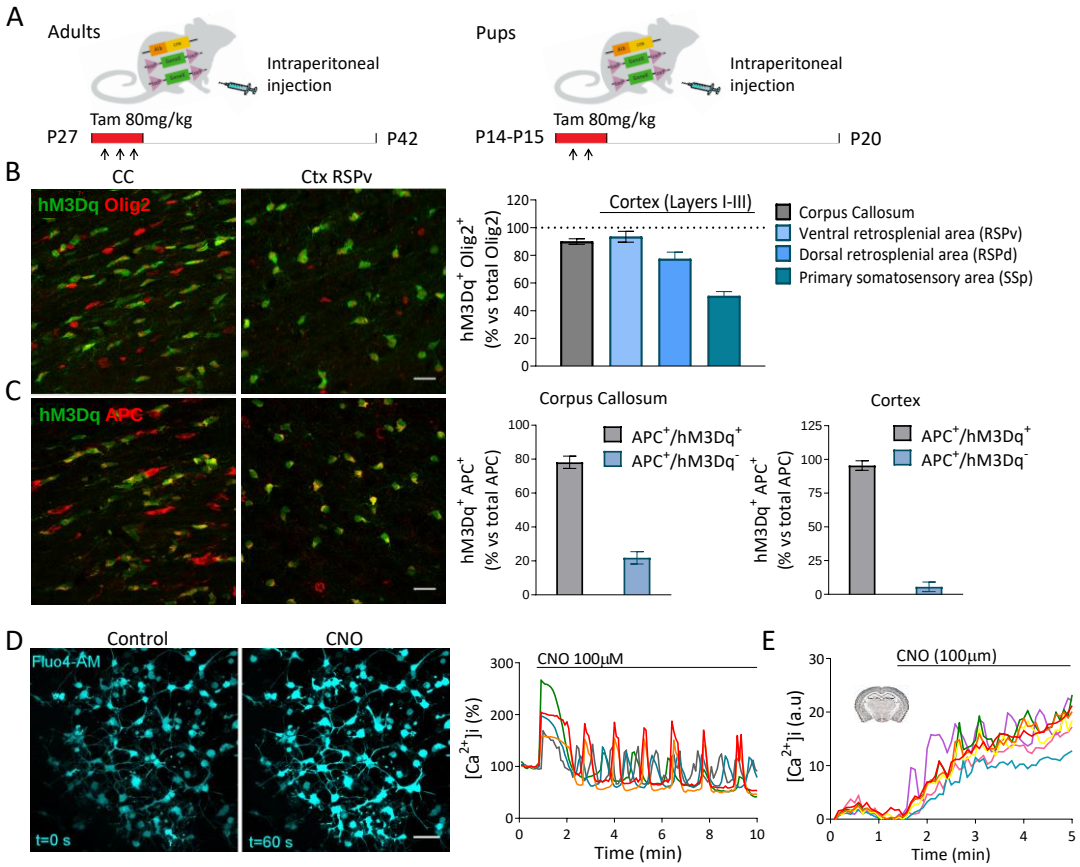

Figure 24. Functional characterization of the pharmacogenetic mice. **A**. Tamoxifen administration protocol in adult mice and pups to perform *in vivo* and *in vitro* assays respectively. In adult (P27), tamoxifen treatment (80mg/kg x 3 IP injections) was followed by 15 days of washout (left). In pups (P14), tamoxifen treatment (80mg/kg x 2 IP injections) was followed by a washout period of 5 days (Right). **B, C**. Histological analysis of the recombination level in *corpus callosum* (cc) and cortex. The number of recombined hM3Dq^{+}GFP^{+} oligodendrocytes was normalized to the total number of oligodendrocytes positive for the pan-OL marker Olig2 (B) or the total number of mature APC^{+} oligodendrocytes (C). n = 3 mice. Scale bar = 20 µm. **D, E**. Recordings of Ca^{2+} responses in oligodendrocytes *in vitro* (D) and in acute slices (E) following application of CNO (100 µM) using Fluo-4. Data represent average ± SEM of values obtained from more than 50 cells from 3 different cultures (D) and n = 3 mice (E).

2.3 Oligodendrocyte stimulation *in vitro* increases myelination

We assessed the impact of chronic oligodendrocyte stimulation on oligodendroglial differentiation and myelination. We first analyzed the impact of chronic pharmacogenetic stimulation with CNO (10 μM; 3 days) in cultured hM3Dq$^+$ oligodendrocytes. hM3Dq$^+$/GFP$^+$ oligodendrocytes treated with CNO showed a massive increase in processes branching, as revealed by *Sholl* analysis, and in cell area **(Figure 25.A, B)**. All hM3Dq$^+$/GFP$^+$ oligodendrocytes were also MBP$^+$ and thus, CNO did not alter the proportion of MBP$^+$ cells versus total cells (data not shown). However, CNO treatment induced an increase in MBP expression as observed by confocal imaging **(Figure 25.A),** and determined by Western blot **(Figure 25.C)**. Therefore, the pharmacogenetic activation of hM3Dq receptors in oligodendrocytes *in vitro* promotes oligodendrocyte processes growth and myelin synthesis, indicative that CNO could lead to an increase in myelination.

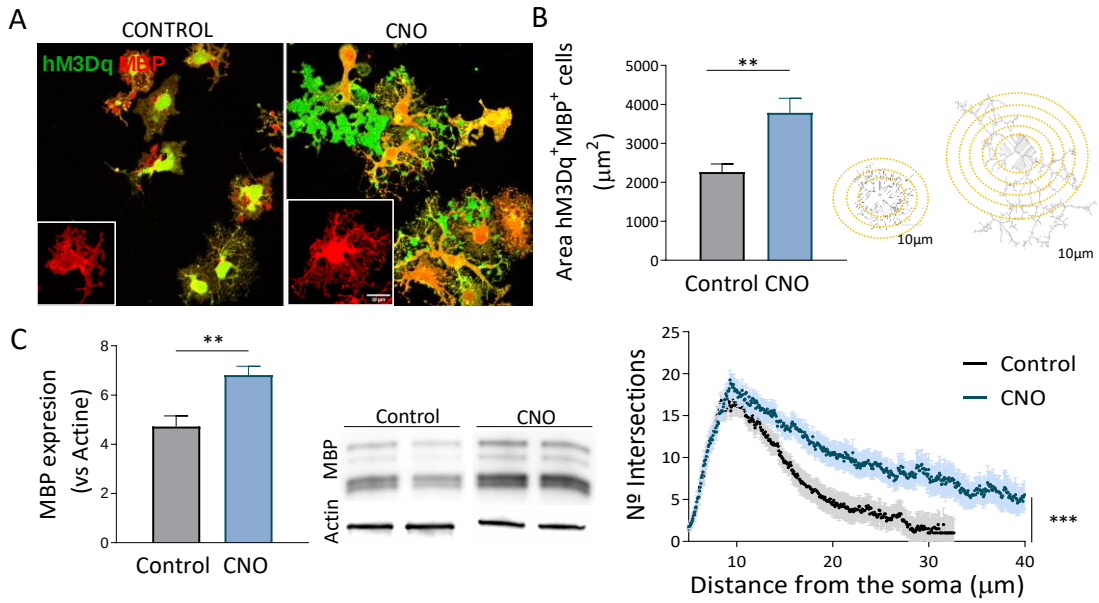

Figure 25. Impact of pharmacogenetic sitmulation of oligodendrocytes *in vitro*. **A**. Representative images showing the morphological changes in oligodendrocytes after *in vitro* stimulation with CNO (10 μM). Scale bar = 10 μm. **B**. Representative skeletonized images of oligodendroctes used for morphological analysis. Scale bar = 10 μm. Graphs show average of the area (top) and sholl analysis (bottom) of hM3Dq$^+$MBP$^+$ oligodendrocytes in the absence or in the presence of CNO. **C**. Western blot analysis of MBP expression in oligodendrocytes *in vitro* after CNO stimulation. n = 3 independent experiments. **p<0.01; ***p<0.001.

2.4 Mature oligodendrocytes stimulation *in vivo* increases myelination and axonal conduction velocity

Recent data suggest that myelination is plastic and that it may respond to changes in the environment, not only during postnatal development but also in adulthood (Chapman & Hill, 2020). MRI studies have revealed structural changes in white matter myelin in children, adolescents, and adults with learning fine motor skills (Gibson *et al*., 2014). However, how this experience translates to cells of the oligodendroglial lineage is still unknown.

We then analyzed the effect of chronic pharmacogenetic stimulation in oligodendrocyte differentiation and myelination *in vivo*. Specifically, we induced recombination in P27 PLP-CreERT2^{+}/hM3Dq$^{+/+}$ mice by tamoxifen administration for three consecutive days. After 15 days of tamoxifen washout, we injected CNO (1 mg/kg, i.p.) daily for 15 consecutive days **(Figure 26.A)**. Mice were perfused at P60 for immunohistochemical and confocal analysis. Recombinant CreERT2^{+}/hM3Dq$^{+/+}$ littermate mice without CNO treatment were used as control mice.

First, we determined the impact of pharmacogenetic sitmulation on oligodendrocyte differentiation. CNO treatment did not induce any significant change in the number of mature APC^{+} oligodendrocytes in *corpus callosum* **(Figure 26.B)**. Thus, pharmacogenetic stimulation did not alter oligodendrogenesis as described *in vitro*. We next analyzed the impact of pharmacogenetic stimulation in *corpus callosum* and cerebral cortex myelination. CNO treatment seemed to increase myelin density, although the tendency was not statistically significant **(Figure 26.C)**. In order to analyze myelination in more detail, we immunolabeled sections of the retrosplenial cortex corresponding to layers II-III (in which the axons are cut transversely) with antibodies to neurofilament (NF-L) to identify axons and antibodies to MBP to identify myelin rings. With the collaboration of Dr. Jorge Valero, we designed an *ImageJ* macro able i) to select axons on the basis of their morphology, circularity and size, and ii) to determine if they are covered by a myelin ring. CNO treatment increased the density of myelinated axons in cerebral cortex **(Figure 26.E)**.

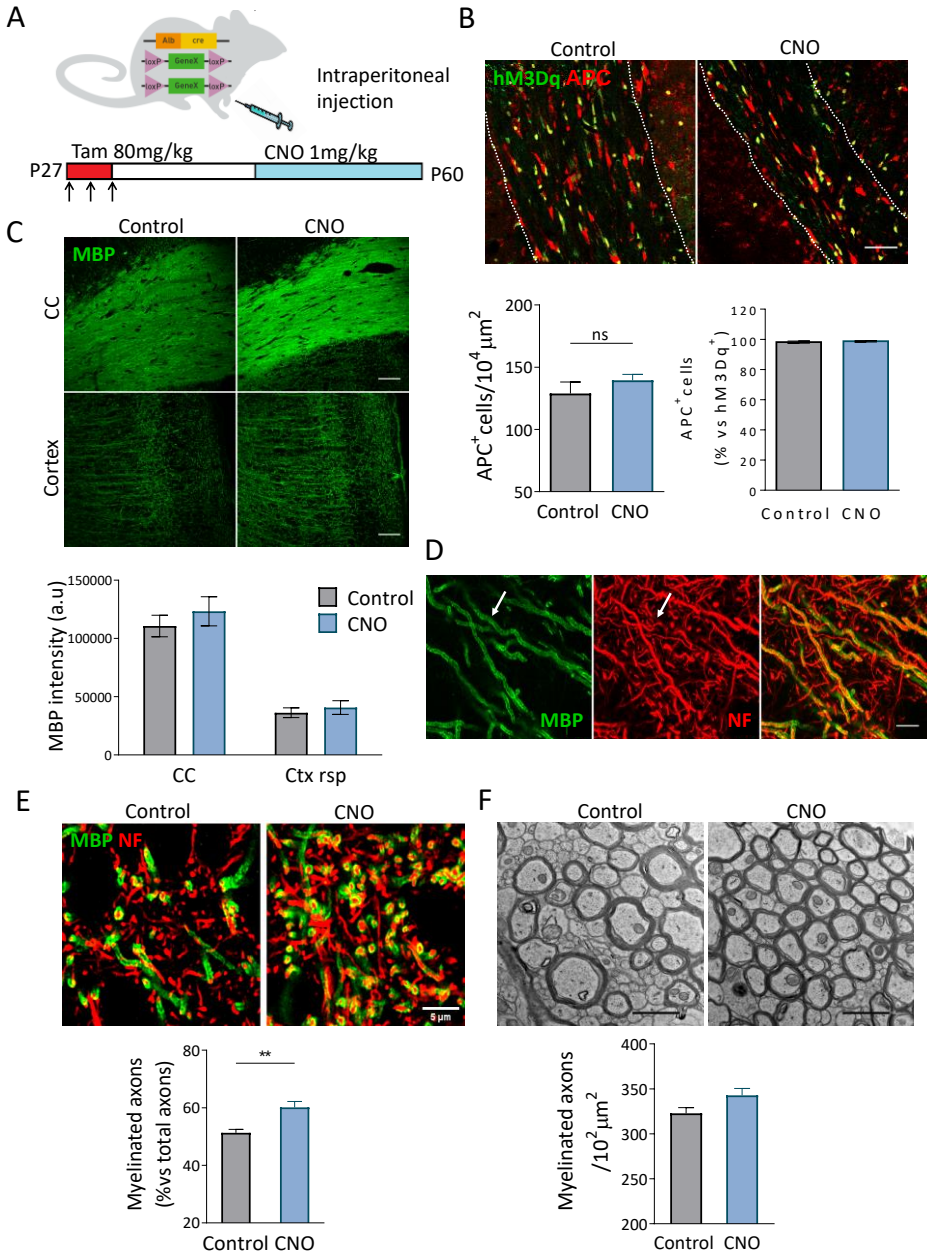

Figure 26. Impact of pharmacogenetic stimulation of oligodendrocytes in myelination *in vivo*. **A**. Schematic representation of the protocol of recombination and treatment with CNO (1 mg / kg, ip). **B**. Chronic treatment with CNO did not alter the number of mature oligodendrocytes (APC^+ cells). **C.** CNO treatment induced an increase in myelin density at the level of the *corpus callosum* (not significant) Scale bar = 50 µm. **D.** Representative image of the artifact produced in longitudinal myelinated axon labeled with MBP and neurofilament (NF-L) markers. Scale bar = 10 µm **E**. Quantification of the percentage of myelinated transverse axons in layers II-III of the cerebral cortex. Data showed a significant increase in CNO treated mice compared to control group. Scale bar = 5 µm. Data come from n = 6 control animals; n = 6 animals treated with CNO. **F.** Quantification of the number of myelinated axons per area analyzed by TEM. Data come from n = 3 animals per group. ** p-value < 0.01.

Due to the limitations of confocal microscopy to distinguish individual myelin sheaths within *corpus callosum* **(Figure 26.C)**, we further analyze myelination using transmission electron microscopy in another cohort of hM3Dq$^{+/+}$ CNO-treated mice. We took TEM images from anatomically equivalent tissue sections in control and CNO-treated mice. We detected an increase in the number of axons that were myelinated in the *corpus callosum* of hM3Dq$^{+/+}$ CNO-treated mice compared to control mice **(Figure 26.F)**. Altogether, the data suggested that pharmacogenetic activation of oligodendrocytes increases myelination.

As myelin sheaths wide longitudinally along the axons, lateral cytoplasmic loops form the paranode and voltage-gated sodium channels get clustered forming the nodes of Ranvier. Thus, adaptive myelination and new myelin sheath formation could change the number or the cytoarchitecture of the node of Ranvier (Arancibia-Cárcamo *et al*., 2017). Therefore, to determine whether the increase in myelination in response to pharmacogenetic stimulation of oligodendrocytes changes nodes of Ranvier structure, we analyzed the number and length of them in the *corpus callosum* and cerebral cortex. As described in the previous section, we immunolabeled coronal brain sections with antibodies against Caspr and Nav1.6 channels and we identified the nodes of Ranvier as Nav1.6^{+} regions flanked by Caspr^{+} paranodes. As expected, the number of nodes of Ranvier in the *corpus callosum* as well as in cerebral cortex was significantly higher in hM3Dq$^{+/+}$ CNO-treated mice in comparison to hM3Dq$^{+/+}$ control mice **(Figure 27.A)**.

These results corroborated that pharmacogenetic stimulation of oligodendrocytes promote new myelin sheath and node of Ranvier formation. Surprisingly, we also detected that nodes of Ranvier were shorter in hM3Dq$^{+/+}$ CNO-treated mice in comparison to hM3Dq$^{+/+}$ control mice **(Figure 27.A)**. Moreover, shortening of node length correlates with an increase in paranode length in hM3Dq$^{+/+}$ CNO-treated mice **(Figure 27.B)**. These data indicate that pharmacogenetic stimulation of oligodendrocytes also tune node of Ranvier cytoarchitecture.

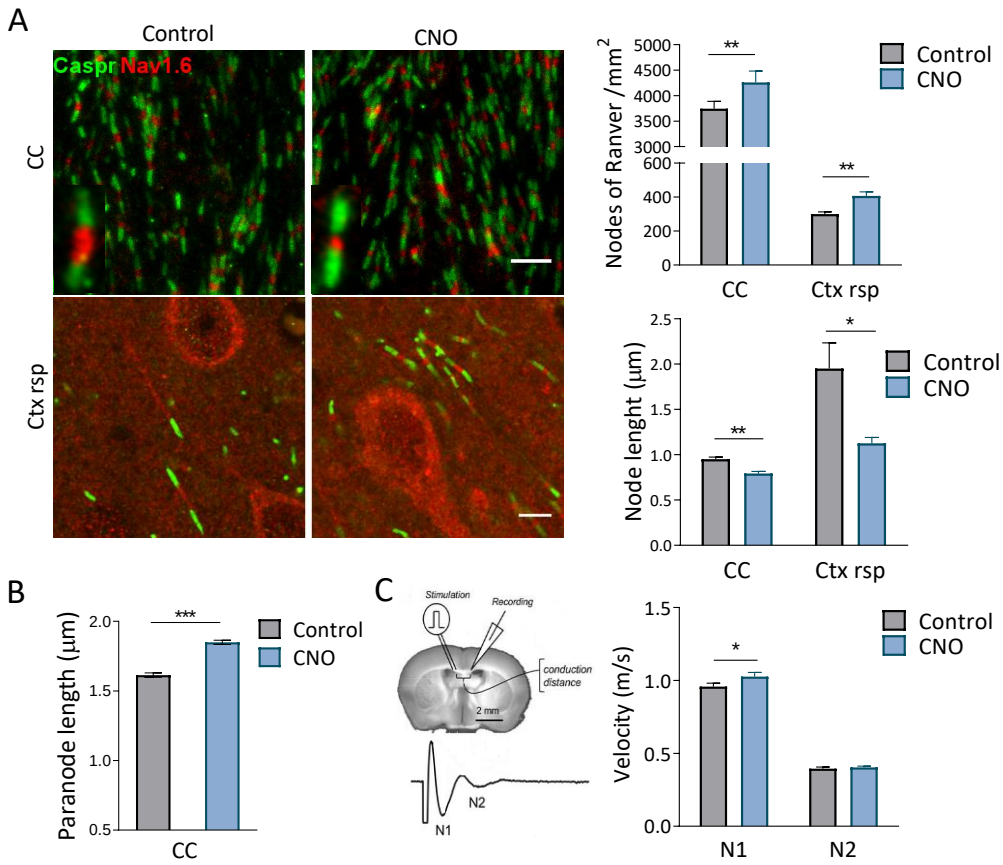

Figure 27. Impact of pharmacogenetic stimulation of oligodendrocytes in myelination and axonal conduction *in vivo* **A.** Representative confocal images of nodes of Ranvier ($Na_v1.6$; red) and paranodes (Caspr; green) in *corpus callosum* and cerebral cortex of control and CNO-treated mice. Scale bar = 5 µm. Rigth, histograms shows average node of Ranvier number and length in control and CNO-treated mice (n= 6 per experimental group). **B.** Histograms show average paranode length in control and CNO-treated mice (n= 6). **C**. Conduction velocity corresponding to N1 and N2 peaks in vehicle (n= 6) and CNO-treated mice (n= 6). Analysis was performed with t-Student. * p-value < 0.05; ** p-value < 0.01 *** p-value < 0.001

Previous modelling proposes that node length changes could alter conduction speed by ~20%, similar to the changes produced by altering the number of myelin wraps or the internode length (Arancibia-Cárcamo *et al*., 2017). Assuming that the number of ion channels at the node is held constant, the predicted conduction speed falls with increasing node length. In contrast, if we assume that the density of ion channels (not the absolute number) at the node is constant, and then conduction speed falls with decreasing node length. In order to corroborate the global impact of new myelin sheath formation and the changes at

node of Ranvier in tuning axonal conduction speed, we measured the conduction velocity of compound action potential (CAPs) in the *corpus callosum* in acute coronal brain slices. CAPs were evoked by a bipolar stimulating electrode and recorded by a field electrode placed at varying distances across the *corpus callosum*. CNO treatment induced an increase in the conduction speed of myelinated fibers (N1), but not in non-myelinated or less myelinated fibers (N2) in hM3Dq$^{+/+}$ mice **(Figure 27.C)**. Overall, pharmacogenetic stimulation of oligodendrocytes could tune myelination and axonal conduction velocity in the absence of electrical activity changes. Therefore, PLP-CreERT2^{+}/hM3Dq$^{+/+}$ mice could be useful to study the selective impact of myelin in brain physiology and/or pathology.

2.5 Mature oligodendrocytes stimulation promotes remyelination and decreases axonal damage in demyelinating diseases

Multiple sclerosis, the main demyelinating disease of the CNS, is an autoimmune disease characterized by oligodendroglial loss and demyelination that leads to axonal damage. One of the therapeutic strategies under study is the promotion of remyelination to preserve axons, for which it is necessary to understand in detail the mechanisms that regulate this process. Most approaches to increase the endogenous remyelination capacity are based on accelerating OPC differentiation (Kotter *et al*., 2006; Valny *et al*., 2017). However, the role of mature oligodendrocytes in multiple sclerosis lesions outcome is much less known. New myelin is also generated throughout life in humans, but the low rate of OL turnover suggests that myelin remodelling is performed primarily by mature oligodendrocytes (Yeung *et al*., 2014). Moreover, selective manipulation of ERK1/2 activity in mature oligodendrocytes resulted in increased myelin thickness, faster conduction speed and accelerated remyelination (Jeffries *et al*., 2016).

As pharmacogenetic stimulation of mature oligodendrocytes increases myelination, we next analyzed whether this strategy could also help to increase remyelination after demyelination using the experimental autoimmune encephalitis (EAE) model of multiple sclerosis. The EAE model shares many clinical and pathophysiological features with multiple sclerosis and is based on the reaction of the immune system against myelin antigens such as the myelin oligodendrocyte glycoprotein (MOG). We induced recombination in another cohort of P60

PLP-CreERT2^{+}/hM3Dq$^{+/+}$ mice by tamoxifen administration following the previous protocol. After tamoxifen washout, mice were immunized with myelin oligodendrocyte glycoprotein (MOG) as described previously (Matute *et al*., 2007) and treated daily with CNO (1 mg / kg; i.p.) or saline from the onset of the disease at 10 days post-immunization to avoid interfering with immune priming **(Figure 28.A)**.

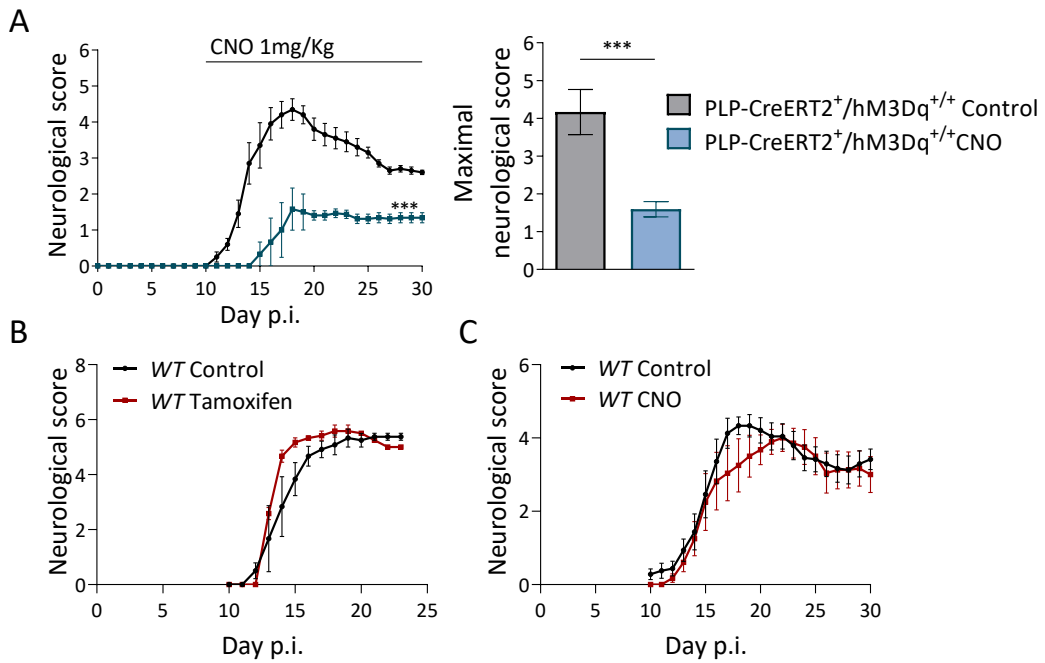

Figure 28. Impact of pharmacogenetic stimulation of oligodendrocytes in EAE neurological score. myelination and axonal conduction in vivo **A.** Clinical score of vehicle and CNO (1 mg/kg, i.p.)-treated PLP-CreERT2^{+}/hM3Dq$^{+/+}$ mice after EAE induction (two independent experiments performed with n=7-8 mice per group). **C, D**) Clinical score in control and tamoxifen-treated or CNO-treated (D) wild type mice (n= 8-10 mice per group). Neither tamoxifen or CNO administration affect EAE neurological score in control mice, indicating that the effect observed was specific of hM3Dq^{+} oligodendrocytes stimulation. Statistical analysis was performed with Mann-Whitney U test (neurological score curve) and t-student (maximal neurological score). * p-value < 0.05; ** p-value < 0.005; *** p-value < 0.0005

The neurological score or the motor symptoms in the EAE progressively increases after EAE onset (around 9-10 days postimmunization) until reaching a maximum neurological score at the peak of the disease, with paralysis of the hind and forelimbs. Thereafter, this model shows a partial recovery or remyelination in the EAE chronic phase. Pharmacogenetic stimulation of mature oligodendrocytes significantly ameliorated EAE disease. Thus, CNO treatment induced a delay in the appearance of symptoms and reduced neurological symptoms at EAE peak **(Figure 28.A)**. Neither tamoxifen nor CNO administered alone induced any effect in EAE neurological score in wild type mice **(Figure 28.B, C)**, thus corroborating that the effect of CNO is mediated specifically by mature oligodendrocyte activation.

Histologically, hM3Dq$^{+/+}$ CNO-treated mice showed a massive reduction in the lesion area, defined on the basis of MBP^{+} myelin damage or loss and Iba1^{+} microglia/macrophage accumulation **(Figure 29.A)**. These data suggested that pharmacogenetic stimulation of oligodendrocytes either promotes an accelerated recovery or remyelination, or prevents demyelination. We also observed that axonal damage is massively reduced in hM3Dq$^{+/+}$ CNO-treated mice in comparison to control treated mice **(Figure 29.B)**. Because axonal damage is secondary to demyelination and also because the differences observed in the neurological score were detected at early stages of the disease, we challenged the hypothesis that pharmacogenetic stimulation of mature oligodendrocytes prevents oligodendroglial and axonal damage.

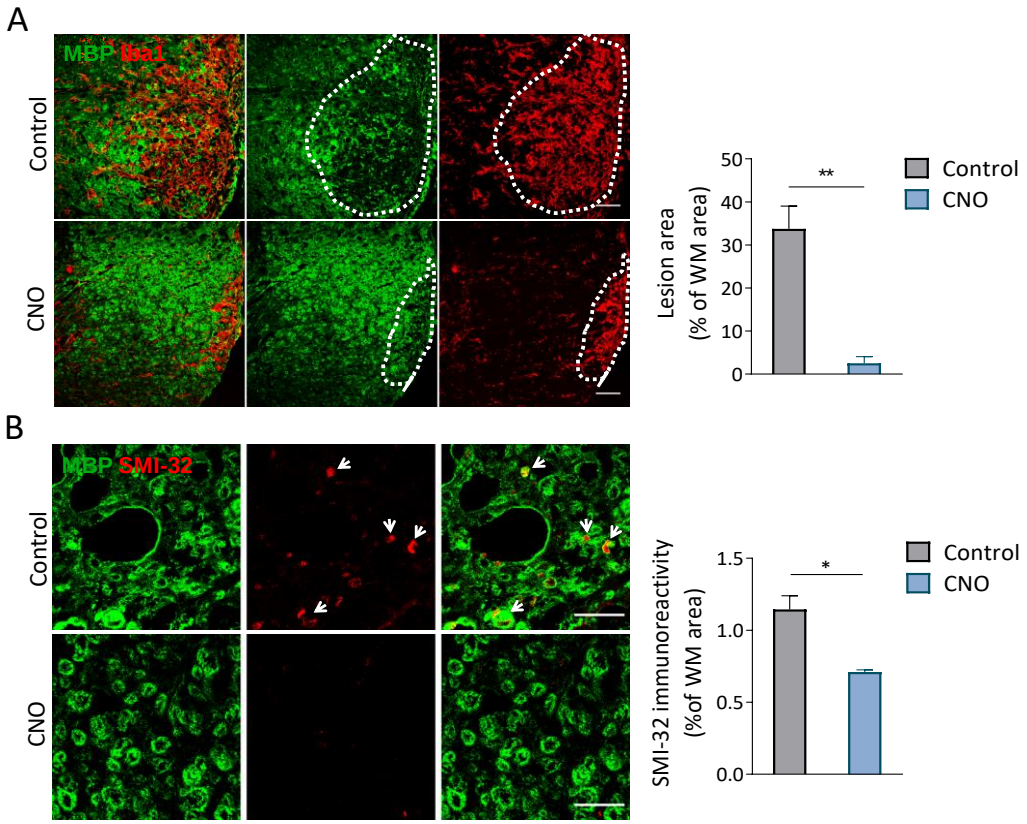

Figure 29. Pharmacogenetic stimulation of oligodendrocytes prevents axonal damage in EAE **A, B.** Spinal cord immunolabelling for MBP (green) and Iba1 (red) (**A**) to define the lesions and the inflammatory reaction (dotted area); and for MBP (green) and SMI-32 (red) (**B**) to define axonal damage (arrowheads). *Right*, quantification of the lesion area (A) and axonal damage (D) in the spinal cord of control and CNO-treated PLP-CreERT2^{+}/hM3Dq$^{+/+}$ mice (n=4). Scale bar 20µm. * p-value < 0.05; ** p-value < 0.005.

2.6 Mature oligodendrocytes stimulation increases oligodendrocyte survival under pathological conditions

Next, to determine whether the increase in axonal survival could be related to lower oligodendrocyte death, we quantified the percentage of apoptotic hM3Dq$^+$GFP$^+$ oligodendrocytes within the lesions in control and CNO-treated mice using antibodies to cleaved-Caspase-3. Caspase-3 activates caspase-8 and caspase-9, leading to a signaling cascade involved in the execution-phase of cell apoptosis. Pharmacogenetic stimulation of oligodendrocytes induced a significant decrease of apoptotic Casp3$^+$/hM3Dq$^+$ oligodendrocytes within the lesion **(Figure 30.A)**. We therefore concluded that CNO treatment increases oligodendroglial survival.

To further test whether pharmacogenetic stimulation of oligodendrocytes prevents their cell death, we performed experiments in cultured oligodendrocytes using a model of ischemia induced by oxygen-glucose deprivation (OGD), as previously described (Domercq *et al*., 2007). hM3Dq$^+$ oligodendrocytes were exposed to CNO (10 μM) both during the OGD and the recovery period (24h) and cell death was assessed using Calcein-AM fluorimetry (Ruiz *et al*., 2014). CNO treatment induced a significant reduction of hMd3q$^+$ oligodendrocyte cell death induced by a mild stimulus **(Figure 30.B)**.

One of the signaling pathways pivotal for mature oligodendrocyte differentiation and myelination/remyelination is mediated through ERK1/2 (Ishii *et al*., 2016; Jeffries *et al*., 2016). We therefore analyzed whether hM3Dq is linked to ERK1/2 activation in oligodendrocytes by immunocytochemistry. Thus, we confirmed that CNO stimulation increased the intensity of pERK staining in hM3Dq$^+$ oligodendrocytes **(Figure 30.C)**. Altogether we concluded that pharmacogenetic stimulation of oligodendrocytes activates survival signaling pathways that prevent oligodendroglial and axonal damage in EAE mice.

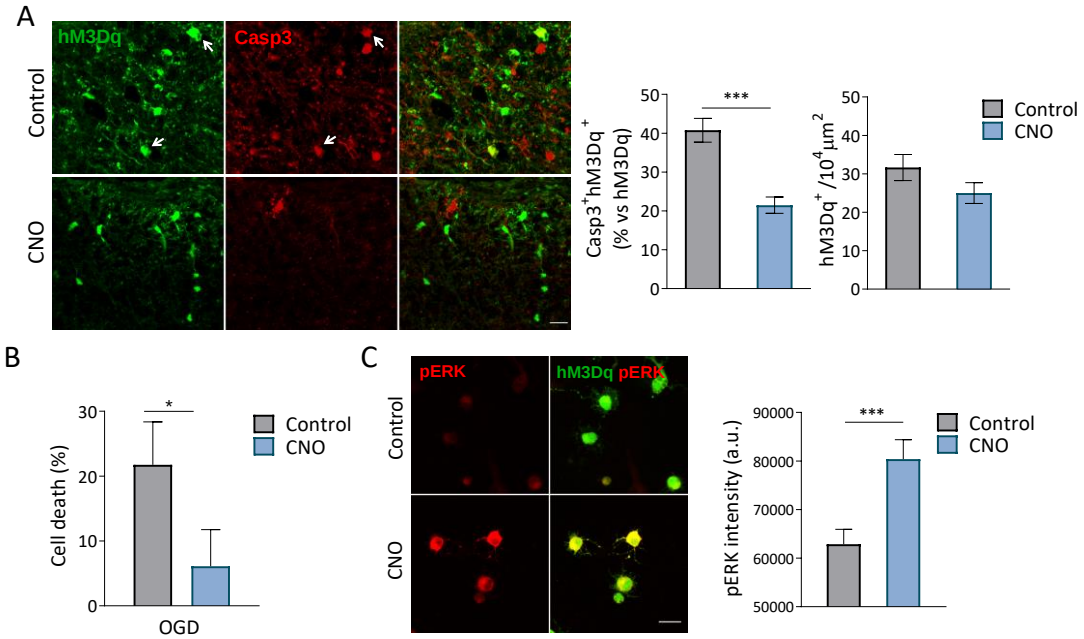

Figure 30. Pharmacogenetic stimulation of oligodendrocytes increases oligodendrocytes survival. **A.** hM3Dq$^+$oligdoendrocytes labelled with Casp3 antibody to analyze the proportion of apoptotic oligodendrocytes within the lesion of control and CNO-treated mice (n=4 per group) (arrowheads). **B.** Cell viability assay of control and CNO-treated hM3Dq$^+$ oligdoendrocytes after oxygen-glucose deprivation (OGD). **C.** Imaging analysis of pERK immunoreactivity after treatment with CNO. Scale bar = 20µm. * p-value < 0.05; *** p-value < 0.001.

2.7 Acute oligodendrocyte stimulation boosts oligodendrocyte metabolic activity

Previous data in the literature indicate that oligodendrocytes support axon survival and function through a mechanism independent of myelination and their dysfunction leads to axon degeneration in several diseases. Thus, mouse models of oligodendrocyte injury, including proteolipid protein 1 (Plp1)-null mice3 and Cnp (also known as Cnp1 and CNPase) mutant mice4, demonstrate axon loss without considerable demyelination, suggesting that oligodendroglia support axon survival through a myelin-independent mechanism, possibly as a result of insufficient axonal energy support (Lee *et al.*, 2012b). Myelinated axons are only exposed to extracellular energy substrates at the nodes of Ranvier, and therefore may require specialized transport of energy metabolites from myelinating oligodendroglia to meet their high metabolic needs. Indeed , a new model of axon-oligodendroglia metabolic coupling has been proposed, in which the products derived from glycolysis in

oligodendrocytes such as pyruvate and lactate are transported to axons through specific transporters of these metabolites (MCT1 and MCT2) (Funfschilling *et al*., 2012; Lee *et al*., 2012a). As this metabolic coupling known as "lactate shuttle" is essential for axonal survival, we hypothesized that pharmacogenetic stimulation of oligodendrocytes could modulate oligodendroglial metabolism and the metabolic support to axons. We therefore asked the impact of pharmacogenetic stimulation of oligodendrocytes in their metabolism.

First, we measured oxygen consumption rate (OCR) and extracellular acidification rate (ECAR) in real time as indicative of mitochondrial respiration and glycolysis respectively in cultured hM3Dq$^+$ oligodendrocytes. To measure OCR, we used the Mito Stress Kit using the Seahorse XFe96 Analyzer (Agilent). Acute stimulation of oligodendrocytes with CNO did not modify basal respiration **(Figure 31.A)**. However, acute CNO increased the spare respiratory capacity of oligodendrocytes, defined as the difference between basal ATP production and its maximal activity **(Figure 31.A)**. Mitochondrial spare respiratory capacity (SRC) is the extra capacity available in cells to produce energy in response to increased stress or work, and as such is associated with cellular survival. This data further supports the higher survival of CNO-treated hM3Dq$^+$ oligodendrocytes after OGD.

In addition to the increase in the oxidative phosphorylation (OXPHOS), we also found that CNO induced an acute increase in the extracellular acidification basal rate (ECAR) **(Figure 31.B)**, suggesting that activation of oligodendrocytes induces an acute increase in glycolysis. As lactate is one of the end products of glycolysis, we measured lactate released to the medium by oligodendrocytes after pharmacogenetic activation of oligodendrocytes. CNO (10 μM; 72h) produced a significant increase in lactate in the extracellular medium **(Figure 31.C)**. To more accurately detect intracellular lactate production in oligodendrocytes, we expressed Laconic, a lactate sensor based on Forster Resonance Energy Transfer (FRET) that encodes the fluorescence proteins mTFP and mVenus. Recordings were carried out in the presence of CHC, a pan inhibitor of lactate transporters (MCTs), to avoid lactate release and amplify the FRET signal. As a positive control we used azide, which blocks mitochondrial respiration and increases glycolysis and lactate production (Mächler *et al*., 2016; San Martín *et al*., 2013). Azide induces a massive increase in FRET signal **(Figure 31.D)**. Pharmacogenetic activation of oligodendrocytes with CNO induced a progressive increase in the accumulation

of lactate in the cells **(Figure 31.D)**. We therefore confirmed that metabotropic activation of oligodendrocytes activates metabolism, in particular increases glycolysis and lactate release.

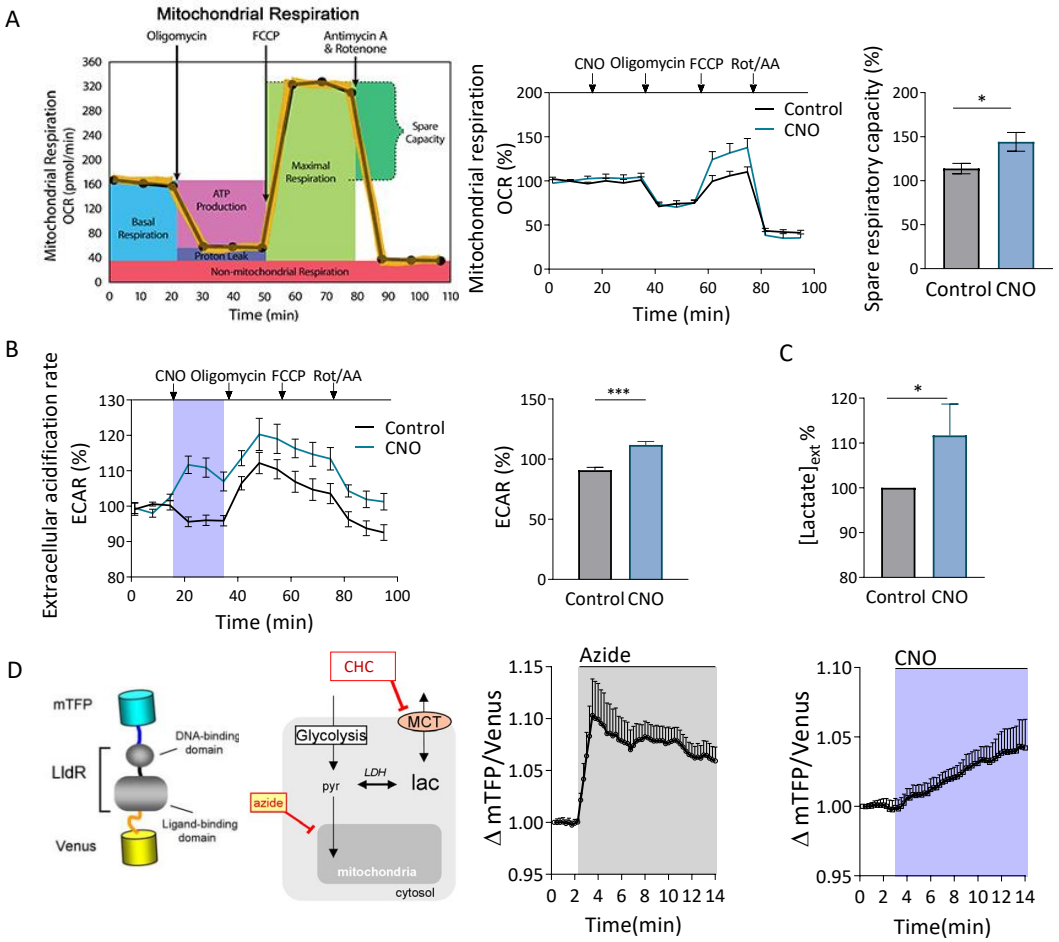

Figure 31. Impact of pharmacogenetic stimulation of oligodendrocytes in metabolism. **A**. Schematic representation of the metabolic profile of mitochondrial respiration (oxygen consumption rate, OCR) obtained with the Seahorse XF cell mito stress equipment. *Left*, Rate of oxygen consumption (OCR) and maximum respiratory capacity in control and CNO (10 μM; 24h)-treated hM3Dq$^{+/+}$ oligodendrocytes (n= 3 independent experiments performed with 8 replicates). *Right*, histogram show the spare respiratory capacity obtained by the analysis of the metabolic profile and expressed in % versus control cells. **B**. ECAR (extracellular cell acidification rate) profile, indicative of glycolysis, in control and acutely CNO (10 μM)-treated oligodendrocytes. The histogram shows the basal level of this parameter as well as the increase provoked by the acute treatment with CNO, relative to the control cells, in basal glycoslisis (n= 3 independent experiments performed with 8 replicates). **C.** Analysis of extracellular lactate accumulation in control and CNO (10 μM; 72h)-treated hM3Dq $^{+}$ oligodendrocytes (n = 3). **D.** Structural configuration of the FRET sensor to measure intracellular lactate. The assay was performed in presence of CHC, an inhibitor of lactate transporters (MCT). Acute stimulation with azide (5 mM), used as a positive control, and CNO induce an increase in the intracellular lactate within 10 minutes after the stimulation. T-student test * p-value < 0.05; *** p-value < 0.001)

2.8 Axon-oligodendrocyte metabolic coupling promotes axonal survival

In line with these results, we hypothesized that lactate release secondary to oligodendroglial stimulation could increase the metabolic support of axons and their survival. We tested this hypothesis experimentally using electrophysiological recordings of CAPs in *corpus callosum*. Callosal fibers were stimulated by short burst with a gradual increase in frequency (between 1 and 100 Hz). As expected, the recorded CAP area dropped drastically as we increased frequency **(Figure 32.A)**. Interestingly, when acute slices were perfused with CNO (10 μM), high-frequency conductivity was maintained at higher rates **(Figure 32.A)**. Indeed, CNO-treated slices were able to maintain nearly intact axonal conduction at 25 Hz, whereas control slices showed a conduction decline of about 50%. These results suggest that pharmacogenetic activation of oligodendrocytes provides lactate to electrically compromised axons.

Previous studies reported that the protective capacity of glial cells against neuronal death is mediated by released metabolites, including L-lactate (Magistretti & Allaman, 2018). Next, we examined myelinated *corpus callosum* under metabolic stress in order to assess their ability to recover from transient oxygen-glucose deprivation (OGD), a well-established model of acute ischemia and axonal injury. Within minutes after OGD onset, axonal conductivity declined rapidly as expected due to the energy blockage. After 30 min, reperfusion only induced a low recovery of axonal conductivity, a process associated to Ca^{2+}-dependent axonal damage (Domercq *et al*., 2010; Tekkök *et al*., 2007). Pharmacogenetic stimulation of oligodendrocytes during OGD and recovery phase significantly increased the recovery of axonal function **(Figure 32.B, C)**. Moreover, the increase in axonal survival induced by pharmacogenetic stimulation of oligodendrocytes was blocked in the presence of CHC, a generic lactate transporters inhibitor **(Figure 32.B, C)**. This data suggest that lactate released by oligodendrocytes is involved in axonal survival after metabolic stress.

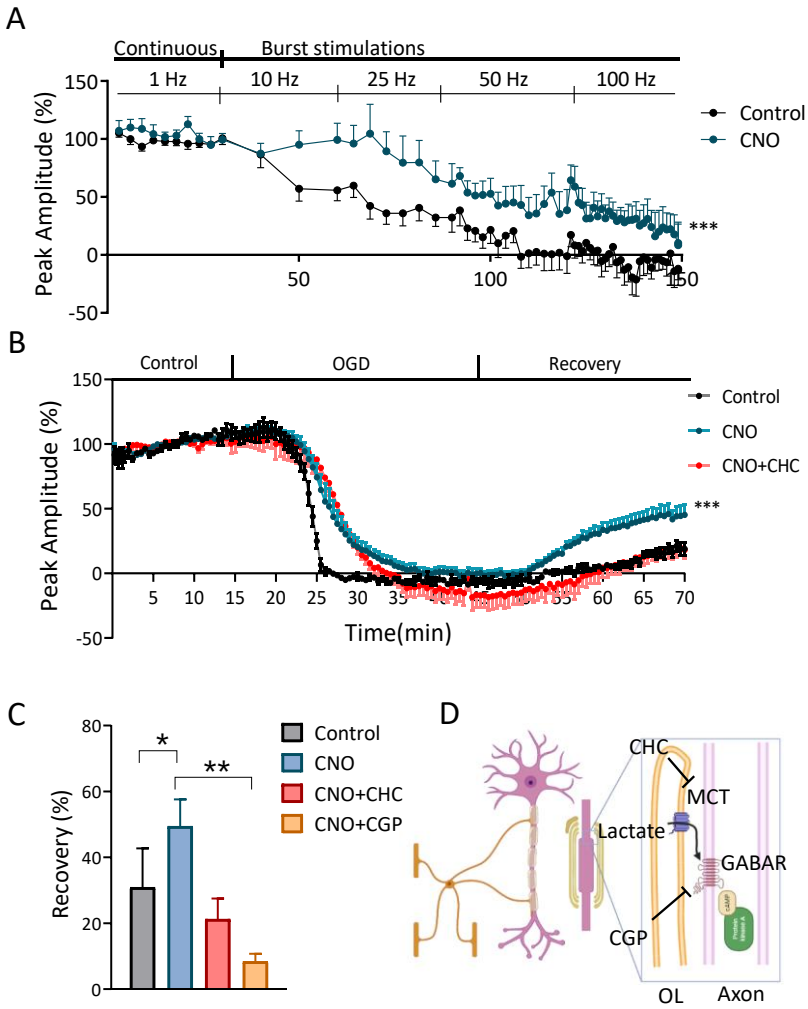

Figure 32. Pharmacogenetic stimulation of oligodendrocytes increases lactate shuttle to axons. **A.** Compound action potentials (CAPs) recording in *corpus callosum* of 400µm coronal slices before and after high frequency stimulation (HFS). The amplitude area was normalized versus basal conditions before HFS stimulation. Notice that slices treated with CNO to active hM3Dq$^+$ oligodendrocytes show a slower decline of CAP area at higher frequencies (n= 4 mice). **B, C.** Pharmacogenetic stimulation of oligodendrocytes prevents loss of axonal function after oxygen glucose deprivation (OGD). Normalized CAP amplitude recorded before, during and after 30 min OGD in control conditions and after oligodendrocytes stimulation with CNO in the presence of CHC, a lactate transporter blocker; in the presence of CGP, a GABA-B receptor antagonist, and control drug-free aCSF (n = 4-6 mice per experimental group). Mann-Whitney U (A, B) and Student's t-tests (C) * p-value < 0.05; ** p-value < 0.01; *** p-value < 0.001. **D,** Schematic hypothesis: lactate released by oligodendrocytes after CNO stimulation protects axons by GABA-B receptor activation

Previous data have already demonstrated that upregulation of glycolysis in glial cells can improve axonal survival after spinal cord injury (F. Li *et al*., 2020). Importantly, these authors also demonstrated that glycolytic products lactate and L-2-hydroxyglutarate are functioning by modulating extracellular GABA-B receptors in neurons (Li *et al*., 2020), rather than through transport into neurons where they can be used as metabolic fuel, as originally proposed by astrocyte-neuron lactate shuttle (Magistretti & Allaman, 2018) **(Figure 32.D)**. We therefore analyzed whether the protection obtained after pharmacogenetic stimulation of oligodendrocytes is mediated through this signaling pathway. To asses that, we used the GABA-B receptor antagonist CGP. In the presence of CGP (3 mM), the protective effect of CNO was significantly blocked **(Figure 32.C)**. Further experiments are ongoing to confirm that lactate released by pharmacogenetic activation of oligodendrocytes activates GABA-B receptors, preventing axonal damage.

2.9. Pharmacogenetic stimulation of oligodendrocytes increases axon excitability

The conduction of action potential along axons imposes widely varying delays on synaptic transmission, and hence shapes the dynamics and timing of signal processing in the brain. In myelinated axons, the conduction speed of action potentials depends crucially on myelin. However, it is unknown whether myelin and node of Ranvier are dynamic and acutely regulated by activity-dependent mechanisms, which could affect the timing of information transfer between cells and brain areas. We next decided to analyze the acute impact of pharmacogenetic stimulation of oligodendrocytes in axonal conduction velocity. We measured action potential latency in callosum fibers before and after mature oligodendrocyte stimulation in acute slices from recombined hM3Dq$^{+/+}$mice **(Figure 33. A)**. After 10 min of basal recordings, we applied CNO (10 μM) for 20 minutes. We did not detect any impact of CNO on the latency of AP transmission, suggesting that oligodendrocytes did not modulate conduction velocity acutely (data not shown). However, we observed that CNO increased the amplitude of N1 and N2 peaks **(Figure 33.B, C)**, which indicates that mature oligodendrocyte stimulation can dynamically modulate the excitability of axonal fibers. Again, the increase in axonal amplitude was blocked in the presence of the lactate transporters inhibitors suggesting that the acute increase in metabolism in oligodendrocytes

is involved in myelin-axon dynamic regulation (data not shown). Further experiments are required to characterize the mechanism involved and, more importantly, to analyze the physiological impact of this finding in synaptic transmission.

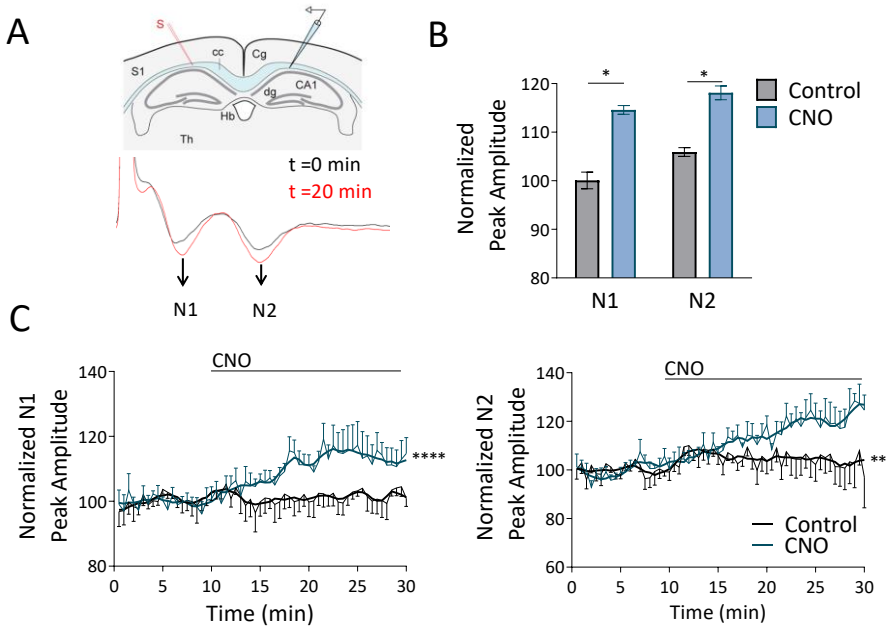

Figure 33. Pharmacogenetic stimulation of oligodendrocytes increases axon excitability. **A**. Graphic representation of the coronal sections and representative recordings of N1 (myelinated fibers) and N2 (partially-myelinated fibers) CAPs before and after CNO stimulation (10 µM; 20 min). **B,** Graph showing the variation in N1 and N2 CAP amplitude after CNO stimulation over time. **C**, Histograms showing the increase in CAP amplitude at the end of the stimulation (n = 5-6 mice per group). Student's t-tests (B) and Mann-Whitney U (C) * p-value < 0.05; ** p-value < 0.01; **** p-value < 0.0001.

PART III. ROLE OF OLIGODENDROGLIAL NMDA RECEPTORS IN AUTOIMMUNE ENCEPHALITIS

3.1 NMDAR are activated by NMDA in cultured oligodendrocytes

NMDARs are highly permeable to Ca^{2+} upon activation by their endogenous ligands. Because of that, we set an assay to evaluate whether patients' antibodies were able to alter NMDAR function using Fluo-4, a calcium indicator that exhibits an increased fluorescence upon binding Ca^{2+}, and time-lapse fluorescence microscopy. Cultured oligodendrocytes exposed to NMDA applied together with glycine induced a robust and fast increase in cytosolic Ca^{2+} with a peak amplitude of 159 ± 4% compared with resting levels (100%) that progressively decreased to baseline by around 5 to 10 minutes of stimulation **(Figure 34)**. To assess the specificity of the responses triggered by NMDA and glycine, we used CGP39551 (1µM) and AP5 (100µM), 2 potent, selective and competitive NMDAR antagonists, as well as MK801 (50µM), a noncompetitive antagonist that binds to a site located within the NMDAR-associated ion channel and thus prevents Ca^{2+} flux. In all instances, the responses to NMDA and glycine were abolished in the presence of these antagonists **(Figure 34)**.

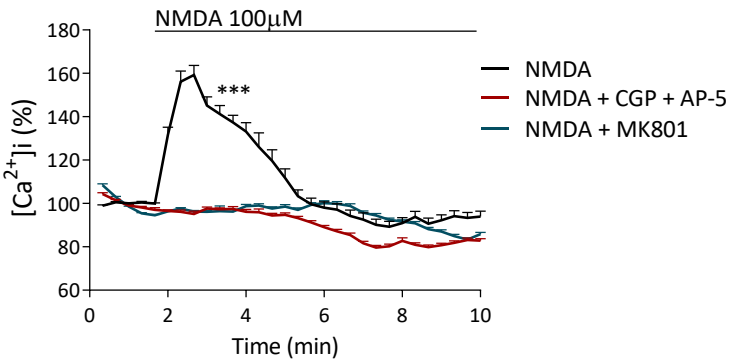

Figure 34. Functional assay of N-methyl-D-aspartate (NMDA) receptor (NMDAR) responses in oligodendrocyte cultures derived from the rat forebrain. Recordings of Ca^{2+} responses following application of NMDA plus glycine (both at 100µM) using Fluo-4. Responses are blocked in the presence of NMDAR antagonists CGP39551 (1µM) and AP5 (100µM) (NMDA + CGP + AP5); and MK801 (50µM) (NMDA + MK801). In all instances, data represent the average ± SEM of values obtained from at least 2 to 3 different cultures and analyzed using one-way analysis of variance with Tukey post-test (NMDA alone vs NMDA plus antagonists, *** p-value < 0.001).

3.2 NMDARs are functionally blocked by autoantibodies from CSF of autoimmune encephalitis patients.

The profile and amplitude of agonist responses were not significantly altered by preincubation of oligodendrocytes (experimental procedure **Figure 35.A**) for 4 hours with CSF obtained from controls (peak response = 140 ± 7% vs 154 ± 13% for naive oligodendrocytes; **Figure 35.B**). Instead, after preincubation with CSF from patients with anti-NMDAR encephalitis, the cytosolic Ca^{2+} responses to NMDA plus glycine exhibited a sharp reduction (maximal amplitude = 111 ± 5%), indicative of a strong reduction in the number of receptors being available to the agonists in the oligodendrocyte plasma membrane **(Figure 35.B)**.

To further analyze the changes in the responses during the whole period of recording, we calculated the area under the curve to compare the levels of Ca^{2+} accumulated over the time window examined. This analysis revealed that CSF from healthy donors on average did not significantly alter Ca^{2+} cytosolic load over time after incubation with the agonists (336 ± 87% vs 355 ± 91% in naive cells). In contrast, CSF from patients with anti-NMDAR encephalitis nearly abolished the response (106 ± 30% vs agonists alone or control CSF, $p < 0.05$, in both instances; **Figure 35.C**). An individual analysis of the effects of CSF from patients showed different levels of NMDAR remaining functionality ranging from 15 to 47% **(Figure 35.D)**, whereas CSF from controls had little or no effect (>76% or higher functionality preserved). The intensity of effects of patients' CSF antibodies correlated with CSF antibody titers in 6 of 7 patients (data not shown).

As AMPA receptors (AMPARs) are highly expressed in oligodendrocytes (Matute *et al*., 1997), we tested whether activation of these receptors with AMPA applied together with cyclothiazide (both at 100μM) was affected by patients' CSF. Contrary to the robust effect of patients' CSF on the NMDAR-mediated responses, no effects were observed on the profile of AMPAR-mediated responses **(Figure 36.A)**, strongly suggesting the specific blockade of NMDARs by patients' CSF.

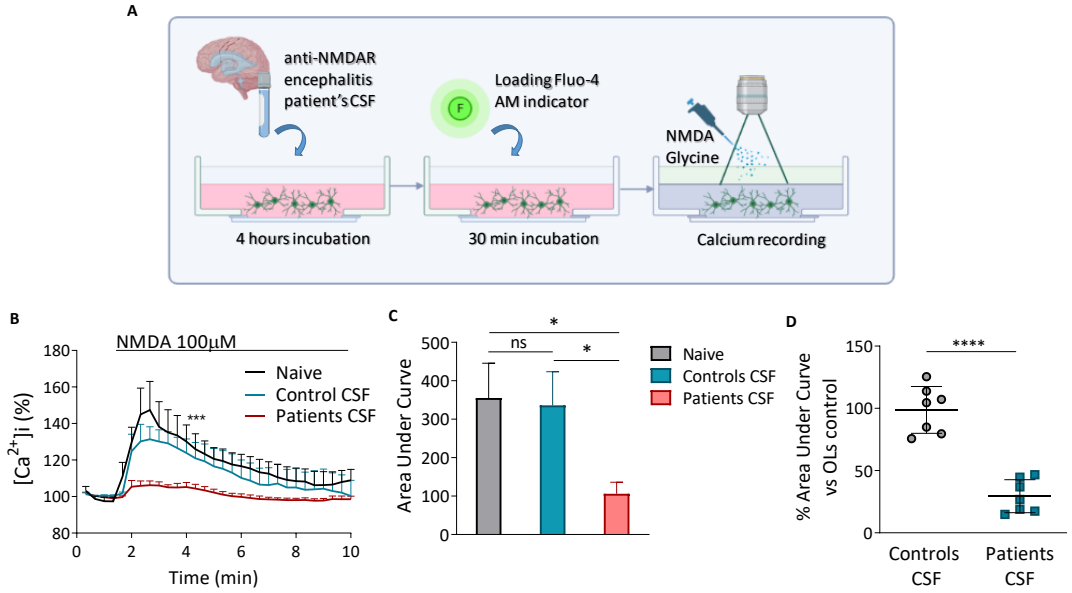

Figure 35. Specific N-methyl-D-aspartate (NMDA) receptor (NMDAR) activity in oligodendrocytes in response to agonist application after incubation with patients and control cerebrospinal fluid (CSF). **A**. Graphic representation of the experimental procedure. **B.** Recordings of the basal Ca^{2+} responses in naive oligodendrocytes were not significantly modified after incubation with CSF from control subjects (mean value of 7 control CSF samples in 3 different experiments) but were significantly reduced following exposure to patients' CSF (mean value of 7 patients' CSF samples in 3 different experiments); *** p-value < 0.001, one-way analysis of variance (ANOVA) with Tukey *post-hoc* test. **C.** Histogram depicting the area under the curve displayed by the recordings in B. Note that the values after preincubation with CSFs from patients are lower than in control naive oligodendrocytes or after preincubation with control CSF; *p < 0.05, one-way ANOVA with Tukey *post-hoc* test. **D.** Graph showing the effects of each individual CSF from controls or patients on the NMDAR responses in naive oligodendrocytes (100%); ****p < 0.001, unpaired 2-tailed Student t test.

The specificity of the changes in NMDAR-mediated responses caused by patients' CSF antibodies was further assessed with 2 different approaches. First, we used pooled patients' CSF samples preabsorbed with HEK293 cells expressing GluN1 or with cells not expressing this subunit (mock transfected cells). These experiments showed that the effect of patients' CSF antibodies was abrogated when CSF samples were preabsorbed with HEK293 cells expressing GluN1, but not with samples preabsorbed with HEK293 mock transfected cells **(Figure 36.B)**. Second, we assessed the changes in oligodendrocyte NMDAR mediated responses using a previously reported monoclonal human GluN1 antibody (SSM5) and the corresponding isotype control (12D7). We found that pre-treatment of oligodendrocytes with SSM5, but not 12D7, efficiently blocked the NMDAR-mediated responses **(Figure 36.C)**.

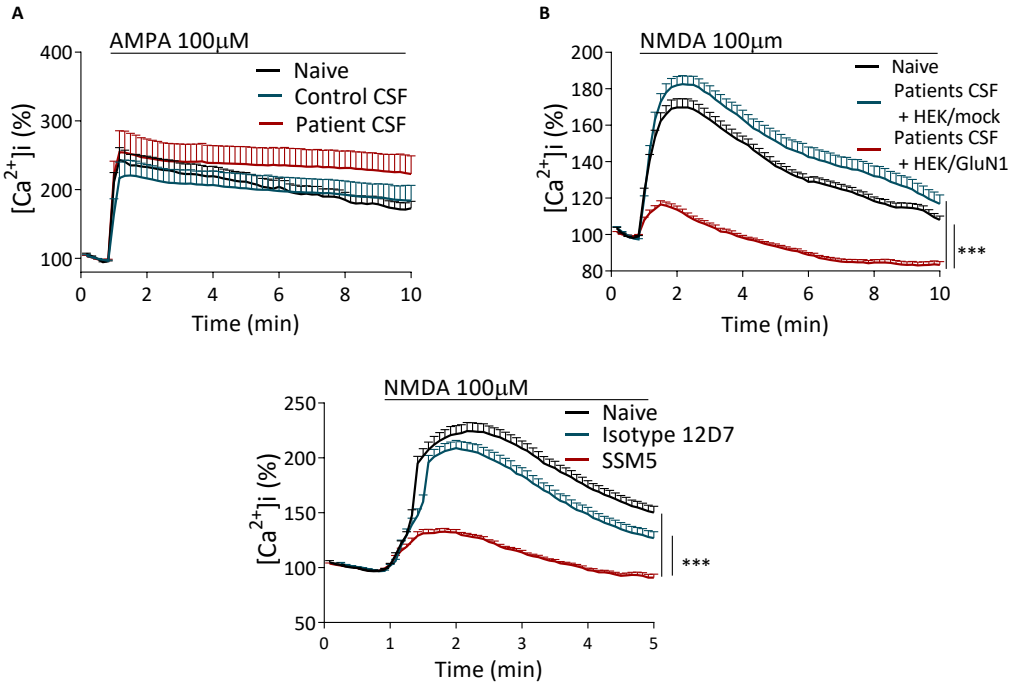

Figure 36. **A**. The α-amino- 3-hydroxy-5-methyl-4-isoxazolepropionic acid (AMPA) receptor responses are similar in oligodendrocytes not preincubated with CSF and those preincubated with control CSF or patients' CSF. **B.** Preabsorption of pooled patients' CSF in HEK cells transfected with GluN1, but not with HEK mock transfected cells, results in NMDA responses similar to those of naive oligodendrocytes (naive vs patients' CSF + HEK/mock, *** $p < 0.001$; patients' CSF + HEK/GluN1 vs patients' CSF + HEK/ mock, *** $p < 0.001$; one-way ANOVA with Tukey *post-hoc* test). **C.** Pretreatment of oligodendrocytes with the human monoclonal NMDAR antibody SSM5, but not isotype control 12D7, abolishes the NMDA response (naive vs SSM5, *** $p < 0.001$; 12D7 isotype vs SSM5, *** $p < 0.001$; one-way ANOVA with Tukey *post-hoc* test). In all graphs, data of each sample represent the average ± SEM of values obtained from 3 different cultures.

Taken together, these 2 sets of experiments provide robust evidence that the reduction of NMDAR-mediated responses in oligodendrocytes is mediated by patients' GluN1 antibodies. NMDAR activity in oligodendrocytes mediates the translocation of GLUT1 to the membrane and myelin compartment, a feature that has structural consequences for the white matter (Saab *et al*., 2016). Therefore, our findings suggest a link between antibody-mediated dysfunction of NMDARs in oligodendrocytes and the white matter alterations reported in patients with this disorder.

DISCUSSION

Clemastine induces an impairment in developmental myelination

Here we report that clemastine treatment during development promotes oligodendrocyte differentiation and alters myelination. In addition, our results also demonstrate that clemastine reduces the density of $CD11c^{+}$ microglial cells, a transient microglia subtype present during development that it is involved in myelinogenesis. These findings strongly suggest that clemastine final outcome on myelination may depend on microglia-oligodendrocytes crosstalk.

Clemastine was identified in a high-throughput study (Mei *et al*., 2014) as a drug inducing oligodendrocyte progenitor differentiation *in vitro*. The drug facilitates remyelination after demyelination (Li *et al*., 2015; Mei *et al*., 2016). Thus, clemastine promotes remyelination in animal models of multiple sclerosis and after ischemic insults (Cree *et al*., 2018; Wang *et al*., 2018). Myelin renewal induced by clemastine also prevents cognitive symptoms secondary to aging and Alzheimer's disease (Wang *et al*., 2020; Chen *et al*., 2021). Finally, it has been described to promote myelination and to rescue behavioral phenotype in socially isolated mice (Liu *et al*., 2016). In contrast, no clinical benefit of clemastine was obtained in animal models of Pelizaeus Merzbacher disease (Turski *et al*., 2018), a dysmyelinating disorder of the central nervous system caused by impaired differentiation of oligodendrocytes during development. In accordance, we found that developmental myelination is not increased after chronic clemastine treatment, even if clemastine induced an increase in oligodendrocyte differentiation. The dose used in our study was similar to those used in other studies (Liu *et al*., 2016). In addition, clemastine crosses the blood brain barrier and reaches the CNS parenchyma, as determined by mass spectrometry (Turski *et al*., 2018).

Of note, the study of Tursky and colleagues, and ours tested the therapeutical potential of clemastine during development, whereas all the previous studies analyzed the effect of clemastine on adult mice after demyelination or altered myelination. The other important difference is that mice either do not have demyelination (in our study) or have a primary myelination disorder in *Pelizaeus Merzbacher* disease mice (Turski *et al*., 2018), whereas in the other models in which clemastine has been tested, myelination deficits were induced by

toxins, inflammation or social deprivation and most of the studies are associated with chronic inflammation.

Although the beneficial effect of clemastine is extended to different insults and diseases, the underlying mechanisms are still unclear. *In vitro* screening proposes muscarinic M1 receptor as the target for the effect in OPCs promoting its maturation (Deshmukh *et al*., 2013; Mei *et al*., 2014). Indeed, we observed that mice treated with clemastine during development showed an increase in oligodendrocyte maturation, as revealed by the ratio $NG2^+/APC^+$. However, myelin wrapping of axons seemed to be incomplete or delayed in clemastine-treated mice. In addition to oligodendrocytes, it has been reported that clemastine could interact with microglia too as it possess immune suppressive properties. Indeed, clemastine promotes neuronal protection in animal models of ALS and alleviates hypomyelination after hypoxia by modulating microglia inflammatory reaction (Apolloni *et al*., 2016; Xie *et al*., 2021).

Our study also showed that clemastine targets microglia cells during development and induced morphological changes as well as changes in the expression of inflammatory markers, a fact that could indirectly impact developmental myelination. Recent findings highlight the important role played by microglia cells in developmental myelination. Microglial cells engulf myelin sheaths during development to sculpt myelination according to axonal activity (A. N. Hughes & Appel, 2019). On the other hand, a particular $CD11c^+$ microglia subset that predominates in primary myelinating areas of the developing brain is essential for myelinogenesis (Wlodarczyk *et al*., 2017). These cells promote myelinogenesis because they are the major source of insulin-like growth factor (IGF), a factor critical for proper myelin formation (Goebbels *et al*., 2010; Harrington *et al*., 2010). The primary signaling receptor, insulin-like growth factor-1 receptor (IGF1R), is a transmembrane tyrosine kinase receptor that binds insulin-like growth factors 1 and 2 (IGF1 and IGF2) and signals through the PI3K-AKT-mTOR, a signaling pathway whose precise regulation is critical for proper myelin formation. IGF modulates lipid metabolism (Hackett *et al*., 2020), a pathway essential for myelination, not for oligodendrocyte differentiation. Thus, expression of constitutively active Akt in oligodendrocytes and their progenitor cells generated no more

oligodendrocytes, but dramatically more myelin, indicating that this signaling pathway could affect myelin generation without affecting oligodendrocytes differentiation (Flores *et al*., 2008). Similarly, IGF-1-overexpressing mice showed a dramatic increase in the amount of myelin per oligodendrocyte, but normal numbers of oligodendrocytes (Carson *et al*., 1993). More recent studies involve the Akt-mTOR signaling pathway in myelin sheath growth (Fedder-Semmes & Appel, 2021). In our study we showed a significant reduction of IGF and of $CD11c^+$ microglia cells in the *corpus callosum* of clemastine-treated mice. It could be possible that clemastine, under these particular circumstances, blocks the process of myelin wrapping by mature myelinating oligodendrocytes. Further experiments are necessary to confirm this hypothesis.

Pharmacogenetic stimulation of mature oligodendrocytes promotes myelination

Myelin plasticity has recently emerged as an important focus of research, as it opens a novel therapeutic approach for neurodegenerative and neuropsychiatric disorders. The ability to dynamically regulate myelination in response to environmental cues or neuronal activity is increasingly thought to be critical also for normal brain function and learning (Gibson *et al*., 2014; McKenzie *et al*., 2014). Apart from the myelination of previously unmyelinated axons, circuit function could also be modified by either altering the length of myelin internodes (Ford *et al*., 2015) or the number of wraps (myelin thickness) of existing myelin (Castelfranco & Hartline, 2015). The general mechanism proposed for myelin plasticity is driven by new oligodendrogenesis (McKenzie *et al*., 2014), but few studies have analyzed the impact of mature oligodendrocyte stimulation in neuronal function. In addition to generating myelin sheaths and directing node of Ranvier formation, oligodendrocytes support axonal function by communicating with axons via the periaxonal space and providing metabolic support (Y. Lee *et al*., 2012b; Saab *et al*., 2013), i.e. lactate, a metabolite involved in learning and memory at synaptic level. In this study, we addressed the effect of mature oligodendrocytes stimulation on myelination and remyelination by generating a specific pharmacogenetic mice model. Our study demonstrates that mature oligodendrocyte stimulation ameliorates neurological symptoms in EAE mice and prevent axonal damage after oxygen and glucose deprivation. We demonstrated that selective activation of hM3Dq excitatory receptors promotes myelination and oligodendrocyte metabolism. Importantly, CNO activates glycolysis and lactate production and release, that signals through $GABA_B$ receptors to promote axonal survival.

MRI studies of myelination *in vivo* reported that myelin deposition occurs in an orderly and predictable fashion, that generally proceeds in a caudocranial direction, from deep to superficial and from posterior to anterior (Ballesteros *et al*., 1993; Jakovcevski *et al*., 2009; Welker & Patton, 2012). Consistent with this developmental pattern of myelination, we observed a higher number of $hM3Dq^+/GFP^+$ recombinant oligodendrocytes in *corpus callosum* (at P27-29), which corresponds to a higher number of differentiated

oligodendrocytes in *corpus callosum* at that age. Despite the fact that levels of recombination decay in cerebral cortex, this rate was notably high in all the regions analyzed, and the activation of hM3Dq receptors in oligodendrocytes with CNO led to a massive increase in intracellular calcium. Altogether, we validated PLP-CreERT2^{+}/ hM3Dq$^{+/+}$ mice as a very valuable tool to specifically activate oligodendrocytes.

Consistently with the fact that hM3Dq is expressed in PLP^{+} mature oligodendrocytes, we did not observe any effect on OPC proliferation nor in the number of mature APC^{+} oligodendrocytes. Importantly, chronic hM3Dq activation in oligodendrocytes is linked to an increase in myelination and axon conduction velocity. These results suggest an upregulation of the intrinsic machinery for myelin formation upon hM3Dq receptor activation. Our results point to an increase in new myelin sheaths synthesis, as we detected an increase in the number of nodes of Ranvier. In contrast, we did not observe alterations in the number of myelin wraps or g-ratio (de Faria *et al*., 2021). Surprisingly we also detected that pharmacogenetic stimulation of oligodendrocytes tunes the node of Ranvier structure, another plastic structure of the axon-myelin unit (Young *et al*., 2013) . The node length decreases, whereas the paranode length increases. Alterations in node length may involve modifications in the paranodal cell adhesion between the myelin and the axon. These paranodal junctions, mediated by Caspr, neurofascin 155 and contactin, are formed before the establishment of nodal structure, suggesting important glia-dependent mechanisms for nodal Na^{+} channel clustering (Rasband & Peles, 2021). Accordingly, the increase observed in paranode length could indicate longitudinal growth of the myelin sheaths, favouring high-density accumulation of nodal voltage-gated sodium channels, with subsequent enhanced conduction velocity (Freeman *et al*., 2015). In fact, the density of the channels, more that nodal length, seems to be relevant for conduction speed. Computer modelling developed by Arancibia-Cárcamo and colleagues predicts that node length changes will alter conduction speed by ~20%, similar to the changes produced by altering the number of myelin wraps or the internode length. This model could constitute a potentially energy-efficient and rapid mechanism for tuning CNS information transmission (Arancibia-Cárcamo *et al*., 2017). However, the impact of nodal length on axonal conduction velocity depends on whether this

change is accompanied by alterations in the total number of Na^+ channels. If the number of channels is constant at each node, then the predicted conduction speed raises with decreasing node length, as we observed. However, if the density of Na^+ channels remains constant, the decrease in nodal length reduced the number of Na^+ channels leading to a decrease of conduction velocity. Based on these predictions, we assumed that CNO stimulation do not alter the total number of sodium channels at node of Ranvier. Otherwise, it is possible that fine changes in the node structure are less relevant than the increase in the number of myelin sheaths and nodes because of the *de novo* myelination.

In addition to an increase in conduction speed, pharmacogenetic stimulation of oligodendrocytes induces an acute increase in axon excitability. We detected an increase in the amplitude of CAPs of callosal fibers after acute application of CNO in $hM3Dq^+$ mice, indicative of changes in axonal action potential waveform or in fiber recruitment. Although the increase in axon excitability was blocked in the presence of lactate transporters, further experiments are required to characterize the mechanism involved. Importantly, this finding suggest that oligodendrocyte can signal to axons. It is well known that astrocytes can modulate synaptic transmission in grey matter, but how glia can modulate transmission in white matter is less known. Recent data suggest that astrocytes, are able to modulate axon excitability in white matter through the release of adenosine (Lezmy *et al*., 2021). Importantly, changes in axonal action potential amplitude greatly alter neurotransmitter release (Sabatini & Regehr, 1997), and these effects can be even passively transmitted at distal synaptic release sites (Alle & Geiger, 2006; Shu *et al*., 2006). The impact of the data obtained in this thesis offer a new study on the role of oligodendrocytes in synaptic transmission.

Pharmacogenetic stimulation of mature oligodendrocytes drives myelin-axon metabolic coupling and prevents axonal damage.

The ability of mature oligodendrocytes to induce *de novo* myelination highlights their therapeutic potential to promote remyelination in demyelinating diseases, and to increase neural plasticity in the adult CNS (Jeffries *et al*., 2016; Macchi *et al*., 2020). Indeed, we observed that chronic stimulation of mature oligodendrocytes significantly ameliorated neurological symptoms in EAE mice. Although previous evidences suggest that remyelinating oligodendrocytes arise from OPCs (Münzel & Williams, 2013), a recent work proposes that some demyelinated axons maintain the location and components of the nodes, which could indeed guide the remyelination by pre-existing oligodendrocytes (Orthmann-Murphy *et al*., 2020). At histological level, PLP-CreERT2^{+}/hM3Dq$^{+/+}$ mice showed smaller myelin lesions and lower axonal damage. The fact that the differences in the neurological symptoms were detected at EAE onset may suggest that pharmacological stimulation of oligodendrocytes prevents demyelination and axonal damage, more than accelerates remyelination.

Myelin synthesis is energetically expensive and time-consuming, hence, oligodendrocytes uptake large amounts of glucose to support their energetic demands during myelination and remyelination (Harris & Attwell, 2012; Tepavčević, 2021). Glucose is primarily metabolized in the cytosol via glycolysis to generate pyruvate, which provides acetyl CoA for myelin lipids synthesis and ATP generation by oxidative phosphorylation in the mitochondria. Alternatively, once myelination is complete, oligodendrocytes undergo a metabolic reprogramming process, from oxidative phosphorylation to glycolysis in which pyruvate is reversibly converted into lactate in the cytosol (Rosko *et al*., 2019). This suggests a strategy to reduce the production of reactive oxygen species coupled to the activity of mitochondrial electron transport chain, while lactate supports axonal energetic demands and contributes to myelin maintenance and axonal integrity (Fünfschilling *et al*., 2012). Pathological conditions such as metabolic stress injury also promotes a metabolic switch in oligodendrocytes to glycolysis to promote survival, rather than the maintenance of myelin membranes (Rone *et al*., 2016). Here we report that acute stimulation of oligodendrocytes

increases glycolysis, lactate production and lactate shuttle to axons, as previously described in the proposed model of axon-glial metabolic coupling (Fünfschilling *et al*., 2012; Lee *et al*., 2012; Saab *et al*., 2016), a fact that contributed to higher oligodendroglial and axonal survival in EAE. The hypermetabolic activity in acute multiple sclerosis lesions suggests that improving oligodendrocyte bioenergetics would promote neuroprotection. Indeed, lactate release by oligodendrocytes in response to CNO increased axonal recovery and survival after ischemia. Of note, other study revealed that glycogen-derived lactate could also promote remyelination in a cuprizone model (Ichihara *et al*., 2017).

The specific role of lactate on axonal survival has been a subject of considerable interest (Magistretti & Allaman, 2018). Previous findings described that the abolishment of compound action potentials following glucose deprivation was rescued with exogenous glucose more efficiently than with L-lactate or pyruvate (Meyer *et al*., 2018), while other independent work observed the opposite outcome (F. Li *et al*., 2020). Li and colleagues proposed that L-lactate and L-2-hydroxyglutarate not only act as an energetic metabolite, but also as a survival signaling molecule in a model of axonal damage (F. Li *et al*., 2020). During injury, extracellular lactate released by reprogrammed oligodendrocytes modulates neuronal metabotropic GABA-B receptors, increasing cAMP-related pathways and subsequent axonal survival. By contrast, intracellular accumulation of L-2-hydroxyglutarate in neurons inhibits ATP synthase and mTOR signaling, reducing axonal regeneration (Fu *et al*., 2015; Hunt *et al*., 2019). These observations indicate that metabolites acting as signaling molecules could exert different effects on neurons extracellularly and intracellularly, depending on the extrinsic environment and glial metabolism reprogramming (Barros, 2013; Mosienko *et al*., 2015).

Oligodendroglial cells express several metabotropic receptors, including GABA and NMDA receptors, involved in OPC migration and oligodendrocyte myelination. On the other hand, the G-protein coupled receptor GPR17 is considered to play a role in the repair of demyelinating plaques and in oligodendrocyte differentiation under physiological condition (Dziedzic *et al*., 2020). Therefore, the molecular activity of hM3Dq receptors proposes this

pharmacogenetic model as a promising tool to deeply study the role of mature oligodendrocyte, both under physiological and pathological conditions.

N-Methyl-D-Aspartate receptor antibodies in autoimmune encephalopathy alter oligodendrocyte function

In this study we show that treatment of oligodendrocytes with CSF from patients with anti-NMDAR encephalitis or a recombinant monoclonal antibody derived from plasma cells of a patient, but not the corresponding controls, decreased receptor activation by NMDA. These pathogenic effects were abrogated when patients' CSF were preabsorbed in NMDAR-expressing HEK293 cells, confirming the pathogenic role of the antibodies. Moreover, patients' CSF antibodies did not alter AMPAR function, suggesting a specific impairment in NMDAR activation. These antibody-mediated effects could be associated with a reduced expression of GLUT1 in the distal processes of oligodendrocytes. Because expression of GLUT1 is important for axonal function, the findings suggest a novel pathogenic mechanism beyond the reported antibody effects on neuronal synaptic receptors and plasticity.

In oligodendrocytes, NMDARs control the supply of energy substrates to support the proper function of axons via GLUT1 translocation to the oligodendrocyte membrane (Saab *et al*., 2016). Studies have shown that the amplitude of the action potentials in axons during high frequency stimulation decreases in the absence of NMDAR in oligodendrocytes, and recovers more slowly when returning at low frequency *stimuli* (Saab *et al*., 2016). Prolonged loss of NMDAR function in oligodendroglia leads to axonal pathology and neuroinflammation in white matter tracts resulting in neurological symptoms and motor dysfunction. Although astrocytes can also support axonal function by releasing lactate in the white matter (Mächler *et al*., 2016), the direct oligodendrocyte-axon interaction is needed to adjust energy demands and prevent long-term structural damage. In a series of 577 patients with anti-NMDAR encephalitis, 67% had normal clinical MRI studies, and for the most part the other patients had mild or transient cortical-subcortical FLAIR abnormalities (Titulaer *et al*., 2013).The high frequency of normal findings using standard MRI sequences was also indicated in a systematic review of the literature that included 1167 patients, showing that

62% had normal MRI. Moreover, among the 38% of patients with abnormal findings, the subcortical white matter was as frequently involved as the grey matter (Bacchi *et al*., 2018). In contrast, when a cohort of 24 patients was examined using MRI DTI sequences, all patients had widespread changes in white matter integrity that correlated with disease severity. Interestingly, 17 (71%) of these patients had normal standard clinical MRIs (Finke *et al*., 2013). In another study of 46 patients with anti-NMDAR encephalitis (36 recovered and 10 non-recovered from the disease), the non-recovered patients showed widespread superficial white matter damage compared with the recovered patients and healthy controls that had normal findings (Phillips *et al*., 2018). Thus, anti-NMDAR encephalitis is associated with characteristic alterations of functional connectivity and widespread changes of white matter integrity despite normal findings in routine clinical MRI (Finke *et al*., 2013).

Based on the current findings and previously reported clinical and pathological studies, in which cellular inflammatory infiltrates are usually mild without clear involvement of the white matter (Dalmau *et al*., 2007), we postulate that the indicated MRI white matter changes may be directly mediated by NMDAR antibodies. This white matter effects, along with the previously reported impairment of synaptic function and plasticity (Moscato *et al*., 2014; Planagumà *et al*., 2016), would contribute to explain the dissociation between symptoms severity and frequently normal MRI clinical sequences (despite almost constant DTI changes). A task for the future is to determine whether patients´ antibodies alter white matter integrity in an existing animal model of passive transfer of antibodies (Planagumà *et al*., 2015), examining changes in expression of GLUT1, how these changes correlate with white matter abnormalities (using rodent MRI studies), and the degree of reversibility of these alterations. These studies are important because there are currently no biomarkers of the course of the disease (Dalmau *et al*., 2019), thus a better understanding of the white matter changes during the disease may lead to a potentially useful biomarker.

CONCLUSIONS

The conclusions of this work are as follows:

1. Clemastine increases OPC differentiation into mature oligodendrocytes during development.
2. Despite that, clemastine reduces myelination and axonal conduction velocity in developing mice brain.
3. Clemastine treatment in neonatal mice, reduces the subpopulation of $CD11c^+$ microglia, and the expression of IGF.

During development, microglia act as "architects" who organize and coordinate the patterns and wiring of the CNS, including myelination. We propose that clemastine interacts and affects microglia development too **(Figure 37)**. Clemastine reduces the population of microglia $CD11c^+$ cells, a transient subset that regulates CNS myelinogenesis via release of IGF-1, an essential factor for myelination (Wlodarczyk *et al*., 2017). Although clemastine has arisen as a promising pro-myelination drug that promote OPC differentiation *in vitro* and remyelination after demyelinating lesions, our results suggest that correct myelination during development may depend also in microglia-oligodendrocyte crosstalk.

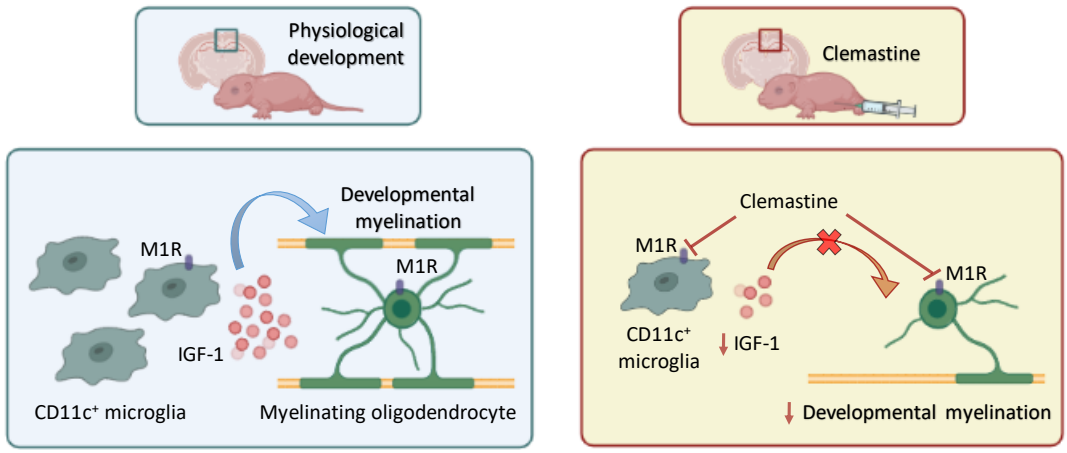

Figure 37. Scheme showing the effect of clemastine treatment on developing mouse brain.

4. Pharmacogenetic stimulation of mature oligodendrocytes promotes myelination *in vitro* and *in vivo*, and increases axonal conduction velocity.
5. Pharmacogenetic activation of oligodendrocytes boosts their metabolic activity, enhancing glycolysis and lactate production.
6. Pharmacogenetic stimulation of mature oligodendrocytes ameliorates neurological symptoms in EAE and prevents axonal damage.
7. Pharmacogenetic stimulation of oligodendrocytes promotes axonal recovery by lactate release and GABA-B receptor activation.

In this study, we demonstrated that selective mature oligodendrocyte stimulation using pharmacogenetics increases myelination and metabolism in oligodendrocytes. Thus, the pharmacogenetic mice line developed in this study is as a promising tool to elucidate the contribution of mature oligodendrocytes to myelin remodeling in physiological and pathological conditions. We propose that the mechanism of axonal protection described in two different models, EAE and OGD, is due to the myelin-axon metabolic coupling preserving axonal integrity. Stimulation of mature oligodendrocytes increases glycolysis and lactate production, promoting axonal survival through GABA-B receptors-related signalling **(Figure 38)**.

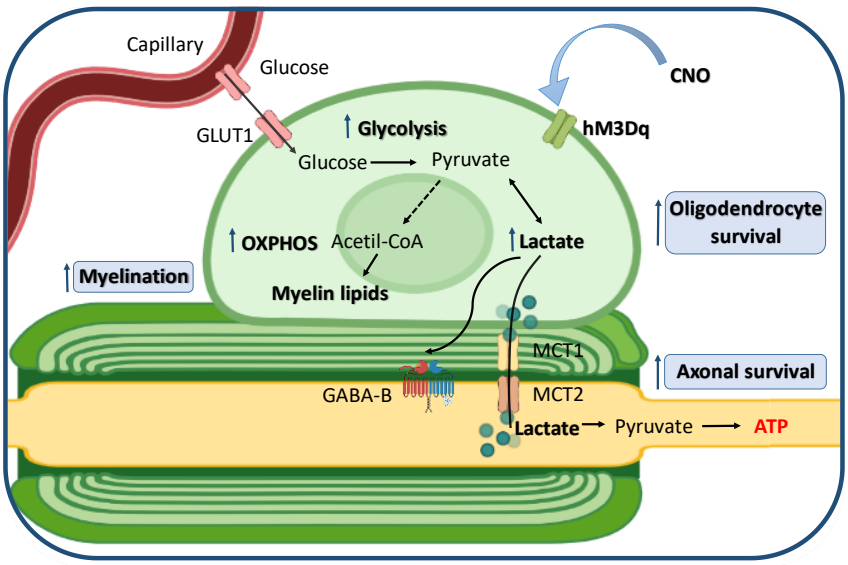

Figure 38. Model of metabolic coupling between hM3Dq^{+} oligodendrocytes and myelinated axons.

8. N-Methyl-D-Aspartate receptor antibodies in autoimmune encephalopathy downregulates the activation of NMDAR in oligodendrocytes.

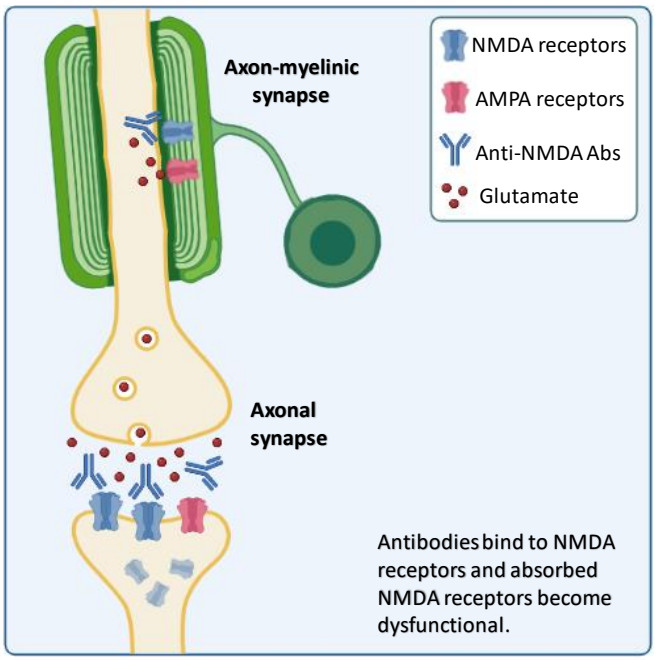

Figure 39. Proposed pathological consequences of anti-NMDAR antibodies on oligodendrocyte and axonal function.

NMDA receptors has been located at the axon-myelin synapse unit, which mediate activity-dependent communication between oligodendrocytes and axons. Our results suggest that the function of the axon-myelinc synapses could be affected by NMDA downregulation in patients with anti-NMDAR encephalitis. We propose that the recruitment of resources for myelin maintenance and axon metabolic support by oligodendrocytes could also be altered in these patients, leading to white matter lesions.

In summary, the results obtained in the different research lines of this Thesis could contribute to the future development of innovative therapies for demyelinating disorders.

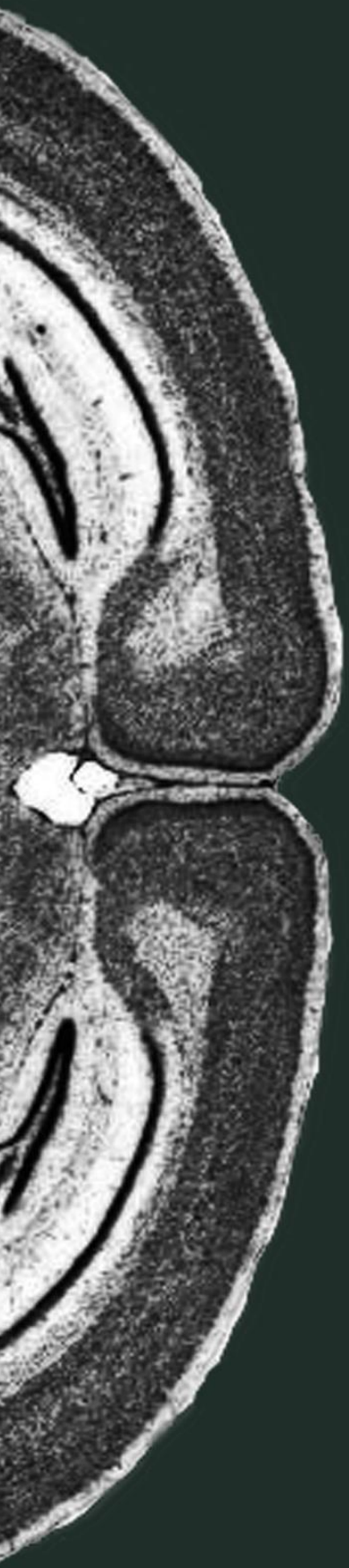

REFERENCES

Alle, H., & Geiger, J. R. P. (2006). Combined analog and action potential coding in hippocampal mossy fibers. *Science*, *311*(5765), 1290–1293. https://doi.org/10.1126/science.1119055

Almeida, R. G., & Lyons, D. A. (2017). On myelinated axon plasticity and neuronal circuit formation and function. *Journal of Neuroscience*, *37*(42), 10023–10034. https://doi.org/10.1523/JNEUROSCI.3185-16.2017

Alonso, A., & Hernán, M. A. (2008). Temporal trends in the incidence of multiple sclerosis: A systematic review. *Neurology*, *71*(2), 129–135. https://doi.org/10.1212/01.wnl.0000316802.35974.34

Apolloni, S., Fabbrizio, P., Amadio, S., & Volonté, C. (2016). Actions of the antihistaminergic clemastine on presymptomatic SOD1-G93A mice ameliorate ALS disease progression. *Journal of Neuroinflammation*, *13*(1), 1–15. https://doi.org/10.1186/s12974-016-0658-8

Arancibia-Cárcamo, I. L., Ford, M. C., Cossell, L., Ishida, K., Tohyama, K., & Attwell, D. (2017). Node of ranvier length as a potential regulator of myelinated axon conduction speed. *ELife*, *6*, 1–15. https://doi.org/10.7554/eLife.23329

Armbruster, B. N., Li, X., Pausch, M. H., Herlitze, S., & Roth, B. L. (2007). Evolving the lock to fit the key to create a family of G protein-coupled receptors potently activated by an inert ligand. *Proceedings of the National Academy of Sciences of the United States of America*, *104*(12), 5163–5168. https://doi.org/10.1073/pnas.0700293104

Aurangzeb, S., Symmonds, M., Knight, R. K., Kennett, R., Wehner, T., & Irani, S. R. (2017). LGI1-antibody encephalitis is characterised by frequent, multifocal clinical and subclinical seizures. *Seizure*, *50*, 14–17. https://doi.org/10.1016/j.seizure.2017.05.017

Bacchi, S., Franke, K., Wewegama, D., Needham, E., Patel, S., & Menon, D. (2018). Magnetic resonance imaging and positron emission tomography in anti-NMDA receptor encephalitis: A systematic review. *Journal of Clinical Neuroscience*, *52*, 54–59. https://doi.org/10.1016/j.jocn.2018.03.026

Back, S. A., Tuohy, T. M. F., Chen, H., Wallingford, N., Craig, A., Struve, J., Ning, L. L., Banine, F., Liu, Y., Chang, A., Trapp, B. D., Bebo, B. F., Rao, M. S., & Sherman, L. S. (2005). Hyaluronan accumulates in demyelinated lesions and inhibits oligodendrocyte progenitor maturation. *Nature Medicine*, *11*(9), 966–972. https://doi.org/10.1038/nm1279

Ballesteros, M. C., Hansen, P. E., & Soila, K. (1993). MR imaging of the developing human brain. Part 2. Postnatal development. *Radiographics : A Review Publication of the Radiological Society of North America, Inc*, *13*(3), 611–622. https://doi.org/10.1148/radiographics.13.3.8316668

Barnett, M. H., & Prineas, J. W. (2004). Relapsing and Remitting Multiple Sclerosis: Pathology of the Newly Forming Lesion. *Annals of Neurology*, *55*(4), 458–468. https://doi.org/10.1002/ana.20016

Barres, B. A., Hart, I. K., Coles, H. S. R., Burne, J. F., Voyvodic, J. T., Richardson, W. D., & Raff, M. C. (1992). Cell death and control of cell survival in the oligodendrocyte lineage. *Cell*, *70*(1), 31–46. https://doi.org/10.1016/0092-8674(92)90531-G

Barres, B. A., & Raff, M. C. (1993). Proliferation of oligodendrocyte precursor cells depends on electrical activity in axons. *Nature*, *361*(6409), 258–260. https://doi.org/10.1038/361258a0

Barros, L. F. (2013). Metabolic signaling by lactate in the brain. *Trends in Neurosciences*, *36*(7), 396–404. https://doi.org/10.1016/j.tins.2013.04.002

Bartzokis, G. (2004). Age-related myelin breakdown: A developmental model of cognitive decline and Alzheimer's disease. *Neurobiology of Aging*, *25*(1), 5–18. https://doi.org/10.1016/j.neurobiolaging.2003.03.001

Bartzokis, G., Beckson, M., Lu, P. H., Nuechterlein, K. H., Edwards, N., & Mintz, J. (2001). Age-related changes in frontal and temporal lobe volumes in men: A magnetic resonance imaging study. *Archives of General Psychiatry*, *58*(5), 461–465. https://doi.org/10.1001/archpsyc.58.5.461

Bartzokis, G., Sultzer, D., Lu, P. H., Nuechterlein, K. H., Mintz, J., & Cummings, J. L. (2004). Heterogeneous age-related breakdown of white matter structural integrity: Implications for cortical "disconnection" in aging and Alzheimer's disease. *Neurobiology of Aging*, *25*(7), 843–851. https://doi.org/10.1016/j.neurobiolaging.2003.09.005

Battefeld, A., Popovic, M. A., de Vries, S. I., & Kole, M. H. P. (2019). High-Frequency Microdomain Ca 2+ Transients and Waves during Early Myelin Internode Remodeling. *Cell Reports*, *26*(1), 182-191.e5. https://doi.org/10.1016/j.celrep.2018.12.039

Baumann, N., & Pham-Dinh, D. (2001). Biology of oligodendrocyte and myelin in the mammalian central nervous system. *Physiological Reviews*, *81*(2), 871–927. https://doi.org/10.1152/physrev.2001.81.2.871

Bechler, M. E., Swire, M., & ffrench-Constant, C. (2018). Intrinsic and adaptive myelination—A sequential mechanism for smart wiring in the brain. *Developmental Neurobiology*, *78*(2), 68–79. https://doi.org/10.1002/dneu.22518

Bengtsson, S. L., Nagy, Z., Skare, S., Forsman, L., Forssberg, H., & Ullén, F. (2005). Extensive piano practicing has regionally specific effects on white matter development. *Nature Neuroscience*, *8*(9), 1148–1150. https://doi.org/10.1038/nn1516

Bercury, K. K., & Macklin, W. B. (2015). Dynamics and mechanisms of CNS myelination. *Developmental Cell*, *32*(4), 447–458. https://doi.org/10.1016/j.devcel.2015.01.016

Bergles, D. E., & Jahr, C. E. (2000). Glutamatergic synapses on oligodendrocyte precursor cells in the hippocampus. *Nature*, *15439*(1996), 187–191.

Bitsch, A., Schuchardt, J., Bunkowski, S., Kuhlmann, T., & Brück, W. (2000). Acute axonal injury in multiple sclerosis. Correlation with demyelination and inflammation. *Brain*, *123*(6), 1174–1183. https://doi.org/10.1093/brain/123.6.1174

Broadley, J., Seneviratne, U., Beech, P., Buzzard, K., Butzkueven, H., O'Brien, T., & Monif, M. (2019). Prognosticating autoimmune encephalitis: A systematic review. *Journal of Autoimmunity*, *96*(October 2018), 24–34. https://doi.org/10.1016/j.jaut.2018.10.014

Browne P, Chandraratna D, Angood C, Tremlett H, Baker C, Taylor BV, & Thompson AJ. (2014). Atlas of Multiple Sclerosis 2013: A growing global problem with widespread inequity. *Neurology*, *93*(11), 1022–1024. http://www.msif.org/about-ms/publications-

Bujalka, H., Koenning, M., Jackson, S., Perreau, V. M., Pope, B., Hay, C. M., Mitew, S., Hill, A. F., Lu, Q. R., Wegner, M., Srinivasan, R., Svaren, J., Willingham, M., Barres, B. A., & Emery, B. (2013). MYRF Is a Membrane-Associated Transcription Factor That Autoproteolytically Cleaves to Directly Activate Myelin Genes. *PLoS Biology*, *11*(8). https://doi.org/10.1371/journal.pbio.1001625

Burzomato, V., Frugier, G., Pérez-Otaño, I., Kittler, J. T., & Attwell, D. (2010). The receptor subunits generating NMDA receptor mediated currents in oligodendrocytes. *Journal of Physiology*, *588*(18), 3403–3414. https://doi.org/10.1113/jphysiol.2010.195503

Byun, J. I., Lee, S. T., Moon, J., Jung, K. H., Shin, J. W., Sunwoo, J. S., Lim, J. A., Shin, Y. W., Kim, T. J., Lee, K. J., Park, K. il, Jung, K. Y., Lee, S. K., & Chu, K. (2015). Cardiac sympathetic dysfunction in anti-NMDA receptor encephalitis. *Autonomic Neuroscience: Basic and Clinical*, *193*, 142–146. https://doi.org/10.1016/j.autneu.2015.08.002

Carson, M. J., Behringer, R. R., Brinster, R. L., & McMorris, F. A. (1993). Insulin-like growth factor I increases brain growth and central nervous system myelination in tTransgenic mice. *Neuron*, *10*(4), 729–740. https://doi.org/10.1016/0896-6273(93)90173-O

Castelfranco, A. M., & Hartline, D. K. (2015). The evolution of vertebrate and invertebrate myelin: a theoretical computational study. *Journal of Computational Neuroscience*, *38*(3), 521–538. https://doi.org/10.1007/s10827-015-0552-x

Chang, A., Staugaitis, S. M., Dutta, R., Batt, C. E., Easley, K. E., Chomyk, A. M., Yong, V. W., Fox, R. J., Kidd, G. J., & Trapp, B. D. (2012). Cortical remyelination: A new target for repair therapies in multiple sclerosis. *Annals of Neurology*, *72*(6), 918–926. https://doi.org/10.1002/ana.23693

Chang, K. J., Redmond, S. A., & Chan, J. R. (2016). Remodeling myelination: Implications for mechanisms of neural plasticity. *Nature Neuroscience*, *19*(2), 190–197. https://doi.org/10.1038/nn.4200

Chan, J. R., Watkins, T. A., Cosgaya, J. M., Zhang, C., Chen, L., Reichardt, L. F., Shooter, E. M., & Barres, B. A. (2004). NGF controls axonal receptivity to myelination by Schwann cells or oligodendrocytes. *Neuron*, *43*(2), 183–191. https://doi.org/10.1016/j.neuron.2004.06.024

Chapman, T. W., & Hill, R. A. (2020). Myelin plasticity in adulthood and aging. *Neuroscience Letters*, *715*(July 2019), 134645. https://doi.org/10.1016/j.neulet.2019.134645

Chari, D. M. (2007). Remyelination In Multiple Sclerosis. *International Review of Neurobiology*, *79*(07), 589–620. https://doi.org/10.1016/S0074-7742(07)79026-8

Charles, P., Hernandez, M. P., Stankoff, B., Aigrot, M. S., Colin, C., Rougon, G., Zalc, B., & Lubetzki, C. (2000). Negative regulation of central nervous system myelination by polysialylated-neural cell adhesion molecule. *Proceedings of the National Academy of Sciences of the United States of America*, *97*(13), 7585–7590. https://doi.org/10.1073/pnas.100076197

Chen, C., Westenbroek, R. E., Xu, X., Edwards, C. A., Sorenson, D. R., Chen, Y., McEwen, D. P., O'Malley, H. A., Bharucha, V., Meadows, L. S., Knudsen, G. A., Vilaythong, A., Noebels, J. L., Saunders, T. L., Scheuer, T., Shrager, P., Catterall, W. A., & Isom, L. L. (2004). Mice Lacking Sodium Channel β1 Subunits Display Defects in Neuronal Excitability, Sodium Channel Expression, and Nodal Architecture. *Journal of Neuroscience*, *24*(16), 4030–4042. https://doi.org/10.1523/JNEUROSCI.4139-03.2004

Chen, J. F., Liu, K., Hu, B., Li, R. R., Xin, W., Chen, H., Wang, F., Chen, L., Li, R. X., Ren, S. Y., Xiao, L., Chan, J. R., & Mei, F. (2021). Enhancing myelin renewal reverses cognitive dysfunction in a murine model of Alzheimer's disease. *Neuron*, *109*(14), 2292-2307.e5. https://doi.org/10.1016/j.neuron.2021.05.012

Chen, Y., Wu, H., Wang, S., Koito, H., Li, J., Ye, F., Hoang, J., Escobar, S. S., Gow, A., Arnett, H. A., Trapp, B. D., Karandikar, N. J., Hsieh, J., & Lu, Q. R. (2009). The oligodendrocyte-specific G protein-coupled receptor GPR17 is a cell-intrinsic timer of myelination. *Nature Neuroscience*, *12*(11), 1398–1406. https://doi.org/10.1038/nn.2410

Chomiak, T., & Hu, B. (2009). What is the optimal value of the g-ratio for myelinated fibers in the rat CNS? A theoretical approach. *PLoS ONE*, *4*(11). https://doi.org/10.1371/journal.pone.0007754

Chrast, R., Saher, G., Nave, K. A., & Verheijen, M. H. G. (2011). Lipid metabolism in myelinating glial cells: Lessons from human inherited disorders and mouse models. *Journal of Lipid Research*, *52*(3), 419–434. https://doi.org/10.1194/jlr.R009761

Compston, A., & Coles, A. (2008). Multiple sclerosis. *The Lancet*, *372*(9648), 1502–1517. https://doi.org/10.1016/S0140-6736(08)61620-7

Cree, B. A. C., Niu, J., Hoi, K. K., Zhao, C., Caganap, S. D., Henry, R. G., Dao, D. Q., Zollinger, D. R., Mei, F., Shen, Y. A. A., Franklin, R. J. M., Ullian, E. M., Xiao, L., Chan, J. R., & Fancy, S. P. J. (2018). Clemastine rescues myelination defects and promotes functional recovery in hypoxic brain injury. *Brain*, *141*(1), 85–98. https://doi.org/10.1093/brain/awx312

Cullen, C. L., Pepper, R. E., Clutterbuck, M. T., Pitman, K. A., Oorschot, V., Auderset, L., Tang, A. D., Ramm, G., Emery, B., Rodger, J., Jolivet, R. B., & Young, K. M. (2021). Periaxonal and nodal plasticities modulate action potential conduction in the adult mouse brain. *Cell Reports*, *34*(3), 108641. https://doi.org/10.1016/j.celrep.2020.108641

Cunniffe, N., & Coles, A. (2021). Promoting remyelination in multiple sclerosis. *Journal of Neurology*, *268*(1), 30–44. https://doi.org/10.1007/s00415-019-09421-x

Czopka, T., ffrench-Constant, C., & Lyons, D. A. (2013). Individual oligodendrocytes have only a few hours in which to generate new myelin sheaths invivo. *Developmental Cell*, *25*(6), 599–609. https://doi.org/10.1016/j.devcel.2013.05.013

Dalmau, J., Armangué, T., Planagumà, J., Radosevic, M., Mannara, F., Leypoldt, F., Geis, C., Lancaster, E., Titulaer, M. J., Rosenfeld, M. R., & Graus, F. (2019). An update on anti-NMDA receptor encephalitis for neurologists and psychiatrists: mechanisms and models. *The Lancet Neurology*, *18*(11), 1045–1057. https://doi.org/10.1016/S1474-4422(19)30244-3

Dalmau, J., Geis, C., & Graus, F. (2017). Autoantibodies to synaptic receptors and neuronal cell surface proteins in autoimmune diseases of the central nervous system. *Physiological Reviews*, *97*(2), 839–887. https://doi.org/10.1152/PHYSREV.00010.2016

Dalmau, J., Gleichman, A. J., Hughes, E. G., Rossi, J. E., Peng, X., Lai, M., Dessain, S. K., Rosenfeld, M. R., Balice-Gordon, R., & Lynch, D. R. (2008). Anti-NMDA-receptor encephalitis: case series and analysis of the effects of antibodies. *The Lancet Neurology*, *7*(12), 1091–1098. https://doi.org/10.1016/S1474-4422(08)70224-2

Dalmau, J., Tüzün, E., Wu, H. Y., Masjuan, J., Rossi, J. E., Voloschin, A., Baehring, J. M., Shimazaki, H., Koide, R., King, D., Mason, W., Sansing, L. H., Dichter, M. A., Rosenfeld, M. R., & Lynch, D. R. (2007). Paraneoplastic anti-N-methyl-D-aspartate receptor encephalitis associated with ovarian teratoma. *Annals of Neurology*, *61*(1), 25–36. https://doi.org/10.1002/ana.21050

de Angelis, F., Bernardo, A., Magnaghi, V., Minghetti, L., & Tata, A. M. (2012). Muscarinic receptor subtypes as potential targets to modulate oligodendrocyte progenitor survival, proliferation, and differentiation. *Developmental Neurobiology*, *72*(5), 713–728. https://doi.org/10.1002/dneu.20976

de Faria, O., Pivonkova, H., Varga, B., Timmler, S., Evans, K. A., & Káradóttir, R. T. (2021). Periods of synchronized myelin changes shape brain function and plasticity. *Nature Neuroscience*, *24*(11), 1508–1521. https://doi.org/10.1038/s41593-021-00917-2

Dendrou, C. A., Fugger, L., & Friese, M. A. (2015). Immunopathology of multiple sclerosis. *Nature Reviews Immunology*, *15*(9), 545–558. https://doi.org/10.1038/nri3871

Derfuss, T., Linington, C., Hohlfeld, R., & Meinl, E. (2010). Axo-glial antigens as targets in multiple sclerosis: Implications for axonal and grey matter injury. *Journal of Molecular Medicine*, *88*(8), 753–761. https://doi.org/10.1007/s00109-010-0632-3

Deshmukh, V. A., Tardif, V., Lyssiotis, C. A., Green, C. C., Kerman, B., Kim, H. J., Padmanabhan, K., Swoboda, J. G., Ahmad, I., Kondo, T., Gage, F. H., Theofilopoulos, A. N., Lawson, B. R., Schultz, P. G., & Lairson, L. L. (2013). A regenerative approach to the treatment of multiple sclerosis. *Nature*, *502*(7471), 327–332. https://doi.org/10.1038/nature12647

Dimou, L., Simon, C., Kirchhoff, F., Takebayashi, H., & Götz, M. (2008). Progeny of Olig2-expressing progenitors in the gray and white matter of the adult mouse cerebral cortex. *Journal of Neuroscience*, *28*(41), 10434–10442. https://doi.org/10.1523/JNEUROSCI.2831-08.2008

Domercq, M., Perez-Samartin, A., Aparicio, D., Alberdi, E., Pampliega, O., & Matute, C. (2010). P2X7 receptors mediate ischemic damage to oligodendrocytes. *Glia*, *58*(6), 730–740. https://doi.org/10.1002/glia.20958

Domercq, M., Sánchez-Gómez, M. V., Sherwin, C., Etxebarria, E., Fern, R., & Matute, C. (2007). System x c − and Glutamate Transporter Inhibition Mediates Microglial Toxicity to Oligodendrocytes . *The Journal of Immunology*, *178*(10), 6549–6556. https://doi.org/10.4049/jimmunol.178.10.6549

Dugas, J. C., Cuellar, T. L., Scholze, A., Ason, B., Ibrahim, A., Emery, B., Zamanian, J. L., Foo, L. C., McManus, M. T., & Barres, B. A. (2010). Dicer1 and miR-219 Are Required for Normal Oligodendrocyte Differentiation and Myelination. *Neuron*, *65*(5), 597–611. https://doi.org/10.1016/j.neuron.2010.01.027

Duncan, I. D., & Radcliff, A. B. (2020). *Myelin plasticity: sculpting circuits in learning and memory*. *January*.

Dziedzic, A., Miller, E., Saluk-Bijak, J., & Bijak, M. (2020). The gpr17 receptor—a promising goal for therapy and a potential marker of the neurodegenerative process in multiple sclerosis. *International Journal of Molecular Sciences*, *21*(5). https://doi.org/10.3390/ijms21051852

Eglen, R. M., Choppin, A., & Watson, N. (2001). Therapeutic opportunities from muscarinic receptor research. *Trends in Pharmacological Sciences*, *22*(8), 409–414. https://doi.org/10.1016/S0165-6147(00)01737-5

Eleuteri, C., Olla, S., Veroni, C., Umeton, R., Mechelli, R., Romano, S., Buscarinu, M. C., Ferrari, F., Calò, G., Ristori, G., Salvetti, M., & Agresti, C. (2017). A staged screening of registered drugs highlights remyelinating drug candidates for clinical trials. *Scientific Reports*, *7*(April), 1–15. https://doi.org/10.1038/srep45780

Emery, B. (2010). Regulation of oligodendrocyte differentiation and myelination. *Science*, *330*(6005), 779–782. https://doi.org/10.1126/science.1190927

Falcão, A. M., van Bruggen, D., Marques, S., Meijer, M., Jäkel, S., Agirre, E., Samudyata, Floriddia, E. M., Vanichkina, D. P., ffrench-Constant, C., Williams, A., Guerreiro-Cacais, A. O., & Castelo-Branco, G. (2018). Disease-specific oligodendrocyte lineage cells arise in multiple sclerosis. *Nature Medicine*, *24*(12), 1837–1844. https://doi.org/10.1038/s41591-018-0236-y

Fedder-Semmes, K. N., & Appel, B. (2021). The akt-mtor pathway drives myelin sheath growth by regulating cap-dependent translation. *Journal of Neuroscience*, *41*(41), 8532–8544. https://doi.org/10.1523/JNEUROSCI.0783-21.2021

Fields, R. D., Dutta, D. J., Belgrad, J., & Robnett, M. (2017). Cholinergic signaling in myelination. *Glia*, *65*(5), 687–698. https://doi.org/10.1002/glia.23101

Fields, R. D., & Stevens-graham, B. (2002). *New Insights into Neuron-Glia Communication*. *298*(October), 556–563.

Finke, C., Kopp, U. A., Scheel, M., Pech, L. M., Soemmer, C., Schlichting, J., Leypoldt, F., Brandt, A. U., Wuerfel, J., Probst, C., Ploner, C. J., Prüss, H., & Paul, F. (2013). Functional and structural brain changes in anti-N-methyl-D-aspartate receptor encephalitis. *Annals of Neurology*, *74*(2), 284–296. https://doi.org/10.1002/ana.23932

Fletcher, J. L., Makowiecki, K., Cullen, C. L., & Young, K. M. (2021). Oligodendrogenesis and myelination regulate cortical development, plasticity and circuit function. *Seminars in Cell and Developmental Biology*, *118*, 14–23. https://doi.org/10.1016/j.semcdb.2021.03.017

Flores, A. I., Narayanan, S. P., Morse, E. N., Shick, H. E., Yin, X., Kidd, G., Avila, R. L., Kirschner, D. A., & Macklin, W. B. (2008). Constitutively active Akt induces enhanced myelination in the CNS. *Journal of Neuroscience*, *28*(28), 7174–7183. https://doi.org/10.1523/JNEUROSCI.0150-08.2008

Ford, M. C., Alexandrova, O., Cossell, L., Stange-Marten, A., Sinclair, J., Kopp-Scheinpflug, C., Pecka, M., Attwell, D., & Grothe, B. (2015). Tuning of Ranvier node and internode properties in myelinated axons to adjust action potential timing. *Nature Communications*, *6*. https://doi.org/10.1038/ncomms9073

Franklin, R. J. M., & Ffrench-Constant, C. (2017). Regenerating CNS myelin - From mechanisms to experimental medicines. *Nature Reviews Neuroscience*, *18*(12), 753–769. https://doi.org/10.1038/nrn.2017.136

Freeman, S. A., Desmazières, A., Simonnet, J., Gatta, M., Pfeiffer, F., Aigrot, M. S., Rappeneau, Q., Guerreiro, S., Michel, P. P., Yanagawa, Y., Barbin, G., Brophy, P. J., Fricker, D., Lubetzki, C., & Sol-Foulon, N. (2015). Acceleration of conduction velocity linked to clustering of nodal components precedes myelination. *Proceedings of the National Academy of Sciences of the United States of America*, *112*(3), E321–E328. https://doi.org/10.1073/pnas.1419099112

Fünfschilling, U., Supplie, L. M., Mahad, D., Boretius, S., Saab, A. S., Edgar, J., Brinkmann, B. G., Kassmann, C. M., Tzvetanova, I. D., Möbius, W., Diaz, F., Meijer, D., Suter, U., Hamprecht, B., Sereda, M. W., Moraes, C. T., Frahm, J., Goebbels, S., & Nave, K. A. (2012). Glycolytic oligodendrocytes maintain myelin and long-term axonal integrity. *Nature*, *485*(7399), 517–521. https://doi.org/10.1038/nature11007

Furusho, M., Ishii, A., & Bansal, R. (2017). Signaling by FGF receptor 2, not FGF receptor 1, regulates myelin thickness through activation of ERK1/2–MAPK, which promotes mTORC1 activity in an Akt-independent manner. *Journal of Neuroscience*, *37*(11), 2931–2946. https://doi.org/10.1523/JNEUROSCI.3316-16.2017

Fu, X., Chin, R. M., Vergnes, L., Hwang, H., Deng, G., Xing, Y., Pai, M. Y., Li, S., Ta, L., Fazlollahi, F., Chen, C., Prins, R. M., Teitell, M. A., Nathanson, D. A., Lai, A., Faull, K. F., Jiang, M., Clarke, S. G., Cloughesy, T. F., … Huang, J. (2015). 2-hydroxyglutarate inhibits ATP synthase and mTOR Signaling. *Cell Metabolism*, *22*(3), 508–515. https://doi.org/10.1016/j.cmet.2015.06.009

Galvez-Contreras, A. Y., Zarate-Lopez, D., Torres-Chavez, A. L., & Gonzalez-Perez, O. (2020). Role of oligodendrocytes and myelin in the pathophysiology of autism spectrum disorder. *Brain Sciences*, *10*(12), 1–17. https://doi.org/10.3390/brainsci10120951

Gdalyahu, A., Lazaro, M., Penagarikano, O., Golshani, P., Trachtenberg, J. T., & Gescwind, D. H. (2015). The autism related protein contactin-associated protein-like 2 (CNTNAP2) stabilizes new spines: An in vivo mouse study. *PLoS ONE*, *10*(5), 1–7. https://doi.org/10.1371/journal.pone.0125633

Geraghty, A. C., Gibson, E. M., Ghanem, R. A., Greene, J. J., Ocampo, A., Goldstein, A. K., Ni, L., Yang, T., Marton, R. M., Paşca, S. P., Greenberg, M. E., Longo, F. M., & Monje, M. (2019). Loss of Adaptive Myelination Contributes to Methotrexate Chemotherapy-Related Cognitive Impairment. *Neuron*, *103*(2), 250-265.e8. https://doi.org/10.1016/j.neuron.2019.04.032

Gibson, E. M., Purger, D., Mount, C. W., Goldstein, A. K., Lin, G. L., Wood, L. S., Inema, I., Miller, S. E., Bieri, G., Zuchero, J. B., Barres, B. A., Woo, P. J., Vogel, H., & Monje, M. (2014). Neuronal activity promotes oligodendrogenesis and adaptive myelination in

the mammalian brain. *Science*, *344*(6183), 1–27. https://doi.org/10.1126/science.1252304

Giovannoni, G., Butzkueven, H., Dhib-Jalbut, S., Hobart, J., Kobelt, G., Pepper, G., Sormani, M. P., Thalheim, C., Traboulsee, A., & Vollmer, T. (2016). Brain health: time matters in multiple sclerosis. *Multiple Sclerosis and Related Disorders*, *9*, S5–S48. https://doi.org/10.1016/j.msard.2016.07.003

Givre, S. (2003). Rakic p. adult neurogenesis in mammals: an identity crisis. *Journal of Neuro-Ophthalmology*, *23*(2), 164. https://doi.org/10.1097/00041327-200306000-00014

Goebbels, S., Oltrogge, J. H., Kemper, R., Heilmann, I., Bormuth, I., Wolfer, S., Wichert, S. P., Möbius, W., Liu, X., Lappe-Siefke, C., Rossner, M. J., Groszer, M., Suter, U., Frahm, J., Boretius, S., & Nave, K. A. (2010). Elevated phosphatidylinositol 3,4,5-trisphosphate in glia triggers cell-autonomous membrane wrapping and myelination. *Journal of Neuroscience*, *30*(26), 8953–8964. https://doi.org/10.1523/JNEUROSCI.0219-10.2010

Goodfellow, J. A., & Mackay, G. A. (2019). Autoimmune encephalitis. *Journal of the Royal College of Physicians of Edinburgh*, *49*(4), 287–294. https://doi.org/10.4997/JRCPE.2019.407

Gould, R. M., Oakley, T., Goldstone, J. v., Dugas, J. C., Brady, S. T., & Gow, A. (2008). Myelin sheaths are formed with proteins that originated in vertebrate lineages. *Neuron Glia Biology*, *4*(2), 137–152. https://doi.org/10.1017/S1740925X09990238

Graciarena, M., Seiffe, A., Nait-Oumesmar, B., & Depino, A. M. (2019). Hypomyelination and oligodendroglial alterations in a mouse model of autism spectrum disorder. *Frontiers in Cellular Neuroscience*, *12*(January), 1–11. https://doi.org/10.3389/fncel.2018.00517

Graus, F., Saiz, A., & Dalmau, J. (2010). Antibodies and neuronal autoimmune disorders of the CNS. *Journal of Neurology*, *257*(4), 509–517. https://doi.org/10.1007/s00415-009-5431-9

Green, A. J., Gelfand, J. M., Cree, B. A., Bevan, C., Boscardin, W. J., Mei, F., Inman, J., Arnow, S., Devereux, M., Abounasr, A., Nobuta, H., Zhu, A., Friessen, M., Gerona, R., von Büdingen, H. C., Henry, R. G., Hauser, S. L., & Chan, J. R. (2017). Clemastine fumarate as a remyelinating therapy for multiple sclerosis (ReBUILD): a randomised, controlled, double-blind, crossover trial. *The Lancet*, *390*(10111), 2481–2489. https://doi.org/10.1016/S0140-6736(17)32346-2

Griffiths, I., Klugmann, M., Anderson, T., Yool, D., Schwab, M. H., Schneider, A., Zimmermann, F., Mcculloch, M., Griffiths, I., Klugmann, M., Anderson, T., Yool, D., Thomson, C., Schwab, M. H., Schneider, A., Zimmermann, F., Mcculloch, M., Nadon, N., & Nave, K. (2016). *Axonal Swellings and Degeneration in Mice Lacking the Major Proteolipid of Myelin Nancy Nadon and Klaus-Armin Nave Published by : American*

Association for the Advancement of Science Stable URL : http://www.jstor.org/stable/2895967 JSTOR is a not-for-profi. *280*(5369), 1610–1613.

Grigoriadis, N., & van Pesch, V. (2015). A basic overview of multiple sclerosis immunopathology. *European Journal of Neurology*, *22*, 3–13. https://doi.org/10.1111/ene.12798

Hackett, A. R., Strickland, A., & Milbrandt, J. (2020). Disrupting insulin signaling in Schwann cells impairs myelination and induces a sensory neuropathy. *Glia*, *68*(5), 963–978. https://doi.org/10.1002/glia.23755.Disrupting

Hagemeyer, N., Hanft, K. M., Akriditou, M. A., Unger, N., Park, E. S., Stanley, E. R., Staszewski, O., Dimou, L., & Prinz, M. (2017). Microglia contribute to normal myelinogenesis and to oligodendrocyte progenitor maintenance during adulthood. *Acta Neuropathologica*, *134*(3), 441–458. https://doi.org/10.1007/s00401-017-1747-1

Harrington, E. P., Zhao, C., Fancy, S. P. J., Kaing, S., Franklin, R. J. M., & Rowitch, D. H. (2010). Oligodendrocyte PTEN is required for myelin and axonal integrity, not remyelination. *Annals of Neurology*, *68*(5), 703–716. https://doi.org/10.1002/ana.22090

Harris, J. J., & Attwell, D. (2012). The energetics of CNS white matter. *Journal of Neuroscience*, *32*(1), 356–371. https://doi.org/10.1523/JNEUROSCI.3430-11.2012

Hartline, D. K. (2008). What is myelin? *Neuron Glia Biology*, *4*(2), 153–163. https://doi.org/10.1017/S1740925X09990263

Hartline, D. K., & Colman, D. R. (2007). Rapid Conduction and the Evolution of Giant Axons and Myelinated Fibers. *Current Biology*, *17*(1), 29–35. https://doi.org/10.1016/j.cub.2006.11.042

Hasan, M., Kanna, M. S., Jun, W., Ramkrishnan, A. S., Iqbal, Z., Lee, Y., & Li, Y. (2019). Schema-like learning and memory consolidation acting through myelination. *FASEB Journal*, *33*(11), 11758–11775. https://doi.org/10.1096/fj.201900910R

Hill, R. A., Li, A. M., & Grutzendler, J. (2018). Lifelong cortical myelin plasticity and age-related degeneration in the live mammalian brain. *Nature Neuroscience*, *21*(5), 683–695. https://doi.org/10.1038/s41593-018-0120-6

Hines, J. H., Ravanelli, A. M., Schwindt, R., Scott, E. K., & Appel, B. (2015). Neuronal activity biases axon selection for myelination in vivo. *Nature Neuroscience*, *18*(5), 683–689. https://doi.org/10.1038/nn.3992

Höftberger, R., Sepulveda, M., Armangue, T., Blanco, Y., Rostásy, K., Cobo Calvo, A., Olascoaga, J., Ramió-Torrentà, L., Reindl, M., Benito-León, J., Casanova, B., Arrambide, G., Sabater, L., Graus, F., Dalmau, J., & Saiz, A. (2015). Antibodies to MOG and AQP4 in adults with neuromyelitis optica and suspected limited forms of the disease. *Multiple Sclerosis*, *21*(7), 866–874. https://doi.org/10.1177/1352458514555785

Hornig, J., Fröb, F., Vogl, M. R., Hermans-Borgmeyer, I., Tamm, E. R., & Wegner, M. (2013). The Transcription Factors Sox10 and Myrf Define an Essential Regulatory Network Module in Differentiating Oligodendrocytes. *PLoS Genetics*, *9*(10). https://doi.org/10.1371/journal.pgen.1003907

Hughes, A. N., & Appel, B. (2019). Oligodendrocytes express synaptic proteins that modulate myelin sheath formation. *Nature Communications*, *10*(1), 1–15. https://doi.org/10.1038/s41467-019-12059-y

Hughes, E. G., Kang, S. H., Fukaya, M., & Bergles, D. E. (2013). Oligodendrocyte progenitors balance growth with self-repulsion to achieve homeostasis in the adult brain. *Nature Neuroscience*, *16*(6), 668–676. https://doi.org/10.1038/nn.3390

Hughes, E. G., Orthmann-Murphy, J. L., Langseth, A. J., & Bergles, D. E. (2018). Myelin remodeling through experience-dependent oligodendrogenesis in the adult somatosensory cortex. *Nature Neuroscience*, *21*(5), 696–706. https://doi.org/10.1038/s41593-018-0121-5

Hunt, R. J., Granat, L., McElroy, G. S., Ranganathan, R., Chandel, N. S., & Bateman, J. M. (2019). Mitochondrial stress causes neuronal dysfunction via an ATF4-dependent increase in L-2-hydroxyglutarate. *Journal of Cell Biology*, *218*(12), 4007–4016. https://doi.org/10.1083/jcb.201904148

Huynh, J. L., & Casaccia, P. (2013). Epigenetic mechanisms in multiple sclerosis: Implications for pathogenesis and treatment. *The Lancet Neurology*, *12*(2), 195–206. https://doi.org/10.1016/S1474-4422(12)70309-5

Ichihara, Y., Doi, T., Ryu, Y., Nagao, M., Sawada, Y., & Ogata, T. (2017). Oligodendrocyte Progenitor Cells Directly Utilize Lactate for Promoting Cell Cycling and Differentiation. *Journal of Cellular Physiology*, *232*(5), 986–995. https://doi.org/10.1002/jcp.25690

Ishii, A., Furusho, M., Dupree, J. L., & Bansal, R. (2014). Role of ERK1/2 MAPK signaling in the maintenance of myelin and axonal integrity in the adult CNS. *Journal of Neuroscience*, *34*(48), 16031–16045. https://doi.org/10.1523/JNEUROSCI.3360-14.2014

Ishii, A., Furusho, M., Dupree, J. L., & Bansal, R. (2016). Strength of ERK1/2 MAPK activation determines its effect on myelin and axonal integrity in the adult CNS. *Journal of Neuroscience*, *36*(24), 6471–6487. https://doi.org/10.1523/JNEUROSCI.0299-16.2016

Jahn, O., Siems, S. B., Kusch, K., Hesse, D., Jung, R. B., Liepold, T., Uecker, M., Sun, T., & Werner, H. B. (2020). The CNS Myelin Proteome: Deep Profile and Persistence After Post-mortem Delay. *Frontiers in Cellular Neuroscience*, *14*(August), 1–15. https://doi.org/10.3389/fncel.2020.00239

Jahn, O., Tenzer, S., & Werner, H. B. (2009). Myelin proteomics: Molecular anatomy of an insulating sheath. *Molecular Neurobiology*, *40*(1), 55–72. https://doi.org/10.1007/s12035-009-8071-2

Jakovcevski, I., Filipovic, R., Mo, Z., Rakic, S., & Zecevic, N. (2009). Oligodendrocyte development and the onset of myelination in the human fetal brain. *Frontiers in Neuroanatomy*, *3*(JUN), 1–15. https://doi.org/10.3389/neuro.05.005.2009

Jeffries, M. A., Urbanek, K., Torres, L., Wendell, S. G., Rubio, M. E., & Fyffe-Maricich, S. L. (2016). ERK1/2 activation in preexisting oligodendrocytes of adult mice drives new myelin synthesis and enhanced CNS function. *Journal of Neuroscience*, *36*(35), 9186–9200. https://doi.org/10.1523/JNEUROSCI.1444-16.2016

Jolles, D., Wassermann, D., Chokhani, R., Richardson, J., Tenison, C., Bammer, R., Fuchs, L., Supekar, K., & Menon, V. (2016). Plasticity of left perisylvian white-matter tracts is associated with individual differences in math learning. *Brain Structure and Function*, *221*(3), 1337–1351. https://doi.org/10.1007/s00429-014-0975-6

Káradóttir, R., Cavelier, P., Bergersen, L. H., & Attwell, D. (2005). NMDA receptors are expressed in oligodendrocytes and activated in ischaemia. *Nature*, *438*(7071), 1162–1166. https://doi.org/10.1038/nature04302

Kasischke, K. A., Vishwasrao, H. D., Fisher, P. J., Zipfel, W. R., & Webb, W. W. (2004). Neural activity triggers neuronal oxidative metabolism followed by astrocytic glycolysis. *Science*, *305*(5680), 99–103. https://doi.org/10.1126/science.1096485

Koch, M., Kingwell, E., Rieckmann, P., & Tremlett, H. (2009). The natural history of primary progressive multiple sclerosis. *Neurology*, *73*(23), 1996–2002. https://doi.org/10.1212/WNL.0b013e3181c5b47f

Kotter, M. R., Li, W. W., Zhao, C., & Franklin, R. J. M. (2006). Myelin impairs CNS remyelination by inhibiting oligodendrocyte precursor cell differentiation. *Journal of Neuroscience*, *26*(1), 328–332. https://doi.org/10.1523/JNEUROSCI.2615-05.2006

Koyama, R., & Ikegaya, Y. (2015). Microglia in the pathogenesis of autism spectrum disorders. *Neuroscience Research*, *100*, 1–5. https://doi.org/10.1016/j.neures.2015.06.005

Krasnow, A. M., & Attwell, D. (2016). NMDA Receptors: Power Switches for Oligodendrocytes. *Neuron*, *91*(1), 3–5. https://doi.org/10.1016/j.neuron.2016.06.023

Lampron, A., Larochelle, A., Laflamme, N., Préfontaine, P., Plante, M. M., Sánchez, M. G., Wee Yong, V., Stys, P. K., Tremblay, M. È., & Rivest, S. (2015). Inefficient clearance of myelin debris by microglia impairs remyelinating processes. *Journal of Experimental Medicine*, *212*(4), 481–495. https://doi.org/10.1084/jem.20141656

Lao, Y., Kang, Y., Collignon, O., Brun, C., Kheibai, S. B., Alary, F., Gee, J., Nelson, M. D., Lepore, F., & Lepore, N. (2015). A study of brain white matter plasticity in early blinds using tract-based spatial statistics and tract statistical analysis. *NeuroReport*, *26*(18), 1151–1154. https://doi.org/10.1097/WNR.0000000000000488

Lappe-Siefke, C., Goebbels, S., Gravel, M., Nicksch, E., Lee, J., Braun, P. E., Griffiths, I. R., & Navel, K. A. (2003). Disruption of Cnp1 uncouples oligodendroglial functions in axonal support and myelination. *Nature Genetics*, *33*(3), 366–374. https://doi.org/10.1038/ng1095

Lau, L. W., Cua, R., Keough, M. B., Haylock-Jacobs, S., & Yong, V. W. (2013). Pathophysiology of the brain extracellular matrix: A new target for remyelination. *Nature Reviews Neuroscience*, *14*(10), 722–729. https://doi.org/10.1038/nrn3550

Lee, S., Leach, M. K., Redmond, S. A., Chong, S. Y. C., Mellon, S. H., Tuck, S. J., Feng, Z. Q., Corey, J. M., & Chan, J. R. (2012). A culture system to study oligodendrocyte myelination processes using engineered nanofibers. *Nature Methods*, *9*(9), 917–922. https://doi.org/10.1038/nmeth.2105

Lee, X., Yang, Z., Shao, Z., Rosenberg, S. S., Levesque, M., Pepinsky, R. B., Qiu, M., Miller, R. H., Chan, J. R., & Mi, S. (2007). NGF regulates the expression of axonal LINGO-1 to inhibit oligodendrocyte differentiation and myelination. *Journal of Neuroscience*, *27*(1), 220–225. https://doi.org/10.1523/JNEUROSCI.4175-06.2007

Lee, Y., Morrison, B. M., Li, Y., Lengacher, S., Farah, M. H., Hoffman, P. N., Liu, Y., Tsingalia, A., Jin, L., Zhang, P., Pellerin, L., Magistretti, P. J., & Rothstein, J. D. (2012a). Oligodendroglia metabolically support axons and contribute to neurodegeneration. *Nature*, *487*(7408), 443–448. https://doi.org/10.1038/nature11314.Oligodendroglia

Lee, Y., Morrison, B. M., Li, Y., Lengacher, S., Farah, M. H., Hoffman, P. N., Liu, Y., Tsingalia, A., Jin, L., Zhang, P. W., Pellerin, L., Magistretti, P. J., & Rothstein, J. D. (2012b). Oligodendroglia metabolically support axons and contribute to neurodegeneration. *Nature*, *487*(7408), 443–448. https://doi.org/10.1038/nature11314

Lezmy, J., Arancibia-Cárcamo, I. L., Quintela-López, T., Sherman, D. L., Brophy, P. J., & Attwell, D. (2021). Astrocyte Ca2+-evoked ATP release regulates myelinated axon excitability and conduction speed. *Science*, *374*(6565), 1–31. https://doi.org/10.1126/science.abh2858

Li, F., Sami, A., Noristani, H. N., Slattery, K., Qiu, J., Groves, T., Wang, S., Veerasammy, K., Chen, Y. X., Morales, J., Haynes, P., Sehgal, A., He, Y., Li, S., & Song, Y. (2020). Glial Metabolic Rewiring Promotes Axon Regeneration and Functional Recovery in the Central Nervous System. *Cell Metabolism*, *32*(5), 767-785.e7. https://doi.org/10.1016/j.cmet.2020.08.015

Lin, W., Lin, Y., Li, J., Fenstermaker, A. G., Way, S. W., Clayton, B., Jamison, S., Harding, H. P., Ron, D., & Popko, B. (2013). Oligodendrocyte-specific activation of PERK signaling protects mice against experimental autoimmune encephalomyelitis. *Journal of Neuroscience*, *33*(14), 5980–5991. https://doi.org/10.1523/JNEUROSCI.1636-12.2013

Liu, J., Dupree, J. L., Gacias, M., Frawley, R., Sikder, T., Naik, P., & Casaccia, P. (2016). Clemastine enhances myelination in the prefrontal cortex and rescues behavioral changes in socially isolated mice. *Journal of Neuroscience*, *36*(3), 957–962. https://doi.org/10.1523/JNEUROSCI.3608-15.2016

Li, Z., He, Y., Fan, S., & Sun, B. (2015). Clemastine rescues behavioral changes and enhances remyelination in the cuprizone mouse model of demyelination. *Neuroscience Bulletin*, *31*(5), 617–625. https://doi.org/10.1007/s12264-015-1555-3

Lourenço, T., Paes De Faria, J., Bippes, C. A., Maia, J., Lopes-Da-Silva, J. A., Relvas, J. B., & Graõs, M. (2016). Modulation of oligodendrocyte differentiation and maturation by combined biochemical and mechanical cues. *Scientific Reports*, *6*(February), 1–17. https://doi.org/10.1038/srep21563

Lublin, F. D., & Reingold, S. C. (1996). Defining the clinical course of multiple sclerosis: Results of an international survey. *Neurology*, *46*(4), 907–911. https://doi.org/10.1212/WNL.46.4.907

Lublin, F. D., Reingold, S. C., Cohen, J. A., Cutter, G. R., Thompson, A. J., Wolinsky, J. S., Banwell, B., Barkhof, F., Bebo, B., Calabresi, P. A., Clanet, M., Fox, R. J., Freedman, M. S., Goodman, A. D., Lincoln, J. A., Lubetzki, C., Miller, A. E., Montalban, X., Connor, P. W. O., & Sormani, M. P. (2014). Defining the clinical course of multiple sclerosis. *Neurology*. https://www.ncbi.nlm.nih.gov/pmc/articles/PMC4117366/pdf/NEUROLOGY2013555623.pdf

Lundgaard, I., Luzhynskaya, A., Stockley, J. H., Wang, Z., Evans, K. A., Swire, M., Volbracht, K., Gautier, H. O. B., Franklin, R. J. M., ffrench-Constant, C., Attwell, D., & Káradóttir, R. T. (2013). Neuregulin and BDNF Induce a Switch to NMDA Receptor-Dependent Myelination by Oligodendrocytes. *PLoS Biology*, *11*(12). https://doi.org/10.1371/journal.pbio.1001743

Macchi, M., Magalon, K., Zimmer, C., Peeva, E., Waly, B. el, Brousse, B., Jaekel, S., Grobe, K., Kiefer, F., Williams, A., Cayre, M., & Durbec, P. (2020). Mature oligodendrocytes bordering lesions limit demyelination and favor myelin repair via heparan sulfate production. *ELife*, *9*, 1–26. https://doi.org/10.7554/eLife.51735

Mächler, P., Wyss, M. T., Elsayed, M., Stobart, J., Gutierrez, R., von Faber-Castell, A., Kaelin, V., Zuend, M., San Martín, A., Romero-Gómez, I., Baeza-Lehnert, F., Lengacher, S., Schneider, B. L., Aebischer, P., Magistretti, P. J., Barros, L. F., & Weber, B. (2016). In

Vivo Evidence for a Lactate Gradient from Astrocytes to Neurons. *Cell Metabolism*, *23*(1), 94–102. https://doi.org/10.1016/j.cmet.2015.10.010

Magistretti, P. J., & Allaman, I. (2018). Lactate in the brain: From metabolic end-product to signalling molecule. *Nature Reviews Neuroscience*, *19*(4), 235–249. https://doi.org/10.1038/nrn.2018.19

Mahad, D. H., Trapp, B. D., & Lassmann, H. (2015). Pathological mechanisms in progressive multiple sclerosis. *The Lancet Neurology*, *14*(2), 183–193. https://doi.org/10.1016/S1474-4422(14)70256-X

Makinodan, M., Rosen, K. M., Ito, S., & Corfas, G. (2012). A critical period for social experience-dependent oligodendrocyte maturation and myelination. *Science*, *337*(6100), 1357–1360. https://doi.org/10.1126/science.1220845

Mangin, J. M., Li, P., Scafidi, J., & Gallo, V. (2012). Experience-dependent regulation of NG2 progenitors in the developing barrel cortex. *Nature Neuroscience*, *15*(9), 1192–1194. https://doi.org/10.1038/nn.3190

Marinelli, C., Bertalot, T., Zusso, M., Skaper, S. D., & Giusti, P. (2016). Systematic review of pharmacological properties of the oligodendrocyte lineage. *Frontiers in Cellular Neuroscience*, *10*(FEB), 1–19. https://doi.org/10.3389/fncel.2016.00027

Marques, S., Zeisel, A., Codeluppi, S., van Bruggen, D., Falcão, A. M., Xiao, L., Li, H., Häring, M., Hochgerner, H., Romanov, R. A., Gyllborg, D., Muñoz-Manchado, A. B., la Manno, G., Lönnerberg, P., Floriddia, E. M., Rezayee, F., Ernfors, P., Arenas, E., Hjerling-Leffler, J., … Castelo-Branco, G. (2016). Oligodendrocyte heterogeneity in the mouse juvenile and adult central nervous system. *Science*, *352*(6291), 1326–1329. https://doi.org/10.1126/science.aaf6463

Mathews, E. S., & Appel, B. (2016). Cholesterol biosynthesis supports myelin gene expression and axon ensheathment through modulation of P13K/Akt/mTor signaling. *Journal of Neuroscience*, *36*(29), 7628–7639. https://doi.org/10.1523/JNEUROSCI.0726-16.2016

Matute, C., Alberdi, E., Domercq, M., Pérez-Cerdá, F., Pérez-Samartín, A., & Sánchez-Gómez, M. V. (2001). The link between excitotoxic oligodendroglial death and demyelinating diseases. *Trends in Neurosciences*, *24*(4), 224–230. https://doi.org/10.1016/S0166-2236(00)01746-X

Matute, C., & Pérez-Cerdá, F. (2005). Multiple sclerosis: Novel perspectives on newly forming lesions. *Trends in Neurosciences*, *28*(4), 173–175. https://doi.org/10.1016/j.tins.2005.01.006

Matute, C., Sánchez-Gómez, M. V., Martínez-Millán, L., & Miledi, R. (1997). Glutamate receptor-mediated toxicity in optic nerve oligodendrocytes. *Proceedings of the*

National Academy of Sciences of the United States of America, *94*(16), 8830–8835. https://doi.org/10.1073/pnas.94.16.8830

Maxfield, F. R., & van Meer, G. (2010). Cholesterol, the central lipid of mammalian cells. *Current Opinion in Cell Biology*, *22*(4), 422–429. https://doi.org/10.1016/j.ceb.2010.05.004

McDougall, S., Riad, W. V., Silva-Gotay, A., Tavares, E. R., Harpalani, D., Li, G. L., & Richardson, H. N. (2018). Myelination of axons corresponds with faster transmission speed in the prefrontal cortex of developing male rats. *ENeuro*, *5*(4). https://doi.org/10.1523/ENEURO.0203-18.2018

McKenzie, I. A., Ohayon, D., Li, H., de Faria, J. P., Emery, B., Tohyama, K., & Richardson, W. D. (2014). Motor skill learning requires active central myelination. *Science*, *346*(6207), 318–322. https://doi.org/10.1126/science.1254960

Mei, F., Fancy, S. P. J., Shen, Y. A. A., Niu, J., Zhao, C., Presley, B., Miao, E., Lee, S., Mayoral, S. R., Redmond, S. A., Etxeberria, A., Xiao, L., Franklin, R. J. M., Green, A., Hauser, S. L., & Chan, J. R. (2014). Micropillar arrays as a high-throughput screening platform for therapeutics in multiple sclerosis. *Nature Medicine*, *20*(8), 954–960. https://doi.org/10.1038/nm.3618

Mei, F., Lehmann-Horn, K., Shen, Y. A. A., Rankin, K. A., Stebbins, K. J., Lorrain, D. S., Pekarek, K., Sagan, S. A., Xiao, L., Teuscher, C., von Büdingen, H. C., Wess, J., Josh Lawrence, J., Green, A. J., Fancy, S. P. J., Zamvil, S. S., & Chan, J. R. (2016). Accelerated remyelination during inflammatory demyelination prevents axonal loss and improves functional recovery. *ELife*, *5*(September), 1–21. https://doi.org/10.7554/eLife.18246

Mensch, S., Baraban, M., Almeida, R., Czopka, T., Ausborn, J., el Manira, A., & Lyons, D. A. (2015). Synaptic vesicle release regulates myelin sheath number of individual oligodendrocytes in vivo. *Nature Neuroscience*, *18*(5), 628–630. https://doi.org/10.1038/nn.3991

Meyer, N., Richter, N., Fan, Z., Siemonsmeier, G., Pivneva, T., Jordan, P., Steinhäuser, C., Semtner, M., Nolte, C., & Kettenmann, H. (2018). Oligodendrocytes in the Mouse Corpus Callosum Maintain Axonal Function by Delivery of Glucose. *Cell Reports*, *22*(9), 2383–2394. https://doi.org/10.1016/j.celrep.2018.02.022

Micu, I., Jiang, Q., Coderre, E., Ridsdale, A., Zhang, L., Woulfe, J., Yin, X., Trapp, B. D., McRory, J. E., Rehak, R., Zamponi, G. W., Wang, W., & Stys, P. K. (2006). NMDA receptors mediate calcium accumulation in myelin during chemical ischaemia. *Nature*, *439*(7079), 988–992. https://doi.org/10.1038/nature04474

Micu, I., Plemel, J. R., Caprariello, A. v., Nave, K. A., & Stys, P. K. (2018). Axo-myelinic neurotransmission: A novel mode of cell signalling in the central nervous system. *Nature Reviews Neuroscience*, *19*(1), 49–57. https://doi.org/10.1038/nrn.2017.128

Miller, D., Barkhof, F., Montalban, X., Thompson, A., & Filippi, M. (2005). Clinically isolated syndromes suggestive of multiple sclerosis, part I: Natural history, pathogenesis, diagnosis, and prognosis. *Lancet Neurology*, *4*(5), 281–288. https://doi.org/10.1016/S1474-4422(05)70071-5

Miller, R. H. (2002). Regulation of oligodendrocyte development in the vertebrate CNS. *Progress in Neurobiology*, *67*, 451–467.

Miron, V. E., Boyd, A., Zhao, J. W., Yuen, T. J., Ruckh, J. M., Shadrach, J. L., van Wijngaarden, P., Wagers, A. J., Williams, A., Franklin, R. J. M., & Ffrench-Constant, C. (2013). M2 microglia and macrophages drive oligodendrocyte differentiation during CNS remyelination. *Nature Neuroscience*, *16*(9), 1211–1218. https://doi.org/10.1038/nn.3469

Miron, V. E., & Franklin, R. J. M. (2014). Macrophages and CNS remyelination. *Journal of Neurochemistry*, *130*(2), 165–171. https://doi.org/10.1111/jnc.12705

Möbius, W., Cooper, B., Kaufmann, W. A., Imig, C., Ruhwedel, T., Snaidero, N., Saab, A. S., & Varoqueaux, F. (2010). Electron microscopy of the mouse central nervous system. In *Methods in Cell Biology* (Vol. 96, Issue C). https://doi.org/10.1016/S0091-679X(10)96020-2

Moore, S., Meschkat, M., Ruhwedel, T., Trevisiol, A., Tzvetanova, I. D., Battefeld, A., Kusch, K., Kole, M. H. P., Strenzke, N., Möbius, W., de Hoz, L., & Nave, K. A. (2020). A role of oligodendrocytes in information processing. *Nature Communications*, *11*(1), 1–15. https://doi.org/10.1038/s41467-020-19152-7

Morris-Rosendahl, D. J., & Crocq, M. A. (2020). Neurodevelopmental disorders-the history and future of a diagnostic concept. *Dialogues in Clinical Neuroscience*, *22*(1), 65–72. https://doi.org/10.31887/DCNS.2020.22.1/macrocq

Moscato, E. H., Peng, X., Jain, A., Parsons, T. D., Dalmau, J., & Balice-Gordon, R. J. (2014). Acute mechanisms underlying antibody effects in anti-N-methyl-D-aspartate receptor encephalitis. *Annals of Neurology*, *76*(1), 108–119. https://doi.org/10.1002/ana.24195

Mosienko, V., Teschemacher, A. G., & Kasparov, S. (2015). Is L-lactate a novel signaling molecule in the brain? *Journal of Cerebral Blood Flow and Metabolism*, *35*(7), 1069–1075. https://doi.org/10.1038/jcbfm.2015.77

Müller, C., Bauer, N. M., Schäfer, I., & White, R. (2013). Making myelin basic protein - From mRNA transport to localized translation. *Frontiers in Cellular Neuroscience*, *7*(SEP), 1–7. https://doi.org/10.3389/fncel.2013.00169

Münzel, E. J., & Williams, A. (2013). Promoting remyelination in multiple sclerosis-recent advances. *Drugs*, *73*(18), 2017–2029. https://doi.org/10.1007/s40265-013-0146-8

Nave, K. A. (2010). Myelination and support of axonal integrity by glia. *Nature*, *468*(7321), 244–252. https://doi.org/10.1038/nature09614

Newman, M. P., Blum, S., Wong, R. C. W., Scott, J. G., Prain, K., Wilson, R. J., & Gillis, D. (2016). Autoimmune encephalitis. *Internal Medicine Journal*, *46*(2), 148–157. https://doi.org/10.1111/imj.12974

Noori, R., Park, D., Griffiths, J. D., Bells, S., Frankland, P. W., Mabbott, D., & Lefebvre, J. (2020). Activity-dependent myelination: A glial mechanism of oscillatory self-organization in large-scale brain networks. *Proceedings of the National Academy of Sciences of the United States of America*, *117*(24), 13227–13237. https://doi.org/10.1073/pnas.1916646117

Onnink, A. M. H., Zwiers, M. P., Hoogman, M., Mostert, J. C., Dammers, J., Kan, C. C., Vasquez, A. A., Schene, A. H., Buitelaar, J., & Franke, B. (2015). Deviant white matter structure in adults with attention-deficit/hyperactivity disorder points to aberrant myelination and affects neuropsychological performance. *Progress in Neuro-Psychopharmacology and Biological Psychiatry*, *63*, 14–22. https://doi.org/10.1016/j.pnpbp.2015.04.008

Orthmann-Murphy, J., Call, C. L., Molina-Castro, G. C., Hsieh, Y. C., Rasband, M. N., Calabresi, P. A., & Bergles, D. E. (2020). Remyelination alters the pattern of myelin in the cerebral cortex. *ELife*, *9*, 1–61. https://doi.org/10.7554/eLife.56621

Palumbo, S., & Pellegrini, S. (2017). Experimental In Vivo Models of Multiple Sclerosis: State of the Art. *Multiple Sclerosis: Perspectives in Treatment and Pathogenesis*, 173–183. https://doi.org/10.15586/codon.multiplesclerosis.2017.ch11

Pellerin, L., & Magistretti, P. J. (1994). Glutamate uptake into astrocytes stimulates aerobic glycolysis: A mechanism coupling neuronal activity to glucose utilization. *Proceedings of the National Academy of Sciences of the United States of America*, *91*(22), 10625–10629. https://doi.org/10.1073/pnas.91.22.10625

Peñagarikano, O., Abrahams, B. S., Herman, E. I., Winden, K. D., Gdalyahu, A., Dong, H., Sonnenblick, L. I., Gruver, R., Almajano, J., Bragin, A., Golshani, P., Trachtenberg, J. T., Peles, E., & Geschwind, D. H. (2011). Absence of CNTNAP2 leads to epilepsy, neuronal migration abnormalities, and core autism-related deficits. *Cell*, *147*(1), 235–246. https://doi.org/10.1016/j.cell.2011.08.040

Phillips, O. R., Joshi, S. H., Narr, K. L., Shattuck, D. W., Singh, M., di Paola, M., Ploner, C. J., Prüss, H., Paul, F., & Finke, C. (2018). Superficial white matter damage in anti-NMDA receptor encephalitis. *Journal of Neurology, Neurosurgery, and Psychiatry*, *89*(5), 518–525. https://doi.org/10.1136/jnnp-2017-316822

Piaton, G., Gould, R. M., & Lubetzki, C. (2010). Axon-oligodendrocyte interactions during developmental myelination, demyelination and repair. *Journal of Neurochemistry*, *114*(5), 1243–1260. https://doi.org/10.1111/j.1471-4159.2010.06831.x

Piña-Crespo, J. C., Talantova, M., Micu, I., States, B., Chen, H. S. V., Tu, S., Nakanishi, N., Tong, G., Zhang, D., Heinemann, S. F., Zamponi, G. W., Stys, P. K., & Lipton, S. A. (2010). Excitatory glycine responses of CNS myelin mediated by NR1/NR3 "NMDA" receptor subunits. *Journal of Neuroscience*, *30*(34), 11501–11505. https://doi.org/10.1523/JNEUROSCI.1593-10.2010

Planagumà, J., Haselmann, H., Mannara, F., Petit-Pedrol, M., Grünewald, B., Aguilar, E., Röpke, L., Martín-García, E., Titulaer, M. J., Jercog, P., Graus, F., Maldonado, R., Geis, C., & Dalmau, J. (2016). Ephrin-B2 prevents N-methyl-D-aspartate receptor antibody effects on memory and neuroplasticity. *Annals of Neurology*, *80*(3), 388–400. https://doi.org/10.1002/ana.24721

Planagumà, J., Leypoldt, F., Mannara, F., Gutiérrez-Cuesta, J., Martín-García, E., Aguilar, E., Titulaer, M. J., Petit-Pedrol, M., Jain, A., Balice-Gordon, R., Lakadamyali, M., Graus, F., Maldonado, R., & Dalmau, J. (2015). Human N-methyl D-aspartate receptor antibodies alter memory and behaviour in mice. *Brain*, *138*(1), 94–109. https://doi.org/10.1093/brain/awu310

Poitelon, Y., Kopec, A. M., & Belin, S. (2020). Myelin Fat Facts: An Overview of Lipids and Fatty Acid Metabolism. *Cells*, *9*(4). https://doi.org/10.3390/cells9040812

Polman, C. H., Reingold, S. C., Banwell, B., Clanet, M., Cohen, J. A., Filippi, M., Fujihara, K., Havrdova, E., Hutchinson, M., Kappos, L., Lublin, F. D., Montalban, X., O'Connor, P., Sandberg-Wollheim, M., Thompson, A. J., Waubant, E., Weinshenker, B., & Wolinsky, J. S. (2011). Diagnostic criteria for multiple sclerosis: 2010 Revisions to the McDonald criteria. *Annals of Neurology*, *69*(2), 292–302. https://doi.org/10.1002/ana.22366

Rasband, M. N., & Peles, E. (2021). Mechanisms of node of Ranvier assembly. *Nature Reviews Neuroscience*, *22*(1), 7–20. https://doi.org/10.1038/s41583-020-00406-8

Rash, J. E. (2010). Molecular disruptions of the panglial syncytium block potassium siphoning and axonal saltatory conduction: pertinence to neuromyelitis optica and other demyelinating diseases of the central nervous system. *Neuroscience*, *168*(4), 982–1008. https://doi.org/10.1016/j.neuroscience.2009.10.028

Rinholm, J. E., Hamilton, N. B., Kessaris, N., Richardson, W. D., Bergersen, L. H., & Attwell, D. (2011). Regulation of oligodendrocyte development and myelination by glucose and lactate. *Journal of Neuroscience*, *31*(2), 538–548. https://doi.org/10.1523/JNEUROSCI.3516-10.2011

Rodenas-Cuadrado, P., Ho, J., & Vernes, S. C. (2014). Shining a light on CNTNAP2: Complex functions to complex disorders. *European Journal of Human Genetics*, *22*(2), 171–178. https://doi.org/10.1038/ejhg.2013.100

Rogan, S. C., & Roth, B. L. (2011). Remote control of neuronal signaling. *Pharmacological Reviews*, *63*(2), 291–315. https://doi.org/10.1124/pr.110.003020

Rone, M. B., Cui, Q. L., Fang, J., Wang, L. C., Zhang, J., Khan, D., Bedard, M., Almazan, G., Ludwin, S. K., Jones, R., Kennedy, T. E., & Antel, J. P. (2016). Oligodendrogliopathy in multiple sclerosis: Low glycolytic metabolic rate promotes oligodendrocyte survival. *Journal of Neuroscience*, *36*(17), 4698–4707. https://doi.org/10.1523/JNEUROSCI.4077-15.2016

Rosko, L., Smith, V. N., Yamazaki, R., & Huang, J. K. (2019). Oligodendrocyte Bioenergetics in Health and Disease. *Neuroscientist*, *25*(4), 334–343. https://doi.org/10.1177/1073858418793077

Ross Welliver, R., Polanco, J. J., Seidman, R. A., Sinha, A. K., O'bara, M. A., Khaku, Z. M., Santiago González, D. A., Nishiyama, A., Wess, J., Feltri, M. L., Paez, P. M., & Sim, F. J. (2018). Muscarinic receptor M 3 R signaling prevents efficient remyelination by human and mouse oligodendrocyte progenitor cells. *Journal of Neuroscience*, *38*(31), 6921–6932. https://doi.org/10.1523/JNEUROSCI.1862-17.2018

Ruiz, A., Alberdi, E., & Matute, C. (2014). CGP37157, an inhibitor of the mitochondrial Na+/Ca2+ exchanger, protects neurons from excitotoxicity by blocking voltage-gated Ca2+ channels. *Cell Death and Disease*, *5*(4), 1–10. https://doi.org/10.1038/cddis.2014.134

Saab, A. S., Tzvetanova, I. D., & Nave, K. A. (2013). The role of myelin and oligodendrocytes in axonal energy metabolism. *Current Opinion in Neurobiology*, *23*(6), 1065–1072. https://doi.org/10.1016/j.conb.2013.09.008

Saab, A. S., Tzvetavona, I. D., Trevisiol, A., Baltan, S., Dibaj, P., Kusch, K., Möbius, W., Goetze, B., Jahn, H. M., Huang, W., Steffens, H., Schomburg, E. D., Pérez-Samartín, A., Pérez-Cerdá, F., Bakhtiari, D., Matute, C., Löwel, S., Griesinger, C., Hirrlinger, J., … Nave, K. A. (2016). Oligodendroglial NMDA Receptors Regulate Glucose Import and Axonal Energy Metabolism. *Neuron*, *91*(1), 119–132. https://doi.org/10.1016/j.neuron.2016.05.016

Sabatini, B. L., & Regehr, W. G. (1997). Control of neurotransmitter release by presynaptic waveform at the granule cell to Purkinje cell synapse. *Journal of Neuroscience*, *17*(10), 3425–3435. https://doi.org/10.1523/jneurosci.17-10-03425.1997

Salter, M. G., & Fern, R. (2005). NMDA receptors are expressed in developing oligodendrocyte processes and mediate injury. *Nature*, *438*(7071), 1167–1171. https://doi.org/10.1038/nature04301

Salzer, J. L., Brophy, P. J., & Peles, E. (2008). Molecular domains of myelinated axons in the peripheral nervous system. *Glia*, *56*(14), 1532–1540. https://doi.org/10.1002/glia.20750

Sand, I. K. (2015). Classification, diagnosis, and differential diagnosis of multiple sclerosis. *Current Opinion in Neurology*, *28*(3), 193–205. https://doi.org/10.1097/WCO.0000000000000206

San Martín, A., Ceballo, S., Ruminot, I., Lerchundi, R., Frommer, W. B., & Barros, L. F. (2013). A Genetically Encoded FRET Lactate Sensor and Its Use To Detect the Warburg Effect in Single Cancer Cells. *PLoS ONE*, *8*(2). https://doi.org/10.1371/journal.pone.0057712

Scholz, J., Klein, M. C., Behrens, T. E. J., & Johansen-berg, H. (2010a). Europe PMC Funders Group Training induces changes in white matter architecture. *Nat Neurosci.*, *12*(11), 1370–1371. https://doi.org/10.1038/nn.2412.Training

Scholz, J., Klein, M. C., Behrens, T. E. J., & Johansen-berg, H. (2010b). Europe PMC Funders Group Training induces changes in white matter architecture. *Nat Neurosci.*, *12*(11), 1370–1371. https://doi.org/10.1038/nn.2412.Training

Sedel, F., Bernard, D., Mock, D. M., & Tourbah, A. (2016). Targeting demyelination and virtual hypoxia with high-dose biotin as a treatment for progressive multiple sclerosis. *Neuropharmacology*, *110*, 644–653. https://doi.org/10.1016/j.neuropharm.2015.08.028

Seehusen, F., & Baumgartner, W. (2010). Axonal pathology and loss precede demyelination and accompany chronic lesions in a spontaneously occurring animal model of multiple sclerosis. *Brain Pathology*, *20*(3), 551–559. https://doi.org/10.1111/j.1750-3639.2009.00332.x

Seidl, A. H., Rubel, E. W., & Harris, D. M. (2010). Mechanisms for adjusting interaural time differences to achieve binaural coincidence detection. *Journal of Neuroscience*, *30*(1), 70–80. https://doi.org/10.1523/JNEUROSCI.3464-09.2010

Sellgren, C. M., Gracias, J., Watmuff, B., Biag, J. D., Thanos, J. M., Whittredge, P. B., Fu, T., Worringer, K., Brown, H. E., Wang, J., Kaykas, A., Karmacharya, R., Goold, C. P., Sheridan, S. D., & Perlis, R. H. (2019). Increased synapse elimination by microglia in schizophrenia patient-derived models of synaptic pruning. *Nature Neuroscience*, *22*(3), 374–385. https://doi.org/10.1038/s41593-018-0334-7

Shu, Y., Hasenstaub, A., Duque, A., Yu, Y., & McCormick, D. A. (2006). Modulation of intracortical synaptic potentials by presynaptic somatic membrane potential. *Nature*, *441*(7094), 761–765. https://doi.org/10.1038/nature04720

Sim, F. J., Zhao, C., Penderis, J., & Franklin, R. J. M. (2002). The Age-Related Decrease in CNS Remyelination Efficiency Is Attributable to an Impairment of Both Oligodendrocyte Progenitor Recruitment and Differentiation. *Journal of Neuroscience*, *22*(7), 2451–2459. https://doi.org/10.1523/jneurosci.22-07-02451.2002

Simon, C., Götz, M., & Dimou, L. (2011). Progenitors in the adult cerebral cortex: Cell cycle properties and regulation by physiological stimuli and injury. *Glia*, *59*(6), 869–881. https://doi.org/10.1002/glia.21156

Slavin, A., Ewing, C., Liu, J., Ichikawa, M., Slavin, J., & Bernard, C. C. A. (1998). Induction of a multiple sclerosis-like disease in mice with an immunodominant epitope of myelin oligodendrocyte glycoprotein. *Autoimmunity*, *28*(2), 109–120. https://doi.org/10.3109/08916939809003872

Snaidero, N., Möbius, W., Czopka, T., Hekking, L. H. P., Mathisen, C., Verkleij, D., Goebbels, S., Edgar, J., Merkler, D., Lyons, D. A., Nave, K.-A., & Simons, M. (2014a). Europe PMC Funders Group Myelin membrane wrapping of CNS axons by PI (3 , 4 , 5) P3-dependent polarized growth at the inner tongue. *Cell*, *156*(1–2), 277–290. https://doi.org/10.1016/j.cell.2013.11.044.Myelin

Snaidero, N., Möbius, W., Czopka, T., Hekking, L. H. P., Mathisen, C., Verkleij, D., Goebbels, S., Edgar, J., Merkler, D., Lyons, D. A., Nave, K. A., & Simons, M. (2014b). Myelin membrane wrapping of CNS axons by PI(3,4,5)P3-dependent polarized growth at the inner tongue. *Cell*, *156*(1–2), 277–290. https://doi.org/10.1016/j.cell.2013.11.044

Snaidero, N., & Simons, M. (2014). Myelination at a glance. *Journal of Cell Science*, *127*(14), 2999–3004. https://doi.org/10.1242/jcs.151043

Sobottka, B., Ziegler, U., Kaech, A., Becher, B., & Goebels, N. (2011). CNS live imaging reveals a new mechanism of myelination: The liquid croissant model. *Glia*, *59*(12), 1841–1849. https://doi.org/10.1002/glia.21228

Stadelmann, C., Timmler, S., Barrantes-Freer, A., & Simons, M. (2019). Myelin in the central nervous system: Structure, function, and pathology. *Physiological Reviews*, *99*(3), 1381–1431. https://doi.org/10.1152/physrev.00031.2018

Steadman, P. E., Xia, F., Ahmed, M., Mocle, A. J., Penning, A. R. A., Geraghty, A. C., Steenland, H. W., Monje, M., Josselyn, S. A., & Frankland, P. W. (2020). Disruption of Oligodendrogenesis Impairs Memory Consolidation in Adult Mice. *Neuron*, *105*(1), 150-164.e6. https://doi.org/10.1016/j.neuron.2019.10.013

Stover, J. F., Pleinesf, U. E., Morganti-Kossmannf, M. C., Kossmannf, T., Lowitzschj, K., & Kempski, O. S. (1997). Neurotransmitters in cerebrospinal fluid reflect pathological activity. *European Journal of Clinical Investigation*, *27*(12), 1038–1043. https://doi.org/10.1046/j.1365-2362.1997.2250774.x

Strachan-Whaley, M., Rivest, S., & Yong, V. W. (2014). Interactions between microglia and T cells in multiple sclerosis pathobiology. *Journal of Interferon and Cytokine Research*, *34*(8), 615–622. https://doi.org/10.1089/jir.2014.0019

Szulzewsky, F., Pelz, A., Feng, X., Synowitz, M., Markovic, D., Langmann, T., Holtman, I. R., Wang, X., Eggen, B. J. L., Boddeke, H. W. G. M., Hambardzumyan, D., Wolf, S. A., & Kettenmann, H. (2015). Glioma-associated microglia/macrophages display an expression profile different from M1 and M2 polarization and highly express Gpnmb and Spp1. *PLoS ONE*, *10*(2), 1–27. https://doi.org/10.1371/journal.pone.0116644

Takahashi, N., Sakurai, T., Davis, K. L., & Buxbaum, J. D. (2011). Linking oligodendrocyte and myelin dysfunction to neurocircuitry abnormalities in schizophrenia. *Progress in Neurobiology*, *93*(1), 13–24. https://doi.org/10.1016/j.pneurobio.2010.09.004

Tawk, M., Makoukji, J., Belle, M., Fonte, C., Trousson, A., Hawkins, T., Li, H., Ghandour, S., Schumacher, M., & Massaad, C. (2011). Wnt/β-catenin signaling is an essential and direct driver of myelin gene expression and myelinogenesis. *Journal of Neuroscience*, *31*(10), 3729–3742. https://doi.org/10.1523/JNEUROSCI.4270-10.2011

Tekkök, S. B., Ye, Z. C., & Ransom, B. R. (2007). Excitotoxic mechanisms of ischemic injury in myelinated white matter. *Journal of Cerebral Blood Flow and Metabolism*, *27*(9), 1540–1552. https://doi.org/10.1038/sj.jcbfm.9600455

Tepavčević, V. (2021). Oligodendroglial energy metabolism and (Re)myelination. *Life*, *11*(3). https://doi.org/10.3390/life11030238

Thompson, A. J., Baranzini, S. E., Geurts, J., Hemmer, B., & Ciccarelli, O. (2018). Multiple sclerosis. *The Lancet*, *391*(10130), 1622–1636. https://doi.org/10.1016/S0140-6736(18)30481-1

Titulaer, M. J., Mccracken, L., Rosenfeld, M. R., & Graus, F. (2013). *Late-onset anti – NMDA receptor encephalitis*.

Tomassy, G. S., Berger, D. R., Chen, H. H., Kasthuri, N., Hayworth, K. J., Vercelli, A., Seung, H. S., Lichtman, J. W., & Arlotta, P. (2014). Distinct profiles of myelin distribution along single axons of pyramidal neurons in the neocortex. *Science*, *344*(6181), 319–324. https://doi.org/10.1126/science.1249766

Tompkins, S. M., Padilla, J., Dal Canto, M. C., Ting, J. P.-Y., van Kaer, L., & Miller, S. D. (2002). De Novo Central Nervous System Processing of Myelin Antigen Is Required for the Initiation of Experimental Autoimmune Encephalomyelitis. *The Journal of Immunology*, *168*(8), 4173–4183. https://doi.org/10.4049/jimmunol.168.8.4173

Torvund-Jensen, J., Steengaard, J., Askebjerg, L. B., Kjaer-Sorensen, K., & Laursen, L. S. (2018). The 3'UTRs of myelin basic protein mrnas regulate transport, local translation and sensitivity to neuronal activity in zebrafish. *Frontiers in Molecular Neuroscience*, *11*(June), 1–14. https://doi.org/10.3389/fnmol.2018.00185

Traiffort, E., Zakaria, M., Laouarem, Y., & Ferent, J. (2016). Hedgehog: A key signaling in the development of the oligodendrocyte lineage. *Journal of Developmental Biology*, *4*(3), 1–20. https://doi.org/10.3390/jdb4030028

Trevisiol, A., Saab, A. S., Winkler, U., Marx, G., Imamura, H., Möbius, W., Kusch, K., Nave, K. A., & Hirrlinger, J. (2017). Monitoring ATP dynamics in electrically active white matter tracts. *ELife*, *6*, 1–17. https://doi.org/10.7554/eLife.24241

Tsunoda, I., & Fujinami, R. S. (2002). Inside-out versus outside-in models for virus induced demyelination: Axonal damage triggering demyelination. *Springer Seminars in Immunopathology*, *24*(2), 105–125. https://doi.org/10.1007/s00281-002-0105-z

Turski, C. A., Turski, G. N., Chen, B., Wang, H., Heidari, M., Li, L., Noguchi, K. K., Westmark, C., Duncan, I., & Ikonomidou, C. (2018). Clemastine effects in rat models of a myelination disorder. *Pediatric Research*, *83*(6), 1200–1206. https://doi.org/10.1038/pr.2018.45

Valny, M., Honsa, P., Kriska, J., & Anderova, M. (2017). Multipotency and therapeutic potential of NG2 cells. *Biochemical Pharmacology*, *141*, 42–55. https://doi.org/10.1016/j.bcp.2017.05.008

Vitaliani, R., Mason, W., Ances, B., Zwerdling, T., Jiang, Z., & Dalmau, J. (2005). Paraneoplastic encephalitis, psychiatric symptoms, and hypoventilation in ovarian teratoma. *Annals of Neurology*, *58*(4), 594–604. https://doi.org/10.1002/ana.20614

Wake, H., Lee, P. R., & Fields, R. D. (2011). Control of local protein synthesis and initial events in myelination by action potentials. *Science*, *333*(6049), 1647–1651. https://doi.org/10.1126/science.1206998

Waly, B. el, Macchi, M., Cayre, M., & Durbec, P. (2014). Oligodendrogenesis in the normal and pathological central nervous system. *Frontiers in Neuroscience*, *8*(8 JUN), 1–22. https://doi.org/10.3389/fnins.2014.00145

Wang, F., Ren, S. Y., Chen, J. F., Liu, K., Li, R. X., Li, Z. F., Hu, B., Niu, J. Q., Xiao, L., Chan, J. R., & Mei, F. (2020). Myelin degeneration and diminished myelin renewal contribute to age-related deficits in memory. *Nature Neuroscience*, *23*(4), 481–486. https://doi.org/10.1038/s41593-020-0588-8

Wang, F., Yang, Y. J., Yang, N., Chen, X. J., Huang, N. X., Zhang, J., Wu, Y., Liu, Z., Gao, X., Li, T., Pan, G. Q., Liu, S. B., Li, H. L., Fancy, S. P. J., Xiao, L., Chan, J. R., & Mei, F. (2018). Enhancing Oligodendrocyte Myelination Rescues Synaptic Loss and Improves Functional Recovery after Chronic Hypoxia. *Neuron*, *99*(4), 689-701.e5. https://doi.org/10.1016/j.neuron.2018.07.017

Weilinger, N. L., Lohman, A. W., Rakai, B. D., Ma, E. M. M., Bialecki, J., Maslieieva, V., Rilea, T., Bandet, M. v., Ikuta, N. T., Scott, L., Colicos, M. A., Teskey, G. C., Winship, I. R., & Thompson, R. J. (2016). Metabotropic NMDA receptor signaling couples Src family kinases to pannexin-1 during excitotoxicity. *Nature Neuroscience*, *19*(3), 432–442. https://doi.org/10.1038/nn.4236

Welker, K. M., & Patton, A. (2012). Assessment of normal myelination with magnetic resonance imaging. *Seminars in Neurology*, *32*(1), 15–28. https://doi.org/10.1055/s-0032-1306382

White, R., & Krämer-Albers, E. M. (2014). Axon-glia interaction and membrane traffic in myelin formation. *Frontiers in Cellular Neuroscience*, *7*(JAN), 1–8. https://doi.org/10.3389/fncel.2013.00284

Wlodarczyk, A., Holtman, I. R., Krueger, M., Yogev, N., Bruttger, J., Khorooshi, R., Benmamar-Badel, A., Boer-Bergsma, J. J., Martin, N. A., Karram, K., Kramer, I., Boddeke, E. W., Waisman, A., Eggen, B. J., & Owens, T. (2017). A novel microglial subset plays a key role in myelinogenesis in developing brain. *The EMBO Journal*, *36*(22), 3292–3308. https://doi.org/10.15252/embj.201696056

Wu, L. M. N., Williams, A., Delaney, A., Sherman, D. L., & Brophy, P. J. (2012). Increasing internodal distance in myelinated nerves accelerates nerve conduction to a flat maximum. *Current Biology*, *22*(20), 1957–1961. https://doi.org/10.1016/j.cub.2012.08.025

Xie, Y.-Y., Pan, T.-T., Xu, D., Huang, X., Tang, Y., Huang, W., Chen, R., Lu, L., Chi, H., & Ma, Q.-H. (2021). Clemastine Ameliorates Myelin Deficits via Preventing Senescence of Oligodendrocytes Precursor Cells in Alzheimer's Disease Model Mouse. *Frontiers in Cell and Developmental Biology*, *9*(October), 1–13. https://doi.org/10.3389/fcell.2021.733945

Xin, W., & Chan, J. R. (2020). Myelin plasticity: sculpting circuits in learning and memory. *Nature Reviews Neuroscience*, *21*(12), 682–694. https://doi.org/10.1038/s41583-020-00379-8

Yeung, M. S. Y., Zdunek, S., Bergmann, O., Bernard, S., Salehpour, M., Alkass, K., Perl, S., Tisdale, J., Possnert, G., Brundin, L., Druid, H., & Frisén, J. (2014). Dynamics of oligodendrocyte generation and myelination in the human brain. *Cell*, *159*(4), 766–774. https://doi.org/10.1016/j.cell.2014.10.011

Young, K. M., Psachoulia, K., Tripathi, R. B., Dunn, S. J., Cossell, L., Attwell, D., Tohyama, K., & Richardson, W. D. (2013). Oligodendrocyte dynamics in the healthy adult CNS: Evidence for myelin remodeling. *Neuron*, *77*(5), 873–885. https://doi.org/10.1016/j.neuron.2013.01.006

Zabala, A., Vazquez-Villoldo, N., Rissiek, B., Gejo, J., Martin, A., Palomino, A., Perez-Samartín, A., Pulagam, K. R., Lukowiak, M., Capetillo-Zarate, E., Llop, J., Magnus, T., Koch-Nolte, F., Rassendren, F., Matute, C., & Domercq, M. (2018). P2X4 receptor controls microglia activation and favors remyelination in autoimmune encephalitis. *EMBO Molecular Medicine*, *10*(8), 1–20. https://doi.org/10.15252/emmm.201708743

Zalc, B., Goujet, D., & Colman, D. (2008). The origin of the myelination program in vertebrates. *Current Biology*, *18*(12), 511–512. https://doi.org/10.1016/j.cub.2008.04.010

Zhang, Y., Chen, K., Sloan, S. A., Bennett, M. L., Scholze, A. R., O'Keeffe, S., Phatnani, H. P., Guarnieri, P., Caneda, C., Ruderisch, N., Deng, S., Liddelow, S. A., Zhang, C., Daneman, R., Maniatis, T., Barres, B. A., & Wu, J. Q. (2014). An RNA-sequencing transcriptome and splicing database of glia, neurons, and vascular cells of the cerebral cortex. *Journal of Neuroscience*, *34*(36), 11929–11947. https://doi.org/10.1523/JNEUROSCI.1860-14.2014

Zonouzi, M., Scafidi, J., Li, P., McEllin, B., Edwards, J., Dupree, J. L., Harvey, L., Sun, D., Hübner, C. A., Cull-Candy, S. G., Farrant, M., & Gallo, V. (2015). GABAergic regulation of cerebellar NG2 cell development is altered in perinatal white matter injury. *Nature Neuroscience*, *18*(5), 674–682. https://doi.org/10.1038/nn.3990

Agradecimientos

Gracias a María Domercq y Alberto Pérez-Samartín, por darme la oportunidad de realizar esta tesis doctoral y transmitir siempre su entusiasmo. A Carlos Matute, por su buen hacer liderando este grupo de investigación. Gracias a cada uno de los miembros del laboratorio por su compañerismo. Confío en que me llevo grandes amigos. Y sobre todo gracias a mis padres, por su apoyo incondicional.